Doctoral Dissertations   Student Theses and Dissertations

Fall 2017

The influence of caprock on blast fragmentation distribution

Matthew Kurtis Coy

Recommended Citation

THE INFLUENCE OF CAPROCK ON

BLAST FRAGMENTATION DISTRIBUTION

by

MATTHEW KURTIS COY

A DISSERTATION

Presented to the Faculty of the Graduate School of the

MISSOURI UNIVERSITY OF SCIENCE AND TECHNOLOGY

In Partial Fulfillment of the Requirements for the Degree

DOCTOR OF PHILOSOPHY
in
EXPLOSIVES ENGINEERING

2017

Approved by:
Paul N. Worsey, Advisor
Jason Baird
Grzegorz Galecki
John Hogan
Braden Lusk
Catherine Johnson

ABSTRACT

This dissertation describes the development of a small-scale model of a caprock-laden quarry blast and discusses the results from that testing. The purpose of this testing was to provide insight into the reasons for poor caprock breakage during blasting.

Small-scale test blocks were poured using a weak mortar mix to represent a limestone formation at a small scale. A cold joint was created in the upper portion of the test specimens to represent the bedding plane that separates caprock and substrate layers in a caprock-laden limestone bench. The scale-model test blocks were blasted using detonating cord. The primary configuration for this work was a single blast hole at a 4" burden and spacing from the outside corner of the test block. The blocks were loaded with detonating cord, and initiated from the bottom. Following blasting, surface breakage of the cap layer was photographed and collected for sizing. Following collection of the cap fragments, substrate breakage was photographed and collected for sieving as well.

Test blocks fragmented well in the substrate portion and poorly in the cap layers. Cap breakage was typically limited to single-digit fragment populations. Annular fracturing sometimes created uncharacteristically large fragments that exceeded the burden and spacing of the blast hole and explains the presence of uncharacteristically large boulders in the field.

This testing provided insight into how a massive, solid layer reacts when blasted from below. Cap breakage remained poor regardless of typical blast hole design. The results of this work indicated that the caprock fragmentation and the substrate fragmentation need to be treated separately by blasters and engineers.

ACKNOWLEDGMENTS

Thanks to Dr. Worsey, a mentor and friend for the past decade. You've given me the opportunity to learn and be the first in my family to accomplish many things. I appreciate your support on this degree, even though we both wanted to pull our hair out.

Thanks to the committee members for reading this monster.

Thanks to the Missouri University of Science and Technology Civil Engineering Lab for their help with concrete materials construction and testing.

Thanks to the Missouri University of Science and Technology Experimental Mine for the use of blasting facilities.

Lastly, thanks to my wife for putting up with this degree.

TABLE OF CONTENTS

LIST OF ILLUSTRATIONS

1. INTRODUCTION

In the mining industry, especially for small mines and quarries, peak cost efficiency is an essential method of operation. Cost efficiency affects many aspects of these operations, from stripping to drilling and blasting, to processing and sale. To maximize revenue and peak efficiency, operations regularly scrutinize the blasting of rock benches to ensure that blasted material can be effectively processed. The primary objective of improving blasting operations is ensuring that fragmentation of the blasted rock is optimum and economically viable for downstream processes. Fragmentation, or the degree and range of rock breakage due to blasting, is optimized to obtain the best results with current methods and equipment. In mining operations, an optimum fragmentation distribution has either the lowest unit cost per saleable ton of material, or highest monetary yield (Engin, 2010); this cost includes secondary crushing and handling. For quarries and mines with fairly stable commodity prices, maintaining the lowest unit cost is a preferred method.

1.1. OPTIMIZATION METHODS

To obtain the fragmentation required for efficient operation, blasters and engineers use many different techniques for designing and improving their blasts. These methods can range from using simple rules of thumb, developed by years of experience, to utilizing complex calculations and computational techniques that provide a more in-depth analysis of the rock mass. By employing these methods, blasters can modify blast designs to obtain the most desirable results. These techniques are intended to produce a

specific mean fragment size of blasted rock that can be easily processed. In addition, oversized fragments and fines are kept to a minimum which may reduce revenue losses.

The rule-of-thumb methods are often employed by smaller mines and quarries. These forms of blast design refer to best practices in the blasting industry and rely heavily on the blaster's previous experience with the specific geologic deposit. A benefit to using these methods is that they require minimal training to employ, and if geologic features remain consistent throughout the rock mass, can obtain adequate results for the operation. A detriment to rule-of-thumb methods is that these methods are not easily employed by newer blasters without experience in the deposit, potentially causing less accurate or inconsistent results than an engineered solution. This loss of accuracy can lead to a lower recovery of revenue compared to an analyzed blasting configuration.

Engineered blasting solutions are typically seen in larger quarries where small percentage changes in blasting procedures have a monetary yield significant enough to justify the additional cost of blasting studies. These blasting configurations are the result of intensive studies, and analysis of blasting conditions and outcomes that meet the needs of downstream processes. Engineered blasting solutions can range from field observations like muck pile analysis, to mathematical modeling methods and computerized simulations. These blasting solutions can lead to higher revenue by highlighting problem areas and revealing solutions to increase mineral recovery.

With typical engineered blasting solutions, a characteristic fragment size is calculated and a distribution coefficient is applied to describe the extent of a muck pile's fragment sizes. These are usually based on the Rosin-Rammler distribution curve, one of the most common means of describing muckpile fragmentation, and will be discussed in

the following section. These estimations are most valuable when there is consistency and uniformity within a rock mass. However, current models that function in this capacity have difficulty accurately accounting for grossly oversized fragments that result from non-uniform geology. These estimations account for stratified and jointed rocks by using an adjustment coefficient obtained from experimental results. They do so only by assuming the discontinuities are relatively uniform in distribution and can be relied upon to adjust a block size estimation that characterizes the bench in its entirety. Deviation from the estimation of these discontinuities can drastically change the results obtained from the model when compared to actual muck pile data.

Inconsistencies in results, especially too much oversize, have led to many traditional blasters dismissing blasting models as useless, or at least superfluous, when compared to proven field methods. Oversize, as a result of adverse geology that is not represented by a modeling or estimation solution, stands in stark contrast to the extra effort required in utilizing engineered estimation methods. The oversize created from inappropriate blast design must usually be re-handled, broken additional times by mechanical means or blasting, then transported to be processed as originally intended. As a result, the cost per unit to mine the material increases, reducing operational efficiency.

Smaller quarrying operations tend to use more basic means to try to deal with oversize by reducing stemming, pattern burden and spacing, or by drilling satellite holes to increase powder factor in problem areas of the bench. These methods are typically applied reactively, depending on breakage of previous blasts.

1.2. CAPROCK

Barring misfires and grossly improper blast design, oversize fragments are typically located near the top of a shot and at locations within the bench that have larger block sizes when compared to the surrounding strata. One of the most common rock formations that can produce these large boulders in a shot is a caprock-laden rock bench. Examples of these types of benches can be found in areas of the Bethany and Winterset limestone seams that are present near Kansas City, Missouri, and discussed in Section 2. These caprock layers can produce oversize fragments that lay on top of the muck pile post-blast.

Caprock is a colloquial term that can have a slightly different meaning depending on the industry that is describing it. The term caprock is used more frequently in petroleum engineering to describe a massive rock formation overlying a petroleum reservoir, or aquifer. Many studies have been performed on these formations for the purposes of resource extraction or sequestration, typically examining the caprock mass for integrity and permeability, with an emphasis on preserving the intact nature of the in-situ cap formation. For the mining and quarrying industry, caprock has a different denotation. In this context, it describes thick overlying layers of rock in a bench that are inconsistent with the underlying layers.

Caprock layers can make blasting operations difficult, especially since the thick upper rock layers often reside in the region of the blast holes that usually contain stemming material. Since quarry blasting typically occurs in an orientation perpendicular to the bedding planes that define the rock layers, the distribution of explosive energy is altered due to the influence of the bedding planes. The change in energy distribution,

coupled with the lack of explosives in the top of the blast hole increases the chances of uncharacteristic oversize occurring in a muckpile.

As stated in Section 1.1, the generated oversize fragments, especially those fragments originating from caprock layers, can be difficult to represent using many of the conventional estimation methods. Discrepancies in size and material properties between the caprock and differing lower layers of rock, make the task difficult for assigning estimation values describing the rock mass in the model. When compared to the results from semi-empirical models such as Kuz-Ram, the oversize portion is severely underestimated, especially if the block size of the rock strata below the caprock is the joint spacing criterion used to define the rock mass. This adverse geology causes these estimation methods to become inappropriate for these applications even though they are an excellent resource for optimizing blasting operations. In this thesis, a better method of describing or assessing the breakage of the oversize fragments in caprock portions of a bench was created to define the workings of caprock and blasting in the stemmed region of a bench.

1.3. OBJECTIVE

The objective of this work is to establish a method to reasonably predict the behavior of caprock relative to normal blasting conditions. The method of testing, as well as interpretation of results can be used to represent operations where caprock causes difficulties with fragmentation. Field blasting design, and practices, need to be modified to make any improvements to the run-of-mine fragment sizes based on indications made by this work.

The objectives of the following literature search were to classify the limits of current fragmentation estimation methods, and analyze current small-scale testing methods.

1.4. CONTRIBUTIONS TO SCIENCE

The following contributions to science are described in this dissertation by the author:

- A small-scale model to examine caprock blasting phenomena was established.

- Caprock breakage must be considered as a separate problem from substrate breakage.

- A major problem typically found in small scale test shots was identified, specifically the need to design the test block with free faces for the first shot hole in a configuration consistent with full scale blast.

- A possible source of uncharacteristic oversize was identified.

- Adjustment of the Kuz-Ram and Swebrec models for uncommon geometry by adjusting to the actual volume of material broken away from the test specimen instead of the theoretical value dependent on burden and spacing.

2. PREVIOUS WORK

2.1. SCOPE OF LITERATURE SEARCHED

The presence of oversize material at the top of a muck pile is a frequently occurring phenomenon when blasting caprock. Oversize fragments or boulders in mining and quarrying may cause additional operating expenses. These expenses include increased bench blasting costs, increased secondary breakage for boulders, or even complete loss of revenue for spoiled oversize material. Engineers and managers can perform a cost analysis based on trends in operating expenses in an attempt to maintain a balanced budget. However, this method of evaluation is reactive to mine conditions and difficult to keep consistent with varying geologic conditions, multiple rock benches, and numerous other factors. A means of anticipating the results of blasting operations, involving caprock as a function of blast design, would provide key information that would allow for a complete cost analysis of the influence of current blasting procedures on downstream revenue recovery. Given geologic and blasting parameters, a model that could estimate an amount and size range for caprock could be readily combined with a cost analysis to determine the most effective solution for a mining operation, similar to the site-specific solution found by Esen in 2007 (Esen, 2007).

Initially, literature was explored to see if there was a reliable model to predict fragment size when blasting and determine if caprock behavior could be adequately taken into account with that model. While there are many models that can predict fragment size and are able to account for varying geology, none were found that could exclusively account for rock breakage in caprock. As a result, a model was selected for this project

that would facilitate simple analysis and be readily adapted once a means for estimating caprock breakage was formed. Although many aspects of other current models are discussed, much of this literature search is centered on the Kuz-Ram fragmentation model that is commonly used for basic fragment size estimation in the mining industry. The Kuz-Ram model was adapted and used as the basis for general fragmentation estimation in this work.

The first section of this literature search focuses on describing the geologic formations that contain caprock. This establishes the basis for many of the assumptions in the experimental design section of this work. After describing caprock geology, an examination of standard bench blasting models was undertaken to determine their viability for assessing the blasting of caprock for this project. Following the explanation of blasting models, a description of the influences of blast forces on rock is presented. This section describes the interaction of blast forces as they are appropriated from bench blasting and applied to scaled model testing.

2.2. GEOLOGY OF CAPROCK

Caprock is a term commonly used by blasters and engineers to describe the portion of a rock bench that has a thick, massive layer at or near the top. This is a regular occurrence with near horizontal sedimentary rock formations. Most often caprock is a concern when remedying fragmentation issues in limestone quarrying.

In the mining industry, rock is commonly classified as resource or waste and therefore the bench configuration (top and or bottom) is often limited to the boundaries of different sedimentary layers. To complicate matters in the quarry industry a bed of say

limestone may have different layers within it differentiated depending on industrial use from chemical characteristics (such as Calcium content) to physical characteristics (such as absorbency), which may necessitate the further subdivision of lithological units into separate benches for extraction purposes.

The most difficult aspect of blasting, in regards to caprock, is that the presence of caprock is a geologic factor and cannot be controlled within the blasting scenario (Atlas Powder Company, 1987). Limestone deposits, with caprock made of all the same type of rock can still vary in properties from layer to layer. Due to the wide variation in geologic scenarios, overall characteristic descriptions of a caprock bench are brief. There may be differences in grain size, strength, and many other diverse rock characteristics (Tulsa Geological Society, 1984). The best course to investigate caprock is by examining and constructing an example of a known rock formation.

The Bethany Falls and Winterset limestone formations in the Kansas City and St. Joseph, Missouri regions are known to produce large oversize from caprock. The strata of these formations are fairly consistent in lamination across the region, with slight variances in thickness and depth as the topography changes. These formations can range from approximately 12 to 30 feet thick for the Bethany Falls formation and 25 to 40 feet thick for the Winterset formation (Cramer, 1983). These are average values, but the author has drilled shallower benches of both formations. These shallow thicknesses can reduce down to 4 feet on the Bethany Falls and dwindle to 5 feet on the Winterset. Where the Winterset and underlying Bethany Falls formation overlap, there lays an inter-burden of 6 to 10 feet of greasy shale. The author notes that the same type of shale lays beneath the Bethany Falls formation as well.

Both of these formations have thick upper layers that are separated from the lower section of their respective formations. When drilling through both formations, their thick top layers of rock are significantly harder than the underlying rock, especially in the Winterset formation. These top layers are separated from the rest of their respective formations by either a slimy mix of clay and shale mud or, in the case of the Bethany Falls member, or by another material that is referred to colloquially as "peanut rock" (Cramer, 1983). Peanut rock is a naturally crushed limestone that resides below the thick top layer. It is an extremely friable and crumbly layer, ranging from 6 inches to 2 feet in thickness. In the author's experience, drilling peanut rock produces fine cuttings and provides very little resistance, sometimes clogging the drill bit if too much feed pressure is used. Conversely, when drilling on a Winterset pattern that is especially wet, drilling productivity is severely reduced due to the stickiness of the 1 to 4-inch thick clay and shale mud seam about 2 ½ to 3 ½ feet below the surface, infilling what is the first bedding plane. While sticky, it also has the consistency of a slippery grease. If drill feed rate is not significantly reduced, and the hole completely flushed at the bedding plane, the clay will more often clog the drill bit than allow constant drilling.

The bedding planes of the Bethany Falls and Winterset formations around Kansas City tend to be relatively flat, with a gentle dip of less than 10% in most places. Because of this regional flatness, most vertical blast holes are drilled approximately perpendicular to the rock strata. Most beds within the limestone are approximately 1 foot in thickness, with the top layer being approximately 3 to 4 feet thick. Vertical joint sets in the Bethany Falls formation range from 20 to 50 feet in average spacing. Joint sets in the Winterset are often harder to identify because the upper layers of the Winterset formation are often

highly weathered and obscured by mud, clay or other intrusive deposits. Figure 2.1 is

photograph taken by the author of a Winterset bench that has been cleared for drilling.

Recorded average compressive strengths of both the Bethany Falls and Winterset

Formations are approximately 12,000 psi to 13,000 psi, with a 700-1,600 psi tensile

strength (Cramer, 1983).

Figure 2.1. Stripped Winterset Bench

Rock quarried from the Bethany Falls and Winterset Formations are typically

used for road rock and concrete, with portions of the Bethany Falls being eligible as

agricultural lime. These formations supply most of the aggregate needs for the Kansas

City and St. Joseph regions. Much of the need for this aggregate is an on-demand basis,

depending on how many development projects are occurring within the region. Most of

the materials sold for these projects are crushed rock, with low demand for rip-rap

materials in the area. The entirety of the bench is usually crushed, but rip-rap scalping

tonnages can change depending on product demand. An emphasis on managing oversize

production while reducing fines is essential in producing the largest tonnage of salable

material. In many instances, models are used to describe the results of blasting operations

in these limestone quarries in an effort to spoil the least amount of the deposit.

2.3. MODELING BLAST FRAGMENTATION

When estimating rock fragmentation from blasting, one of the first steps is to find

what types of mathematical models exist for that purpose, and assess the capabilities of

each. This is a daunting task for someone unfamiliar with blast modeling, as there are

numerous models and as many tertiary articles to their credit. However, the models and

techniques found in this document are works that often refer back to the same source

material for a foundation. From the sources gathered, there are a few distinct types of

models used in estimating rock fragmentation from blasting. Separating the models in

this manner makes it easier to determine their viability and appropriateness. Most models

are generally categorized in two ways, semi-empirical estimations and computer

simulations. An understanding of both is required before attempting to advance or

improve on existing methods.

2.3.1. Semi-Empirical Modeling. Semi-empirical methods of estimating rock

fragmentation were born from the need for quantitative assessment and estimation of

blasting results. These methods were the first ones to be developed, predating computer

simulations by many years. Semi-empirical modeling is often geared towards estimating

different aspects of a blast such as size of fragments, range of fragment sizes, speed of thrown fragments, and crater size. The inputs for these models are fairly simple, as most were developed to be expedient for field use. Many of these equations required manual calculations, which made numerous iterations tedious and time consuming. This is why semi-empirical models often have few parts and are easy to use. However, a simple set of equations can still have a large influence in the improvement of blasting operations.

The disadvantage of semi-empirical modeling, that includes portions of Kuz-Ram and Roth's Scaled Depth of Burial work, is that some additional aspects such as resolution or accuracy in the extended regions of analysis are sacrificed for simplicity. These models are only applicable to a certain range of inputs, and overextending their capabilities can lead to grossly incorrect outputs. Engineers can unwittingly use these models without thought to the practical range of operation for which they are made (Cunningham, 2005). Steps must be taken to ensure that the models are adjusted properly for the intended application and can produce useful outputs. Unlike computer simulations, semi-empirical modeling typically cannot account for properties and behaviors of individual fragments or fractures. This is primarily due to the scale at which these methods function. Semi-empirical methods estimate the behavior of the blast in large sections or as a whole. When these methods were created, they were intended to be used for estimating large amounts of material at a scale that would benefit mine operators and engineers seeking to improve mill and mine tonnages in an expedient manner. Assessing blasted material using these methods yields simple approximations of fragmentation sizes.

Semi-empirical model results are calculated by assigning average numerical values for geology conditions and blast conditions. The most easily recognizable semi-empirical blasting models is the Kuz-Ram model. The need for few inputs, and the output of a distinct result, keep this type of modeling popular and useful. For the laboratory testing discussed later in this dissertation a means of estimating the expected fragmentation of a normal bench blast was required. This was to compare the potential differences in fragmentation as seen in a caprock laden bench blast. The search for such a method began with the Kuz-Ram model.

2.3.1.1. The Kuz-Ram model. The Kuz-Ram model is a semi-empirical rock fragmentation model developed in 1983 by Claude Cunningham. It is a combination of the Kuznetzov estimation of mean fragment size and the Rosin - Rammler size distribution. Kuz-Ram is used as a platform for the development of simple fragmentation optimization programs. The equations can easily be entered into spreadsheets that can be readily modified and adjusted (Cunningham, 2005). Part of the model uses the Kuznetzov equation, or a modified version of it, to estimate the mean fragment size produced by a given energy input into a volume of rock. The more recent iterations employ a rubric to assess rock mass parameters. The Kuz-Ram model has undergone different iterations since its creation and has been modified as new contributions been developed. This section will examine the source material for Kuz-Ram as well as some of the changes made through the various iterations.

2.3.1.2. Mean diameter of rock fragments. In 1973, V.M. Kuznetzov established an equation for estimating the mean fragment size of rocks generated from a single-hole blast. This equation is founded on a specific amount of energy from the

explosives being imparted into a rock mass of known volume and strength, very similar to powder factor, shown in Equation 1 (Kuznetsov, 1973).

$$< x > = A(\frac{V_o}{Q})^{4/5} * Q^{(\frac{1}{6})} \tag{1}$$

Where:

$< x >$ = mean fragment size (cm)

A = strength correction factor; assume 7 for medium hard rocks

V_o = volume of blasted rock (m^3)

Q = TNT equivalent of the explosives weight (kg)

The Kuznetzov equation is a simple relationship that can be adjusted linearly using the correction factor, A, to fit real test data from cratering and bench blasting. It can also be easily utilized from within a spreadsheet.

The Kuznetzov equation does have some drawbacks. It is not easily adapted to fluctuating geology and mineralogy. In its initial iteration, the Kuznetsov equation is only able to adapt in a linear fashion to geologic conditions. In addition, another limitation was found with this equation during the author's Master's Thesis. The equation assumes that the amount of energy imparted to the rock, in the form of powder factor, is completely used by the amount of rock blasted. When tests were in a confined single-borehole configuration, the scaled depth of burial, explained in Section 2.5, was high enough that energy was well confined in the surrounding rock, producing small craters. These smaller craters had a volume that was inconsistent with those used to establish the Kuznetzov equation's relationship, which led to confusing estimation results (Coy, 2014). An accurate means of measuring the volume of blasted rock needs to be established for this equation to be accurate in smaller blasts. Even with its detriments, the Kuznetzov

equation is still a relatively simple and relatively accurate estimation method that, when paired with the Rosin – Rammler equation, comprises the first half of the Kuz-Ram model.

   2.3.1.3. The Rosin - Rammler distribution. In 1933 Rosin and Rammler developed a method for determining the size distribution of powdered coal as cumulative percent of an assayed sample. This method provided a percent passing per sieve size. Rosin and Rammler found that for a given sample, if a sieve of characteristic passing percentage is established and the uniformity of fragments are within a certain range, the distribution of the sample at varying sieve sizes can be determined with reasonable accuracy (Rosin R, 1933). The benefit of this estimation, shown in Equation 2, is that it has few inputs and is easy to calculate, especially when used with modern spreadsheets like Excel. The authors indicate that this distribution is only applicable after a certain degree of grinding and crushing has already been conducted (Rosin R, 1933).

$$R=e^{-(X/X_c)^n} \tag{2}$$

Where:

R = % Failing (Retained) screen size

X = Screen Size

X_c = Characteristic Size (Usually Mean Size)

n= Uniformity Index ($0 < n < 2$)

   The primary application for this type of distribution, as presented by Rosin and Rammler, is to represent the spread of particle sizes after they have undergone a secondary crushing or milling process, commonly found in coal comminution circuits. It is typically applied to a narrow range of particle sizes, so it follows that larger size

differences will lead to a less accurate representation of fragment sizes. The loss of accuracy can be attributed to a change in the amounts of oversize or fines particles compared to the mean portion of the sample that the curve represents. Rosin - Rammler curves are typically applied to represent a sieve analysis of a material that has undergone a milling process. The circumstances for the creation of the fragments must be uniform to properly apply the Rosin - Rammler distribution.

The approximate useful range for this analysis is in the range of 10-100,000 microns (1200 mesh up to 4"). (Wills, 1997) This range does not include the extended sizes that are encountered from run-of-mine fragmentations as they can range from the included fines up to large boulders in excess of 6'. In 1983, Cunningham adapted this distribution for blasting and muckpile fragmentation. It constitutes the second portion of the Kuz-Ram model. The Rosin-Rammler equation is adequate for describing most of the fragment size distribution, but often predicts fewer fines than are measured. Blasting with pre-existing fractures would show less dependence on powder factor and a higher dependency on blast geometry. This is why blasting in rock with small block sizes is more dependent on where the blast hole is located rather than how much explosives are used for that blast hole. (Lownds, 1995)

2.3.1.4. The original Kuz-Ram model. Cunningham's first composition of the Kuz-Ram model was published in 1983. It was a combination of the original Rosin-Rammler and Kuznetzov equations. Cunningham proposed that the mean blasted fragment size obtained from the Kuznetzov equation can be applied as the characteristic size in a Rosin-Rammler distribution. From there, the uniformity index is estimated and the model adjusted based on field data. (Rollins, 1989) This model is readily applied to

mining operations. From measured test blasts, the mean size correction factor and uniformity index are adjusted so that consistent results can be achieved. This model has very basic inputs, but if used properly, can provide usable estimations from blasting operations that may reduce the cost of mining and processing minerals (Cunningham, 1983).

2.3.1.5. Assessing rock blastability. Until now, the Kuz-Ram model has been vague on how the rock quality description has been assessed, with the A correction factor being fairly subjective. This metric is dependent on the investigator's assessment, leading to a wide range of results depending on how the investigator assesses the rock. Peter Lilly proposed a better method of indicating rock blastability based on multiple rock bench attributes. His index is based on a combination of the bench's joint plane spacing and orientation, how blocky or massive it is, hardness, and specific gravity of the rock itself. This relationship was established to work directly with Lilly's assessment of a specific energy input due to blasting, but Lilly also states that it has application when working with Cunningham's Kuz-Ram model to help estimate the mean fragment size (Lilly, 1986). With the addition of this document, Kuz-Ram became much easier to use as it provided a rubric that can be used to quantify rock conditions, removing much of the guesswork needed to describe the rock mass for estimation purposes.

2.3.1.6. Kuz-Ram 2. The second iteration of Kuz-Ram was introduced in 1987, a year after Lilly's blastability index. Most of the model remains the same as its first iteration. The key addition to this version is the inclusion of Peter Lilly's blastability index to help determine the mean fragment size. Other additions to this model are the

adaptation for emulsions and blasting agents, and the recognition that photographic methods can be used in measuring muck pile fragmentation (Cunningham, 1987).

      2.3.1.7. Kuz-Ram 3. The latest version of Cunningham's Kuz-Ram model was published in 2005. It features many changes made in the 20 years since the original (Cunningham, 2005). The first change to note is the modifications made to the Kuznetsov equation. Much of the work done with this version of Kuz-Ram has been to finely adjust the mean fragment size so that powder factor is expanded from the original equation. The weight strength of the utilized explosive has been adjusted for the application of ANFO and related blasting agents, and the exponents have been slightly modified as shown in Equation 3.

$$X = A * (K)^{-0.8} * (Q_e)^{(1/6)} * (115/E)^{(19/30)} \tag{3}$$

Where:

X = Mean Fragment Size (cm)

A = Rock Factor

K = Powder Factor (kg/m3)

Qe = Explosive Weight (kg)

E = Relative Weight Strength to ANFO

      The changes to the sizing portion of the model made it more accurate when used to assess blasting with modern blasting agents. The Rosin-Rammler portion of the distribution remains relatively unchanged since 1987. A correction factor has been added to the rock blastability index to help correct for errors encountered in the field. Delay timing has also been added to the model, making it more applicable to the shot design as a whole than rather than a representative single blast hole. Cunningham does point out

that there are still limitations with the model. He classifies these limitations into unaccounted parameters, limited ability to actually measure fragmentation and difficulty in scaling blast effects. He goes into more detail on the detriments of each of these.

      2.3.1.8. Using computers to run the Kuz-Ram model. The Kuz-Ram model is an easy-to-employ fragmentation prediction model. Its equations may be calculated by hand, or even faster by utilizing a computer spreadsheet and either solving by numerical methods or Microsoft Excel's built in program, Solver. Excel also gives the user the ability to program and run a script that can find the design that produces fragmentation at the lowest unit cost. Mario Morin in 2006, used Microsoft Excel's Visual Basic programming language to construct a Monte Carlo simulation within Excel to run multiple iterations of Kuz-Ram estimations to find the most statistically likely result that would occur with the model and a range of real world values for the blasting conditions (Morin M.A., 2006). In 2010, R.C. Engin used a slightly different but still effective method for solving for the optimum conditions. By inputting the Kuz-Ram model, blasting conditions, and associated costs into Excel's Solver add-on, the lowest unit cost was calculated (Engin, 2010). This method of calculation is faster than creating a numerical equation in Excel to solve for the optimum solution. The results produced from these types of analyses are still sensitive to changes, and the authors did not analyze the changes to see if the maxima obtained would be influenced by small changes in the design or conditions, as would happen in reality. If these kinds of methods are to be used in the future, sensitivity analysis needs to be performed along with the optimization because, while conditions on the actual bench may differ slightly from the optimal inputs obtained in the Excel optimization, the resulting estimated fragmentation may drastically

change. The optimized point can be calculated and used to design the blast, but the design needs to be reliable and repeatable on the bench. The user must ensure that the maxima found via this method is the global maximum for the entire realm of possibilities versus a local maximum (or minimum) which can occur but is not necessarily the maximum gain. This is still the fastest way to complete calculations and analysis through semi-empirical modeling.

Over the years, the Kuz-Ram model has been adapted to be applicable in many different locations with differing geology. There is still a large amount of interpretation that is needed in measuring the geological conditions as well as obtaining a reasonable output (Cunningham, 2005).

2.3.2. The Swebrec Function. Another popular form of semi-empirical fragmentation modeling is the Swebrec model developed by Finn Ouchterlony (Ouchterlony F., 2005). His model is newer than the Kuz-Ram fragmentation model and is very similar in form in that it comprises a two-part model based on Kuznetzov's Mean Diameter of Rock Fragments estimation and a characteristic particle size distribution curve. However, instead of using the Rosin-Rammler equation to approximate the size distribution of rocks, an adapted version of the Gaudin-Schumann equation is used to describe the particle size distribution. This adaptation allows for a better approximation of the fines region of the fragmentation curve. It was selected because Ouchterlony was leading a research effort to better understand and control the generation of fines that result from bench blasting.

Ouchterlony's Swebrec function is very similar to the Kuz-Ram model. However, it takes the estimation used by the Kuz-Ram function and uses it to describe the coarse

section of the fragmentation. The fines section is measured using a new equation that is more accurate in describing breakage in the lower size registers, fragments less than ¾ inch on a full-scale blast. Ouchterlony provides a better description of size distribution and has applied his model to many mining applications. (Ouchterlony F. , What does the fragment size distribution of blasted rock look like?, 2005) Ouctherlony observed that the fines region takes a logarithmic approach instead of following the simple exponential function put forth in the Rosin-Rammler equation. The Swebrec model is appropriate for operations that strive to improve estimation and lower the production of fines in their blasting. (Ouchterlony F. , The Swebrec© function: linking fragmentation by blasting and crushing, 2005).

The Swebrec model enables the user to examine the fines region with a larger degree of scrutiny and anticipate blasting conditions that are creating additional fines. This examination allows the blaster to adjust his methods appropriately. Conversely, Swebrec has a limitation when oversized particles are involved. The limitation is deliberate to ensure a definite upper boundary for the distribution curve, correcting some skewing that occurs as the size distribution function approaches a horizontal asymptote. The upper limit is defined as either the burden or spacing of the blast, whichever is larger. This upper limit is found in both in the function of the distribution curve and the uniformity exponent. Incorporating this upper limit into the Swebrec function allows it to account for a smooth distribution and increased accuracy in the fines region of the size distribution. This is not applicable to extreme scenarios but will work with most applications. Many of the practical applications of Swebrec require an in-depth study of

field conditions such as in-situ block size and varying rock strength characteristics. (Ouchterlony F. , Fragmentation monitoring of production blasts at MRICA, 1990)

Semi-empirical models including the Kuz-Ram and Swebrec can be utilized by hand calculations or formulating a spreadsheet that simplifies the input section and calculates the results easily. By doing so, these models can be applied without requiring a large amount of experience or practice with the methods. Their simplicity allows them to be applied across a broader spectrum of blasting applications. However, there is a second category of blast modeling to consider.

2.4. COMPUTER MODELING

Computer simulations work and behave very differently from semi-empirical methods of assessment. Simulations require the operator to have an intricate knowledge of the materials present and an understanding of their interactions. Unlike the semi-empirical methods, they work from the minute scale of a single simulation element, mimicking the interactions of each specified element as it occurs in the blast.

Computational models are a newer development to blasting, becoming feasible within the past couple decades. Many of these models are based on material and explosives properties, and the physical phenomena that govern them. The models allow for more in-depth analysis of rock breakage because computers can account for many variables and quickly run complex calculations. Two types of computational modeling are examined in this review. Finite element analysis (FEA) and peak particle velocity (PPV) modeling are two distinct forms of computer modeling for rock fragmentation.

2.4.1. Finite Element Analysis. Finite Element Analysis methods are used when a simulation requires exacting detail in describing not only the behavior of a blast, but also the characteristics of individual fragments within the blast. A Finite Element Analysis, or FEA, is constructed by creating a block model that represents the volume of the rock to be simulated. This block model is divided into either smaller blocks or nodes, constituting the smallest possible fragment element that could be created and displaced. With this modeling method, individual elements are the focus of the simulation and are given physical characteristics to represent density, strength, hardness, and as required. When simulating a bench blast, cylinders of material are removed from the block model to represent blast holes.

Once a block model is established, breakage simulated by applying force to a region of the block model, then time-stepped to show the breakage and displacement of the elements. Once the forces have equalized, the nodes or elements are assayed to determine which blocks remain bonded together, representing the fragments generated during a blast. Using an algorithm, these fragments are assigned a size and a distribution curve is created from the data describing overall fragmentation of the simulated blast. The final result is a fragmentation distribution, much like those presented earlier, but is based on exact count of simulated particles, not on general estimations.

The benefit of an FEA simulation is that if the block model remains accurate at a high resolution, it can produce the most accurate prediction of blasting results. Dare-Bryan used a Finite Element Analysis to estimate fragmentation and compared it to the Swebrec function (Dare-Bryan, 2012). He found the simulated results to agree closely with the prediction provided by the Swebrec function. However, the simulations show a

distinct difference between the fragmentation of blast holes located within large blocks and those with narrow or intersecting joint sets. The holes within large blocks showed breakage in all directions, whereas holes located near joints and intersections tended to fracture toward those joints, producing an overall bowtie pattern as shown in Figure 2.2. (Dare-Bryan, 2012) Most of the fractures in this example stop at the joint boundaries because when fractures intersect, the intersection point lacks tensile strength and blast energy cannot cross the boundary (Lownds C. , 1983).

Figure 2.2. Dare-Bryan Simulated Limestone Breakage with Jointing (Dare-Bryan, 2012)

Donze used a 2-dimensional discrete element model to simulate rock breakage from a blast hole in a stress field. Figure 2.3 illustrates the circular elements he used to represent the bonds within the rock material. Fractures and discontinuous regions within the rock mass are demarcations where the elements have no bond with an adjacent element. This method is capable of accounting for discontinuities and rock properties.

However, it is only practical on a small scale due to the high resolution of these elements

(Donze, 1997).

Fractures in this type of model are generated by disassociating bonds of individual

elements at locations where stresses exceed the strength criteria of the block model.

When these fractures intersect, the program recognizes the cluster of associated elements

surrounded by fractures as an individual fragment broken off from the block model.

Margolin's work on numerical simulation of fractures simulates the expansion of existing

cracks in pre-rendered strata (Margolin L.G., 1982). It does so by calculating the change

in forces acting on cracks at fracture tips. This model can be used to estimate the damage

left in strata such as oil shale.
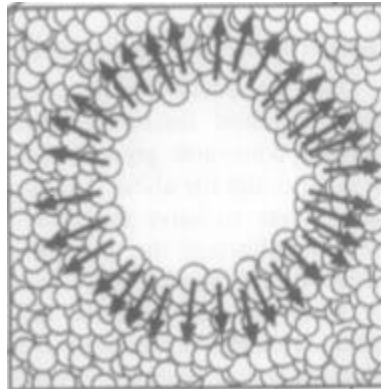
Figure 2.3. Simulation with Circular Elements (Donze F.V., 1997)

Once the generation of fragments is complete, they are categorized by size and a

characteristic curve is generated to describe their distribution (Donze F.V., 1997).

Using finite element methods gives a better understanding of the forces involved, and the movement and breakage of fragments at various times during the simulated blast. These methods show the interaction of forces, as well as the effects that certain geological features can have on the outcome of the blast, provided they are modeled properly and the behavior of the materials involved is accurate. Chung also used the FEA method to analyze the effectiveness of stemming in a blast. He determined that using two different sizes of graded material to constitute the stemming will hold better than using a single graded product (Chung, 2002). Cho's simulation of pressure increased over time, estimated the principal stresses encountered in and around blast holes. This simulation corroborates results on optimal delay times by Langefors and Kihlstrom, and Stagg and Rohll, where the optimal delay periods are shot in relatively fast succession. This study also states that drilling and blasting satellite holes reduces boulders without significantly increasing the number of fines (Cho, 2004).

The materials used in finite element models are usually considered homogenous, so smaller existing fractures are often overlooked and only major joint sets are considered for the block model. Typically, blocks are considered to be uniform and continuous. The lack of impurities and discontinuities within a material lead to less distributions of blast energies. The inability to account for influences from small discontinuities and flaws in a material often leads to the resulting estimated fragmentation differing from what would occur during the actual blast. As the accuracy of these models increases, the errors produced primarily become the responsibility of the individual assessing the rock mass.

The principle detriment to this type of modeling is the time required to use it. These models perform many calculations to account for all the physical interactions

occurring within the simulation at a given time-step. These calculations are not reasonable to solve by hand, and as with semi-empirical modeling, are also only as accurate as the information that is entered into them. Also, many of the higher resolution models are built within software programs like ANSYS AutoDyn, or proprietary programs that require large amounts of computing power. In spite of these detriments, FEA simulations have been used to great effect. Ma used a homogenous AutoDyn model to predict a zone of plastic deformation and failure surrounding a blast hole. He found that faster strain rates caused smaller, more numerous cracks to form (Ma, 1998). Preece also used ANSYS AutoDyn to simulate the effects of timing between blast holes (Preece, 2008). Tawadros used this type of simulation to estimate the production of fines immediately around the blasthole. (Tawadrous, 2012) This method requires a large quantity of work to assemble, but is worthwhile in predicting results where means of measurement are infeasible in real world scenarios.

Smaller operations, especially quarries, will typically not use computational models due to the amount of technical knowledge and training required. The complexity of these methods yields useful results, but is often too cumbersome to use. If modeling is employed in blasting operations, the more simplistic methods are preferred because their ease of use and simple analysis can still influence significant gains. Semi-emperical and most recently PPV modeling still remain popular means of blast modeling.

2.4.2. Peak Particle Velocity (PPV) Modeling. Peak Particle Velocity (PPV) is one of the newest methods of computer modeling employed at large mines for fragmentation optimization and large optimization projects. For complexity, this type of modeling can be considered the bridge between semi-empirical and FEA modeling.

While not as complex as FEA methods, it still provides higher resolution results than the typical Kuz-Ram or Swebrec analysis.

Current iterations of this model are proprietary, along with the large amounts of field observations required to operate the model. PPV modeling is a combination of field observation data and computerized analysis. The primary objective of this type of model is to use ground vibration data from multiple seismographs and estimate the peak particle velocity at different locations within the bench. Persson developed a rough method for estimating the peak particle velocity generated from a blast by relating rock strength and characteristics of the strain wave (Persson, 1997). Prior to the main bench blast, a "signature hole" is fired as a representative to provide a clean seismic signal for the seismographs to record. The remainder of the bench is then shot and the seismic data recorded. Once data is entered into the computer, the vibration data observed by multiple seismographs is trianglulated back to the blastholes once data is entered into the computer (Yang R. a., 2011).

This model cannot accurately account for discontinuities in the rock such as vertical jointing and bedding planes. Discontinuities are not discretely modeled as in finite element models, but areas with a delayed or reduced seismic signal are identified as having a lower integrity. With multiple seismograph recordings from different blasts throughout the rock mass, the understanding of the rock behavior becomes more accurate. By extension, it is possible that PPV modeling cannot explicitly account for thick layers of rock in the upper region of the bench. Due diligence is required when measuring the exact interactions of the blast vibrations in the upper rock layers.

2.4.3. From Theory to Practice. There are many ways to estimate run-of-mine blast fragmentation. For fines, a higher resolution model is required to account for the small particles. When oversize fragments represent a larger portion of the rock mass, making refined resolutions become unnecessary. After examining multiple methods, the semi-empirical modeling methods remain the most viable for assessing the laboratory work in this dissertation. The next section describes fragmentation measurement and acquisition of field data.

2.5. EVALUATING FRAGMENTATION

There are currently two main methods for measuring fragmentation, sieving and photogrammetric analysis. The first is sieving the entire sample of blasted rock, which produces the most accurate results. By obtaining the entire size distribution for all fragments, regardless of their location in the muck pile, the most accurate representation of the size distribution is acquired. Singh describes assessing fragmentation in this manner;

> "Quantitative assessment of fragmentation at a larger scale is a most difficult task. The only fully quantitative method of assessing fragmentation is to screen the entire mass of fragmented material. This, however, is impractical at the production scale. Next to screening there is no known reliable method of evaluating fragmentation quantitatively in a production environment." (Singh, 1993)

This is the more expensive method of measurement, as it is not only time consuming but also requires all of the muck pile to be re-handled.

The second and for many years the predominant measurement method is by taking optical measurements of the muck pile. This method is much quicker and less costly than sieving, but requires more consideration to ensure that the photographs and methods used for analysis produce reliable and useful results.

2.5.1. Measuring Fragmentation Using Standard Photographs. Before the second installation of the Kuz-Ram model, Cunningham discussed an easier method for measuring the muck pile fragmentation. The analysis of a properly scaled photograph allows for a more accurate estimation of muck pile fragmentation. To provide scale and account for distortion, the photograph must have objects of known size placed staggered in a staggered order throughout the muck pile. To provide scale and account for distortion, the photograph is also important to ensure accurate representation of the muck pile. This method can be performed much quicker than sieving a shot, and at a lower cost, as the re-handle costs are not present (Aswegen H.V, 1986).

In his publication, "Methods of Evaluating and Predicting Fragmentation", Cunningham discusses many of the advantages and disadvantages of using sieving and photographic measurements. There is a deceptive nature to using optical methods because a large volume of the shot is not visible. Oversize fragments that appear on top of a shot cause analysis of photographic measurements to underestimate the amount of fines produced in the shot. The less uniform the blast, the less accuracy using optical methods. A reliable means of estimating oversize is by measuring the approximate dimensions of produced boulders and comparing them to the total volume of rock blasted, producing an

oversize index (Singh, 1993). By estimating the oversize portion in this manner, the remainder of the blast can better align with predicted values. Cunningham wrote about these issues twenty years ago, but they still are present whenever photographic measurements are taken (Cunningham, 1995). There have been efforts to try to reduce the influence of these problems, as discussed in the next section.

2.5.2. Digital Image Analysis. There are computerized optical analysis programs that take photographs and, as described in Section 2.5.1, estimate muckpile fragmentation. The most commonly utilized programs are Split Engineering, and Wipfrag. These programs are able to delineate between the different fragments within a scaled photograph. Some assistance from an operator is needed to make sure the computer is accounting for all visible fragments. The computer can then infer content to account for what is not visible; this is still an inference and not completely representative of the actual distribution. However, with proper calibration, these methods can produce consistent, reliable results.

Siddiqui, Shah, and Behan describe how to use digital image processing, more specifically split engineering, to measure size distribution in a muck pile (Siddiqui F.I., 2009). A benefit to using these digital processing programs is the speed at which processing occurs far outpaces measuring and scaling photographs manually. Computerization also allows multiple photographs to be taken of the same shot from different angles and cross-sections of the muck pile and analyzed simultaneously. The produced estimations can then be averaged to provide a more accurate representation of the fragmentation on top of the muck. This method has been used to measure results from blasting and compared to the Kuz-Ram prediction (Engin, 2010). It has also been used for

the calibration of the Swebrec function to ensure accurate prediction of rock breakage. (Ouchterlony, 2006)

2.5.3. Additional Fragmentation Measuring. New technology has been created for measuring muck piles and improving muck pile data using three-dimensional laser scanners to measure the bench face pre-blast. Onederra used lasers scanners to measure fragmentation in 3D which provided a better perspective than estimating fragment size from a two-dimensional photographs. Blindspots are minimized by having a three-dimensional rendering of the rock mass which makes distinguishing the boundaries between fragments easier. (Onederra, 2015)

Sections 2.3 through 2.5 address the acquisition, calculation, and dispensation of muckpile fragmentation. Differing techniques were discussed and common practices for fragmentation estimation have been established. In spite of this wealth of knowledge, there is still a lack of information on how to account for excessive oversize caused by caprock. Section 2.6 examines the basic sciences of breaking rock with explosives explaining specific instances when oversize can occur from bench blasting in caprock.

2.6. BLASTING USED FOR ROCK BREAKAGE

It was difficult to find a fragmentation model that could specifically account for uncharacteristic oversize generated from the blasting of caprock laden rock benches. The Kuz-Ram model was chosen for fragmentation comparison not because of its ability to describe caprock but because of its simplicity and adaptability. Kuz-Ram's description of oversize is not necessarily an accurate depiction of the oversize generated during bench blasting. This section is an examination of the distribution of stresses and fractures,

within a rock mass, that could cause oversize to occur near the top of a blast hole. This examination will provide a more definitive perspective on bench fragmentation that the approximating nature of modeling and estimation cannot encompass.

The current understanding of rock blasting explains the breakage of rock surrounding the blast hole as a two-stage process. First the rock is crushed in the immediate few inches surrounding the blast hole. The rock mass, at the borehole wall and immediate vicinity, experiences a large degree of crushing due to the concentration and interaction of blast forces. Second stage in the process is development of random numerous, radial fractures that eventually taper down to a few primary fractures. These primary fractures will expand with the explosive gasses much later in the blast event (ISEE, 2011). Figure 2.4 illustrates a classic example of how an individual blast hole functions with continuous rock in all directions. Overall rock breakage can vary significantly from the example shown when this process is combined with blast geometry and the interaction of shockwaves with boundaries and discontinuities.
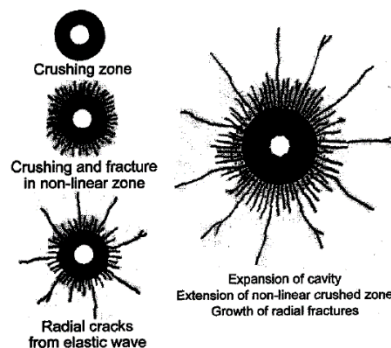
Figure 2.4. Fracture Propagation from a Single Borehole (Donze F.V., 1997)

The two primary forces that cause rock breaking from blasting are shockwave interactions within the rock mass and the gas pressure that follows. There is speculation as to which has greater impact, the initial shock or the gas pressure. However, this is unproductive because both affect the breakage of rock in different ways. One commonality is that the degree to which each explosives property contributes to breakage is dependent on each application. These forces are explained in Section 2.6.1.

When blasting is modeled, described, or evaluated, it is often conducted in 2-dimensional planes; one normal to the blast hole axis and centered on the blast hole, the other running parallel with, and intersecting the axis of the blast hole. Viewing the blast in the normal plane displays the development of radial fractures produced from the blast hole per vertical unit. In a typical bench blast, this display would be the horizontal plane, giving the observer a top-down view of the blast similar to that in Figure 2.4. This type of illustration is not typically applied to an area of the blast hole that contains no explosives, such as the stemmed region of a blast hole. It is assumed that rock in the stemmed region does not to follow this radial breakage process as explosive energy comes from the tip of the explosives column below. In some cases, when stemming consists of one-fourth of the overall bench height, this comprises a large amount of the rock bench that does not receive any radial fracturing directly from the blast hole.

The blast hole profile that is displayed parallel to the axis of the blast hole provides different information than its orthogonal counterpart, as shown in Figure 2.5. This side view shows more of the actual layout of the blast hole relative to the bench, but does not provide as much information as to the extent of radial fracturing. Instead, it does

provide information as to depth and explosives configuration. Both of these perspectives provide insight into the influence of effective blasthole design on rock breakage.
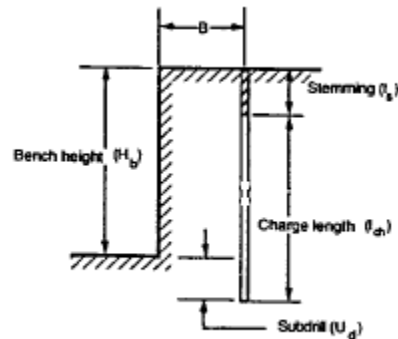
Figure 2.5. Axial Profile of Blasthole (Otterness Rolfe E., 1991)

For metal mines, fine breakage and ore comminution is desirable. Brent proposed a method for improving the blasting of ore, increasing comminution. He proposed using a regular powder factor for the upper portion of a blast, but increasing the powder factor for rock in the lower portion of the blast by using extra holes drilled to full depth. These extra holes are not loaded as high as the main production holes, so that the lower portion of the blast is given a higher powder factor. This increases the amount of fines and comminution so that downstream crushing and refining processes can be accomplished more efficiently. (Brent, 2013)

While increasing the powder factor of explosives has a great effect for ore comminution, it is a significant drawback for aggregate quarries as it reduces the amount of salable tons that can be recovered from a blast. As discussed earlier, the objective for

limestone quarries is to minimize oversize without increasing the amount of fines generated. In an attempt to reduce persistent oversize in a bench blast, one method applies air decks to a bench that would typically not require them, thereby changing the application of blast energy. As previously discussed, blast energy is primarily distributed perpindicular to the blast hole, but by introducing more ends of the powder column into the blast hole, blast energy can have a larger effect vertically in other regions. Air decking also reduces pounds of explosive per delay, vibration, and throw (Jhanwar J. C., 1999). Jhanwar also noted using air deck blasting on jointed rocks increases breakage because the repeated loading extends existing cracks left in damaged fragments (Jhanwar J. C., 2000).

For a single hole blast, it is easier to designate the volume of rock that will be effected by the blast. If multiple holes are blasted within a shot, the shape of the blast distribution changes as burden is removed from previous blastholes (Hjelmberg, 1983). This presents a significant difference between single and multiple hole blasts. This dissertation will primarily examine the effects of a single blast hole.

2.6.1. Stress Distribution. When a confined explosive detonates, the gas products produced by the explosion rapidly pressurize their confines, and for a brief period, induce a stress on the surrounding area. Explosives, located in a blast hole, induce stresses in the surrounding rock. Changing the quantity or geometry of explosives in a blast hole can be used to adjust the stresses so that the rock will break more favorably. There is an occasional attempt to increase fragmentation with higher-pressure explosives, but there is no practical advantage to this effort. Higher blast hole pressures dissipate too quickly into the rock mass to affect the main bulk of fragmentation. The primary result is additional

fines in the region surrounding the blast hole (Hagan, 1974). In addition, Nicholls and Duvall examined the effect of charge diameter on fragmentation and concluded that small diameter charges are less effective than larger diameter charges per respective volumes of rock at inducing stresses in rock (Nicholls, 1966). Siskind, Steckley, and Olson (1973) used rock cores to determine that larger holes have a larger degree of damage, along with a larger blast radius.

2.6.2. Cratering and Scaled Depth of Burial. Livingston's work with single blast hole tests was the beginning of cratering studies. It was the first use of what is now referred to Scaled Depth of Burial (SDOB), which is comprised of analyzing the breakage of rock in the upper region of a blast for shallow charges (Livingston, 1956). Explosive charges loaded above a particular height will crater and cause fragments to be projected from the blasting area. Livingston stated that the damage at the surface is the result of the tensile strain wave reflecting off the surface. Hino continued on Livingston's cratering work to explain slabbing due to shockwave reflection from an explosion near a free face in the blasted medium (Hino, 1956). When Livingston's Cratering Theory is applied, many aspects of cratering can be observed and measured. Crater volume, radius, height, flyrock, and airblast were all associated with burial properties (Bauer, 1961). This cratering theory has been used to anticipate the results of underground nuclear blasts as well, giving these methods a justification on a large scale (Cattermole, 1962). Starfield furthered this cratering theory by examining cratering conditions, scabbing, and extension of radial cracks. He examined the effects of the vertical strainwave in forming the upper portion of a crater. He also observed that if a slab is on top of the shot and no crater is formed, then the strain energy that would be trapped within that upper slab would be

essential in forming the upper portion of a crater (Starfield, 1966). This slab can be considered an allegorical caprock.

With cratering, or the prevention thereof, it is reasonable to believe that the oversize generated from caprock primarily occurs in the upper strata. Once the blast concludes, this same oversize remains on the top of the muckpile and obscures visual analysis. "Observations of a predicted muckpile using throw modelling indicate that the collar of the blast block may mask the fragmentation characteristics of the muckpile" (Katsabanis, 1996). Without mention of jointing or separation near the top of the blast, Katsabanis recognized a clear difference between the main muckpile and the fragments created near the top of the shot.

Scaled depth of burial has been used for a wide range of blast designs. Chiappetta used SDOB for flyrock control during the expansion of the Panama Canal. By designing blasts that would not throw rock, the risk of large rocks finding rest in the shallow bottom of the already established canal was avoided this allowed continuous operation of the canal (Chiappetta, 1998). McKenzie designed from Chiappetta's Scaled Depth of Burial and Roth's flyrock estimations to predict crater volume and flyrock. He used this information to establish more accurate blasting design methods to keep operators and the public safe from the hazards of flyrock (McKenzie, 2009). Chiappetta and McKenzie's designs are two different applications, but they show the efficacy of blast design not only based on powder factor, but the geometry and rock properties that are also present.

Julius Roth constructed a means of comparing performance of blast holes regardless of their size for estimating flyrock by combining Scaled Depth of Burial with Scaled Crater Volume (Roth, 1979). By compensating for the geometry of a blast hole, as

well as explosive properties, a pound-for-pound comparison can be made between differing blasts with results that appropriately scale for each setup. Using this method, differences can be estimated between two different blasts, regardless of size or explosives configuration. Scaled depth of burial is shown in Equation 4 with its associated charge factor in Equation 5.

$$\text{SDOB}_{\text{U.S.}} = \frac{\text{Is} + 0.042 * m * d}{0.305 * (m * d^3 * \rho e)^{0.333}} \qquad (4)$$

Where:

$\text{SDOB}_{\text{U.S.}}$ = U.S. Scaled depth of burial (feet/pound^3)

I_s = Stemming length (feet)

d = Blast hole diameter (inches)

m = Contributing charge length factor

ρ_e = Explosive density (grams/centimeter^3) (ISEE, 2011)

$$m = \frac{12 * \text{Ic}}{d} \qquad (5)$$

Where:

m = Contributing (US) charge length factor

I_c = Charge length (feet)

d = Blast hole diameter (inches) (ISEE, 2011)

This method can also be used to keep small scale tests consistent and representative of larger shots. In crater blasting, it can be fairly accurate in estimating the volume of a crater created by blasting. Scaled Depth of Burial can be paired with the Kuznetzov equation and Roth's estimation of flyrock velocity to give a comparable hazard rating. However, there are issues when pairing the Kuznetzov equation with Scaled Depth of Burial. When just paired together, the scaled depth of burial value must

be at the point with the highest scaled crater volume, otherwise the Kuznetsov equation assumes a higher effective powder factor than in reality. This produces smaller estimated mean fragment size and incredibly fast projection speeds, sometimes predicting speeds nearly as fast as the velocity of detonation. To practically pair the two equations, the calculated scaled depth of burial is used for the actual volume and mass of rock blasted. However, to use the Kuznetzov equation properly, the maximum scaled depth of burial must be used for the volume of rock blasted in the Kuznetzov equation. This contains the results within a reasonable range.

Scaled Depth of Burial can describe the stemmed, upper portion of a bench that does not contain explosives during blasting. The lower portion of the bench is described as a cylindrical geometry that the Kuznetsov equation can be adjusted to estimate easily. Rock breakage in the upper portion of the shot can be estimated independently and described per scaled depth of burial. This description can be added to the Kuz-Ram of the lower portion of the bench for the overall size distribution.

The most critical design a blaster can create is the borehole geometry. Bit size, hole depth, as well as stemming length and type all factor into the overall performance of a blast. Along with the proper selection of explosives product, the physical dimensions of a powder column also play a major role in the performance of a blast.

In most applications, boreholes are divided into two sections where the powder column and the overlying stemming column meet. By examining this type of borehole profile, there is a clear difference between the upper and lower portions. The upper portion has no explosives is broken by excess explosives energy that is used to efficiently break the underlying section. While this configuration allows the lower rock to be broken

efficiently, the upper layers do not receive the same amount of energy and are often the source of oversize in a muckpile. This oversize is further exaggerated by the presence of bedding planes and adverse rock properties.

Figure 2.6 illustrates blasting from this plane and demonstrates how explosive energy moves towards the top of the blast hole, almost like a bubble.
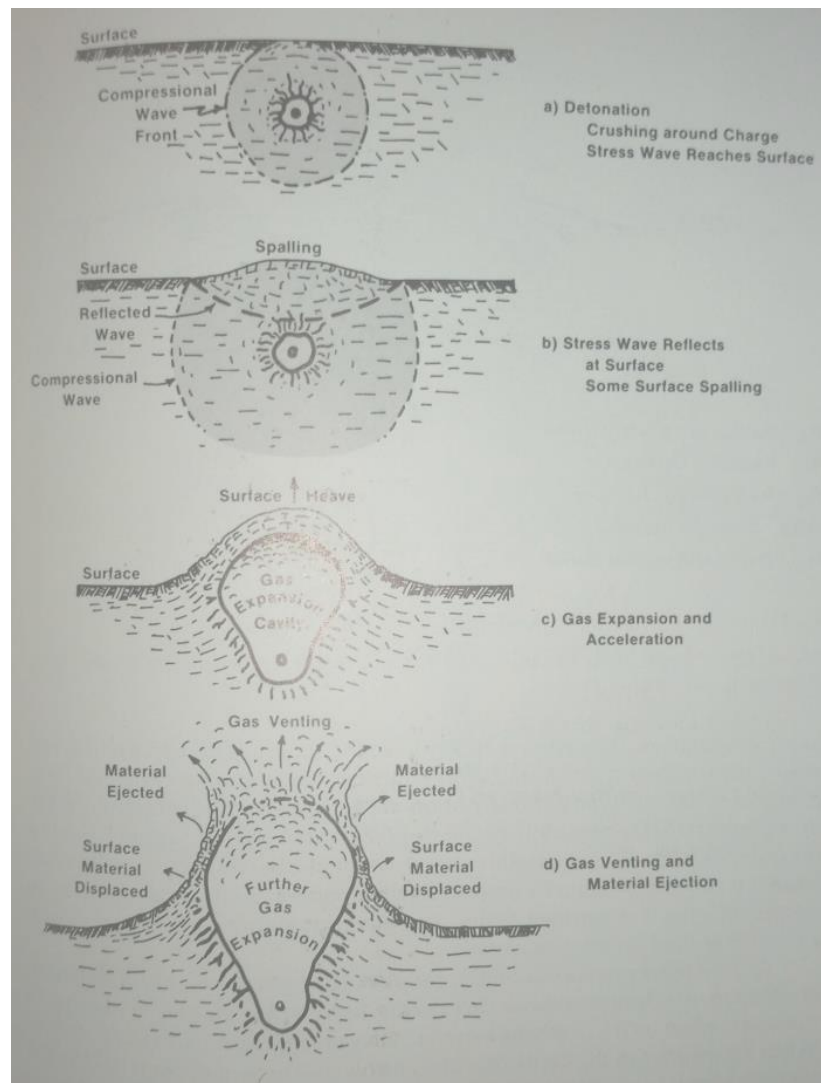
Figure 2.6. Crater Progression (Atlas Powder Company, 1987)

As the explosion progresses, Figure 2.6 illustrates the reflection of blast waves at the surface, creating a cratering scenario. In the example above, the rock at the top of the shot is still cracked by shock, although slightly spread out, and those cracks expanded by the gasses. While this approach seems logical for use in massive rock formations, it is not intuitive for use in laminated rocks. For each additional layer of rock above the powder column, blast energy is reflected, transmitted, and dispersed at diverging angles. As a result, shock energy that does not meet with the next rock layer at a normal angle can be partially transmitted and partially reflected at an angle more parallel with the rock layer than how it entered. This is a possible explanation why cap rock is frequently referenced as the cause for oversize on top of shot rock. The fractures created by shockwaves interacting with the rock do not reach the upper layers. This leads them to break by way of a third mechanism, produced from the underlying rock heaving when the explosives gasses expand existing joints or fractures. This breakage process forms slabs out of the upper layers of laminated rock.

With material creating slabs on top of the shot, a blaster would assume the shot to be too coarse and draw the pattern tighter. In reality is the blaster has reduced the size of the underlying rock, which was likely in the desirable region to begin with, and produced more fines in an attempt to decrease the size and amount of the oversize material. In aggregates, this will result in a higher unit cost per ton because of the amount of unsalable material, fines, created from blasting. It is possible that finding a viable solution to caprock will allow coarser breakage of underlying material and eliminate two problems at one time.

2.6.3. Fracture Behavior. When fractures are induced in rock, they continue to lengthen and expand as long as there is sufficient stress for development. Major fractures will intersect and produce fragments. Oucheterlony proposed that it is possible to estimate a stress intensity factor for a given rock and compare the pressure load rate to estimate the number of primary fractures at the blasthole (Ouchterlony F. , 1974). This estimation is beneficial where blast geometery is more important than powder factor and may be used to estimate the generation large fragments generated during caprock blasting. Figure 2.7 shows one of Livingston's blasts with an 8-pointed star pattern of fractures at the collar. If these primary fractures could be predicted for breakage in the upper strata, the configuration of caprock boulders could be anticipated. This possibilty is examined later in the analysis.

Figure 2.7. Primary Fracturing at Blast Hole Collar (Livingston, 1956)

Rock that experiences slower strain rates, such as that not in contact with the explosives, tend to see fewer primary fractures while the comminution present near the explosives in the blasthole is practically non-existant. In Crichton's hydraulic induced crack propogation testing, the effects of a slower strain rate are visible by the formation of single fractures within such a small medium (Crichton, 1980).

In some areas of the rock, the blast energy is not strong enough to completely cleave a fragment, so it leaves a crack within the fragment. These existing cracks make the fragment more friable and prone to breakage with the introduction of subsequent stresses. Boulders with blast induced cracks are easier to break when dropped from a loader. The larger the fragment, the more likely it is to contain a significant crack (Jaeger, 1986). Monte Carlo simulations of latices can be used to estimate crack densities and internal damage of fragments (Englman, 1984). Most of this type of fracture behavior is observed in ideal rock conditions, but does not account for the effect of discontinuities on blasting.

2.6.4. Influence of Discontinuities on Rock Breakage. The behavior of fractures in ideal conditions is fairly straightforward. However, when discontinuities are introduced, joints and bedding planes tend to take precedence and create boundaries that blasting forces often cannot overcome. When expanding mode-I fractures approach a rock interface, one of three things will occur. The fractures can reach the interface and divert in a direction that follows the interface, the fractures can continue through the interface unhindered, or the separation of the rock material at the interface can precede the arrival of the fracture and the fracture can be stopped dead at the separated interface. This is known as the Cook-Gordon mechanism (Wang and Xu).

The Cook-Gordon mechanism would be difficult, if not impossible to observe in the field. However, the behavior of the mechanism as described by Wang can be used to speculate how a cap layer would break with varying bedding plane conditions. The conditions where separation of interfaces occur are dependent on the angle of incident fracture, the intensity of that fracture, and the shear strength of the interface. In a caprock situation, there is often infill material such as clay, and mud. With these conditions, especially when wet, the shear strength at the bedding plane can be considered minimal. This would indicate that an infilled bedding plane would likely not transmit any sort of fracture, eliminating one of the three possible outcomes. From here an incident fracture can either kink off and split the bedding plane, or just stop completely. The cessation of fracture extension would result in poor breakage of any material on the other side of the bedding plane.

2.6.5. Distribution of Energy Within a Bench Blast.   While the previous Sections 2.6.1-2.6.3 focused on individual aspects of rock blasting, and the interactions of singular elements within the blast, a macroscopic view of the blast needs to be examined as well.

When loading a standard bench blast, drilled holes are filled from the bottom up and stemmed to contain blast energies. This means the majority of the explosives sit toward the bottom of the blast, and associated explosive energies are distributed proportionately. Since the upper portion of the blastholes are filled with stemming material, they have a powder factor that is significantly lower than that of the lower regions of the blast. In the case of caprock-laden bench blasts, a division can be made at the bedding plane to mark a division of the upper and lower sections of the blast. As

described in the previous section, there is a possibility that blast energies are prevented from passing this boundary. In this configuration, the lower section of the blast has explosives along its entire height. The cap portion which contains the stemming will have little to no explosives in that layer. This a disproportionate distribution of explosive energy. In this configuration, the cap material is almost entirely dependent on energy that is confined to the lower rock layers of the blast that may or may not transmit through the bedding plane. A common reaction to oversize on top of a blast is to tighten the blast pattern. If blast energies are only available from underneath the bedding plane, the cap is still dependent on outside energy for breakage and will still break poorly.

In addition to disproportionate loading of explosives, the way explosives energy is portioned into work during a blast must be taken into account. In Joshua Calnan's dissertation, he was able to account for approximately 71% of explosive energy, with rotational and translational kinetic energy comprising 30% of this accounted energy. The energy used in fragmentation was approximately 1% of the accounted energy (Calnan). Calnan indicated that less than half of the energy used in blasting is used in the actual breakage and movement of the rock. In the case of caprock, this energy distribution may be skewed   , with most of the work of the explosives being performed beneath the cap layer.

2.6.6. Estimating the Presence of Oversize. There are methods of loosely accounting for and improving the results of blasting around discontinuities. Drilling the lines of blastholes parallel to major joint sets provide the best breakage (Larson, 1974). Ghosh used natural joints, bedding planes, and other discontinuities to account for larger sized fragments. The spacing of these discontinuities are used as a topsize limit for

fragmentation curves as typical Rosin-Rammler type curves. This allows the curves to have a distinct cutoff size (Ghosh, 1990). The concept of maximum block size bounded by discontinuities is also used with fluid penetrating and underground stowing methods. Fluids will separate blocks or layers of rock at their contacts first, opening and filling exposed discontinuities (Gil, 1991).

An oversize coefficient is used as a practical field method for adjusting for oversize due to blasting. It uses the maximum block size and associates a volume of oversize produced by a particular blast pattern. This is a broad, reactive method as it is measured by overall estimated rock tonnage versus crusher throughput. The transferrence of energy, or similar transition model, uses an idealized version of the rock mass to show how energy is transferred to a highly-jointed rock mass. This model provides a coefficient to compare the effects of different powder factors on the rock mass (Lu, 1998). This model is more appropriate for Armourstone blasts because it was specifically created for estimating the oversize fragments (Latham, 2006). It is also essential for estimating armourstone, as increasing the amount of explosives will not necessarily net a significant gain in fragmentation (Wang, 1991). Armourstone, or very large rip-rap, is used in sea defense structures and can be considered a byproduct of normal quarrying operations, constituting 3-5% of the bench. In blasting operations, some of these blocks are broken, but some are just moved and incur no damage; this lack of damage is due to a loose joint and bedding plane spacing. A low powder factor is used to ensure poor breakage of the armourstone blocks and ensure that fewer blocks are intersected by blast holes. The overall block size is limited by the predominant discontinuities with the larger sections forming a tabular or slab shape (Wang, 1992).

If the amounts of caprock can be estimated, steps could be taken to account for the costs associated with blasting with caprock conditions. In chapter 8 of his dissertation, Joshua Calnan laid out a simple linear program used for optimizing blasting operations. It is used to minimize the total cost with respect to drilling, blasting, transportation and processing of material. This program functions based on the blast design and explosive input into the rock mass. Transport and processing unit costs are associated with processed material tonnages (Calnan). This program can be easily constructed in spreadsheets and is fairly intuitive to use. It is a way that engineers and supervisors can budget for costs and try to improve the efficiency of their operation.

For the above optimization to work for caprock benches, the means of breakage for the caprock needs to be better understood. As geologic conditions in the field vary widely, even across a single blast pattern, the mechanisms that govern caprock breakage will vary accordingly. A repeatable method of examining these mechanisms is through small-scale model testing.

2.7. SCALED MODEL TESTING

Scaled model testing is a widely-used technique for understanding the behavior of blasting. Extrapolation of laboratory tests can be used to anticipate results of full-scale blasts, but cannot be directly correlated due to the methods of assessment between the two types of blasts. These tests are primarily designed to examine the blast mechanics that would not be easily observed in a mining situation.

Scaled model testing can be performed in a variety of materials, and with a range of sizes. The often-cited work performed by Stagg used the rock bench at the University

of Missouri – Rolla's experimental mine to conduct miniature-scaled testing determining the optimum delay timing between blast holes for optimized fragmentation. This testing was performed in the Jefferson City limestone formation (Stagg, 1987). In this case real rock material was used in a reduced shot design to determine a delay coefficient for full scale blasting. Further testing at this site has been correlated to optimal burden and spacing ratios (Otterness, 1991).

Small rock benches are not the only medium useful in determining rock breakage on a small scale. Concrete blocks and benches have been very effective in determining numerous aspects for both experimental and practical shot design.

Work conducted by Tariq and Worsey small scale blocks have shown some aspects that should be considered in shot design. They observed that at wider joint spacing increases the cratering angle available for the blasthole to break out to the face. (Tariq, 1995). They also noted that joints greater than 0.012 inches are open and considered a free face for wave reflection (Tariq, 1996). Both of these observations are important for designing an experiment to exibit the breakage of caprock. They establish which boundaries in the experiment will work as free faces, and influence the fragmentation of the experimental blast. As determined in Kutter's small scale testing, a zone of reflective breakage is present at a certain distance from the surface, after the shockwave reflects. (Kutter H.K., 1971).

Ouctherlony, has also done many tests in concrete blocks at model scale, and has observed that when estimating fragmentation profiles, the model scale tests are typically described using a larger coefficient of uniformity compared to full scale blasts (Ouchterlony, 2006). This means that at a smaller scale, the distribution of particles

across the entire fragmentation profile is spread out across the entire profile, whereas a full-scale blast would have a fairly tight distribution concentrated around the 50% passing size.

Johansson and Ouchterlony furthered testing in concrete blocks with a series of small scale experiments to determine the effect of delays between holes. Holes were loaded in a row, and timed with detonating cord, initiating from the top-down. The sample block was grouted to the test bench to reduce the influence of edge effects. This scaled model project established a better estimation of optimal timing than Stagg (Johansson D, 2013).

While observations of these small-scale tests yield results specific to their respective designs, they can also be useful for validating estimation and analysis tools that are used on a regular basis in the mining and quarrying industry on a regular basis. Katsabanis used a variety of fragmentation estimations, including Kuz-Ram and Swebrec, along with small scale tests in an attempt to estimate optimal timing between consecutively blasted holes. He observed an optimal timing of approximately 10 milliseconds per meter of rock between holes which agrees with many of the previous investigations (Katsabanis P. e., 2014).

Caprock is a unique geologic feature of specific rock formations. Without extensive blasting data on the formation, simulation and general estimation are difficult to perform with a reasonable degree of accuracy. When coupled with the fact that breakage still has not been accounted for, small scale modeling has been determined to be the most viable tool in reproducing caprock blasting results. This section has examined caprock geology, current blast modeling methods, mechanics of rock blasting, and scaled

model testing. All of these aspects are required to perform an assessment of caprock

blasting that is useful with modern blasting techniques. The next section addresses the

experimental design for the small scale caprock tests.

3. EXPERIMENTAL DESIGN

Section 3 describes the design process for small-scale caprock blasting tests. Test specimens were designed to represent quarry blasting situations, but still be adaptable to simulate a variety of geologic conditions. Testing in this manner eliminated aspects of variability by giving the author direct control of the geologic conditions, such as jointing and bedding plane geometry, and uniformity that would not be possible in a quarry setting. The blast pattern and hole design were customized to for examining aspects of the blast that would have interfered with normal blasting operations in a quarry. The testing environment was constructed to be modular and repeatable, eliminating need for small rock benches as used during Stagg's small-scale blasting tests. The general test bench design is suitable to differing scenarios, and easily modified for additional applications and investigations. The beginning of this section establishes the design parameters for the test specimens as they relate to quarry blasting in caprock. This is followed by the small-scale test bench design and accommodations.

3.1. TEST SPECIMEN DESIGN

The scaled-model caprock test specimens were designed to represent geologic conditions that would be encountered during quarry blasting, specifically those involving caprock. Small-scale representations allow for finer observations of the behavior of caprock relative to the blast hole. This type of representation works well since there is no overburden, or other obfuscation. The blast material can be relatively contained and dissected post-blast to observe the fracture patterns and other phenomena. This method is

distinctly more homogenous than actual rock, eliminating the influence of holes, voids, mud pockets, and joints. Scale model testing has the advantage of allowing the user to control previously uncontrolled variables, such as geology, material strength and properties, discontinuities, weather, etc. (Atlas Powder Company).

The design of these tests was initially representative of a generic bench with other features added later. The specimen design was divided into three phases: dimensions for test specimens, initial strength, blasting configuration, and design of caprock layers.

3.1.1. Specimen Sizing and Strength. For the scaled model test specimens to be practical, they needed to be a size that was not only representative of a bench blast, but also transportable during casting and testing. The objective design for these blocks was to design a test block that could be blasted and produce a measurable fragmentation. The end goal for these tests is not to have a direct comparison to a specific full-scale bench, but to provide a small-scale bench that can show some of the caprock breakage phenomena without interference from variables out of the author's control.

Test specimens were sized so that they could be practically cast and moved. A block size of 1.5ft x 1.5ft width and length, and 1ft height was selected. This design made a block that was longer in each horizontal direction than it was tall. The 1ft in height was scaled to represent a 16ft tall rock bench, similar to benches the Winterset rock formation. When blasting in the Winterset formation, a burden and spacing of 12ft is common. At a 1:16 scale, this would be 9in for burden and spacing. From here, borehole size was selected based on available masonry bits and their flexibility. A 3/8in diameter hole was selected because the a 3/8in masonry drill of the required 18in length was much less flexible and by extension less prone to wander during drilling of specimens. At scale,

this equates to a 6in borehole at full scale. A 6in. hole on a Winterset bench is larger than usual. 4in is usually the largest bit used, but the explosive selection for the scale-model tests justifies this increase due to the decoupling of the explosive charge. The test specimen dimensions can be seen in Figure 3.1.
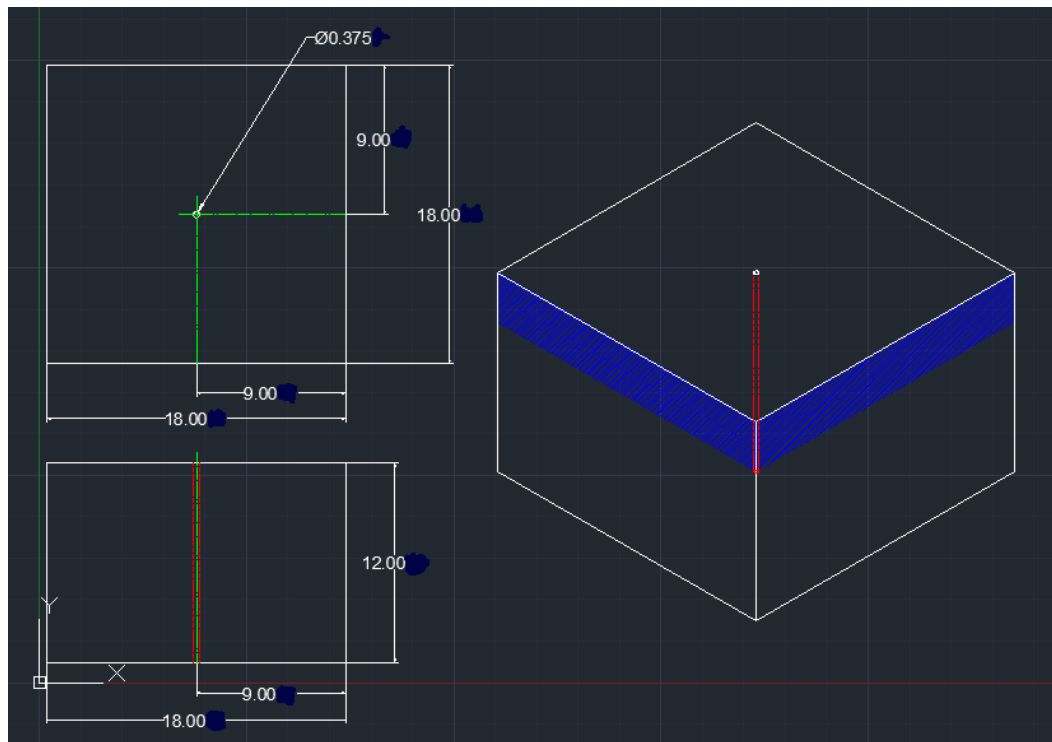
Figure 3.1. Block Dimensions (in) – Top View (Top Left) and Side View (Bottom Left)

The mix design for the blocks was selected by first examining the type of material needed for simulating limestone. The material needed to be fairly homogenous. High strength concrete mixes were out of the question because of the large aggregate within the material. For this reason, a low strength, type S, mortar mix was selected. Mortar mix

does have sand as an aggregate, but it is at a much smaller scale, so it is less likely to affect the creation of oversize fragments. As previously discussed, the compressive strength range for weaker members of Missouri limestones is approximately 7000-13000psi. As the scale of the test decreased, the strength of the material comprising the test specimens had to decrease as well. Keeping with the 1:16 scale, this meant a strength range of approximately 440-800psi. A type S mortar mix was selected to use as the specimen material, with a mix strength of 1800psi compressive strength. It was unknown if an extremely weak mortar mix would stay intact during transportation and handling, so this was the initial value for the solid block test specimens explained later in Section 4.5. The mix was later adjusted to approximately 600psi after initial tests were performed.

Explosive selection at this scale was limited. Blasting agents and most other explosives would not function at a 3/8in diameter. Detonating cord was selected for this reason. It functions at small diameters and could be easily loaded and used in this situation but suffers from decoupling. The detonating cord selected was Dyno Nobel's FireLine 8/40 HMX LS. This is a 40grain/ft detonating cord. A doubled strand of this detonating cord was found to fit snuggly in the 3/8in borehole. This provided a charge of approximately 60 grains of explosive within the specimen for a 9in powder column. The approxmiate associated powder factor for the test specimen was 1.6lb/cyd for the 9in burden and spacing.

This test specimen was blocked on two sides by bumper blocks, as displayed in Figure 3.2. These bumper blocks were intended to provide mass for the back sides of the test specimens to push against, and function as an extended part of the rock bench. They allowed for easy and repeatable placement of the test specimens.
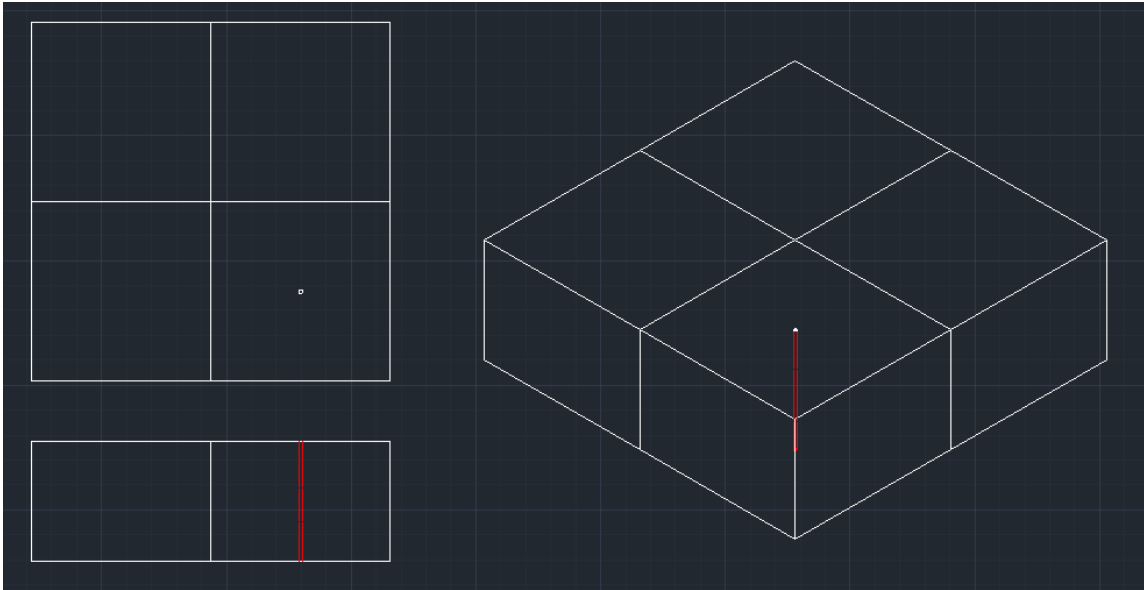
Figure 3.2. Test Bench Block Arrangement Top View (Upper Left), Side View (Lower Left), Isometric View (Right) – Drilled Specimen (with thru-hole) and 3 Bumper Blocks

3.1.2. Caprock Simulation. In the previous subsection, the dimensions and mix design of the test blocks were established. The last phase of caprock simulation is the introduction of the caprock discontinuity into the block design. Pouring the lower portion of the test specimen, waiting a day for it to harden, then pouring the upper portion of the block, created a cold joint in the block and provided a plane of weakness. In caprock laden benches, there is often an infilling of material between the upper layers and the rest of the bench. As mentioned in Section 2.2, this infilled material can consist of clay, shale, mud, or other interstitial media. For the purposes of this testing, infill material was omitted from the joint to maximize the influence of the blast on the caprock layer. A clean cold joint has a small amount of adhesion that would not be present using a filled joint. Adding a dye top section of the block during the pouring process allowed the origin

of a fragment to be distinguished after blasting. The construction of these test specimens and description of caprock test series are discussed in the next section.

3.2. CAPROCK MODEL SCENARIOS

Once the block design was established, the focus shifted to establishing which caprock scenarios would be tested. The test series were conducted in three main stages with key additional tests performed as warranted.

The first set of scaled-model test blocks were poured solid to determine the behavior of the material in the stemmed area of the block without the influence of discontinuities. These tests were designed to be a shakedown and show faults or areas of improvement before the caprock test specimens were poured. These blocks had explosive column heights of three inches. Although they were intended for a different purpose, the design for these tests could be compared to those performed by Tariq for his pre-splitting research, although they were intended for a different purpose (Tariq S. M., 1996). These tests also provided a baseline fragmentation profile for comparison with the remaining tests.

The second set of test blocks was designed to examine the effect of a bedding plane in the stemmed horizon of a blast. This series of test blocks were poured so that a concrete cold-joint, at the top of block, simulated a bedding plane commonly found in cap rock laden rock benches. These blocks were poured so that only the upper layer of the block contained the dye. The thickness of these top sections was poured to 1.5 in, 2.25 in, and 3 in, respective of a 2-foot, 3-foot, and 4-foot thick layer of caprock on a rock bench. They were designed so that the top of the explosives column is below the

bedding plane, level with the bedding plane, and above that level during blasting. For the purposes of this thesis, the height of the powder column is defined by the depth from the top of the test specimen. That is the region nearest the cap layer and the tested powder column heights are based off of the thickness of the cap layer. The varying thicknesses of the simulated cap rock layers and the top of the explosives columns are shown in Figure 3.3. This series of tests examined the effect of cap rock thickness and position of the top of the explosive column relative to the "bedding plane" at the bottom of the cap rock. The results provided insight into the effect of a single blast hole on caprock layers with similar material properties. The next series of tests was designed to examine the effect of harder caprock overlaying a standard bench.

The results from the Series 2 tests provided information that guided the selection of the Series 3 testing parameters, which were designed similar to those in Series 2. Rock strength can vary between layers. This was confirmed by the collected rock samples in Section 3.1.2, which represents one of the more extreme cases of strength differences. The third series of tests were poured so that the caprock section was harder than the block underneath. These layers were comprised of two different hardness degrees and were poured at a set thickness to reduce the number of variables. In addition, a two-layer caprock composite was poured with increasing hardness to determine if this line of testing merited continuation. To conclude the design portion, the test bench and overall blasting configuration were established.
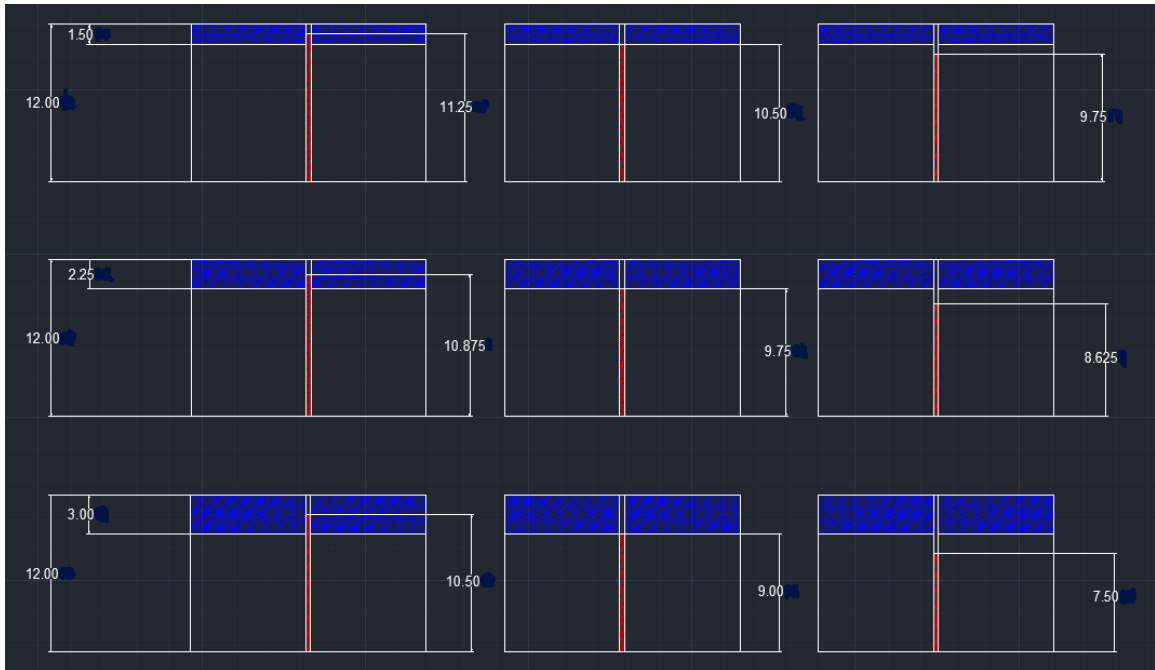
Figure 3.3. Varying Layer Thickness and Explosives Height for Caprock Series 1 Testing

3.3. BLASTING CONFIGURATION

Once the test block was prepared, it was arranged with three other blocks. The blocks surrounding the test block acted as a mass of continuous rock in a bench, allowing only two exposed faces for blasting as shown in Figure 3.2. This block arrangement was assembled on a flat surface that was elevated slightly to allow loading from beneath. Detonating cord was inserted into the drilled hole from beneath the block to the desired explosive column height. Sand was packed into the top of the hole to act as stemming material and confine the explosives energy below. This was assembled to represent a typical blast hole as would be seen in industry, with no explosives in the stemmed region of the blast hole and bottom initiation.

Once the block was fragmented from the blast, it was exposed, beginning at the top. The fragments were examined layer-by-layer for size and position and photographed at each layer of examination for optical analysis. After the fragments had been examined, they were separated and sieved to determine the fragmentation profile of the concrete in the stemmed region of the block as well as the concrete adjacent to the explosive column. This test configuration was used in each of the different test series and was the primary design of the experiments. Alterations and procedure from the described method are explained in Section 4.

4. EXPERIMENTAL PROCEDURE

After the extensive planning performed in the previous section, the actual assembly and execution of the tests was fairly straightforward. Small adjustments were made from the design, as complications were encountered and are described chronologically with the procedure. Section 4 explains test bench construction, the casting and handling of test specimens and bumper blocks, blasting, and data collection.

4.1. CONSTRUCTING THE TEST BENCH

The test bench was constructed for scaled-model testing of caprock with simplicity and utility at the forefront. This bench was constructed to be quickly assembled and disassembled, but still be robust enough to withstand blast forces. It was also constructed to facilitate the loading of explosives as designated in Section 3. The test bench consisted of a flat layer of railroad ties laid tightly together. These ties provided adequate elevation of the test specimens and a heavy, rigid structure for resisting the energy during a blast. The tie placed second from the front of the bench was 2' shorter than the rest and all ties were set even with each other at the left-hand side of the bench, as shown in Figure 4.1. This created a small area on the underneath side where the experiments could be loaded and primed for blasting. Next, two 4x8 foot sheets of ¾ in plywood were placed on top of the ties so that they covered the ties evenly, but still left the priming pocket created by the short tie accessible. The sheets were then fastened to the ties and the floor for the test bench was completed.

Figure 4.1. Test Bench Railroad Tie Configuration
(Note difference in length on second tie)

4.2. MOVING BLOCKS

This test bench was assembled on a level concrete pad using an overhead crane to load test specimens onto the blasting bench. This experiment followed a modular design so that the specimens and barrier blocks could be exchanged once they were no longer needed for testing. The barrier blocks were poured with rebar loops extending from their tops. These loops facilitated easily movement around the test bench with the overhead crane. The specimen blocks, however, had no handles or lifting aids cast into their features. The test specimens varied by strength and features, but the outer dimensions of the untested specimens (1.5ft long, 1.5ft wide, 1ft tall) remained constant for the entirety of the scaled testing.

A set of lifting tongs were created, to work in conjunction with the crane, to transport the test specimens from the forms to their respective location on the test bench. These tongs were similar to logging tongs, with the difference that the set created for these tests had long flat feet consisting of small angle iron instead of the sharp spikes or

barbs that would be present in their logging counterparts. These long feet were positioned underneath opposing edges of the test specimens, providing strong, stable and strong lifting capabilities without risking damage to the specimens. They could then be moved quickly and efficiently and placed near their final location for testing.

The crib was the last piece of extra bench equipment that was constructed. A method of containment was needed to prevent particles, created by blasting, from leaving the test bench. A crib was constructed of 2x12 in planks that surrounded the perimeter of the test block and bumper blocks. This perimeter was reinforced at the corners with 2x4in. wooden blocks to provide additional strength at the joints and eliminate the drawbacks of screwing into end-grain. The inside dimensions of the crib measured 42 in square. This was to accommodate for the horizontal movement and swell of the test material from blasting.

This test was designed to be conducted with a minimal number of steps, and an emphasis on repeatability. As equipment became damaged with testing, it was replaced with minimal disruption to the testing schedule. The following section describes the method in which the tests were arranged and operated.

4.3. TEST OPERATION

The scaled model tests were executed in steps which aided in ensuring test consistency for each of the varying scenarios. This procedure began by inspecting the bumper blocks. Those that were heavily damaged were exchanged, and the three blocks were positioned on the test bench in their respective places. The specimen block was then

placed on the bench so that it was even with the bumper blocks on two sides. This placement was examined to make sure the drilling location on the test specimen was positioned above the small loading pocket at the bottom of the testing bench.

Once the specimen was positioned, the crib was set in place surrounding the specimen and bumpers, so there would be no movement of the test block following drilling. The specimen was drilled through its entirety from a marked location on the top of the specimen. The drilled hole was started by first collaring the hole using a pilot block. The pilot block was a machined block of aluminum with a perpendicular thru-hole to accommodate the drill bit and orient the starter bit true with the top surface of the test specimen. Once the starter bit had completed, the long bit was used to drill through the remainder of the block and underlying plywood. This created a straight through hole that could be loaded from below.

Following the drilling procedure, the test specimens were loaded with FireLine 8/40 HMX detonating cord from the underside of the bench with a specific loading height required for each specimen. A length of used blasting cap wire was folded to create a loop and then used to set the distance from the top of the desired powder column to the top of the test specimen. This distance was marked by wrapping electrical tape around the wire to not only hold the loop together, but delineate a stopping point for loading. The wire loop was then inserted into the top of the drilled hole in the test specimen and pushed through the hole to the underneath side of the block.

After loop installation, a measured length of doubled detonating cord was loaded into the block by threading the cord through the wire loop, and drawing the loop upward until the tape mark on the wire was even with the surface. At this point, the detonating

cord was at the proper height and prepared for priming. The upper portion of the hole was

stemmed slowly with Missouri River sand, same as used in the block construction, to

prevent obstructions and eliminate a change in confinement during the test. A drilled,

loaded, and stemmed test specimen can be seen in Figure 4.2.

Figure 4.2. Loaded and Stemmed Specimen, 5/5/16

After stemming, the specimen was covered with additional plywood and concrete

blocks to confine the particles generated from the blast. The detonating cord was cut from

the spool with additional length so that the ends extended below the test specimen and

into the loading pocket. A detonator was then connected to both extensions, leaving an

even length of detonating cord to the test specimen. At this point, the site was cleared, a

blasting line attached, and the explosives were initiated.

4.4. ANALYSIS OF BLASTED SPECIMENS

Once blasting concluded and the range was designated safe, results were recorded for each test. A general visual inspection was conducted, ensuring that test particles were contained, and if not, which piece of equipment failed for that test. If the equipment performed as expended, the top cover was removed and a top down perspective of the specimen was photographed with a speed-square for scale. This view displayed the major fracture patterns in the upper region of the specimen where caprock would be an issue. In the case of layered specimens, caprock fragments that could be identified as oversize were removed for weighing and measuring at a later time. The remaining substrate was then photographed to compare fractures and fragmentation from the top-down perspective. Crib removal allowed muckpile photographs to be taken using two 1 ¼ in steel ball bearings, placed in the muckpile, as objects of reference. The ball bearings provided two spherical reference points that can be used if the data is correlated with computer fragmentation analysis programs such as Split Desktop or Wipfrag. Once these photographs were taken, the remaining fragments were collected for sieving at a separate location. The bench was cleaned to ensure there was no contamination from previous tests and the procedure was repeated. Small adjustments were made to the testing procedure as testing progressed, and they are documented along with their respective series of results.

4.5. BUMPER BLOCK AND TEST SPECIMEN CONSTRUCTION

For this experiment, the bumper blocks and test specimens were constructed to be modular and more efficient for test setup. When compared to very large, solid blocks,

these specimens were easily moved around the test site, allowing for changing blast

conditions.

Concrete formwork was constructed on top of wooden pallets using ½ in plywood

and 2x4 in bracing. The blocks would remain in the formwork to cure, then moved to the

test site without risk of damaging the specimens. The forms were also designed to be

easily removed from the pallet, while leaving the blocks intact. This allowed the blocks to

be moved with a Bobcat and allow the lifting tongs to fit under the sides of the blocks for

repositioning. Using this modular design, four blocks could be poured per pallet, each

measuring 1.5-foot square and 1-foot in depth as shown in Figure 4.3.

Figure 4.3. Cast Test Specimens in Constructed Forms

Since bumper blocks were required to withstand the forces acting on the specimen

block, they were poured first, using an already designed standard high strength concrete

mix with a ¾-1 in aggregate. Once they were poured, rebar jacks were inserted into the

blocks, leaving a lifting loop extending from the top of the blocks. After the blocks cured, the loops were used in conjunction with the overhead crane to place these blocks in their final position for testing. Test specimens were poured using the same forms, but the process for mixing and pouring them differed completely.

Instead of material strengths equivalent to values observed in the field, the scale model tests required a material strength far lower than that of the real-world counterparts. Therefore, the test specimens were poured in a different manner from the bumper blocks. Due to the low volume of concrete mix needed, a bag mix was more cost effective than an order delivered by truck, narrowing the selection considerably. The next criterion was homogeneity of the concrete materials. Most bagged concrete mixes contained aggregate that, on a small scale, would represent a larger grain size bordering on a conglomerate rock type. Since this test was designed to mimic limestone and other small grained sedimentary rocks, the aggregate in the mix had to be similar in size to that of the cement in the mix. With this in mind, the options were further reduced to a small selection of readily available mortar mixes. Type S mortar was selected because the manufacturer rated the compressive strength of the mix at a minimum of 2400 psi. This compressive strength was significantly lower than that of the rock specimens tested and could be easily prepared. This bag mix was used as the base for the entirety of the testing series and the mix was modified to fit the needs of each test, as indicated in the next section.

4.6. SOLID TEST BLOCK I

Several blocks were poured for use as shake-down tests to determine the appropriate mortar mix that would yield the best results. Blocks were poured using the

type S bag mixture and 11-12lbs of water per bag to wet the mixture, making a workable but still highly saturated mix. For curing purposes, Glenium water displacer was added to the mix to help the blocks dry at faster a faster rate. The blocks were then leveled and smoothed with a trowel and left to firm up for 2 days. Once the blocks had solidified, they were transported to the MST Experimental Mine to finish curing. Cube samples of the mix were also poured and set aside to test the strength of the mix for a 28-day compressive strength. This series of blocks, with the added Glenium, reached a compressive strength of approximately 4000 psi, much higher than the strength advertised on the mix. These blocks were tested using the method described in section 5.3. They did not break in a manner that was useful for this project, which was in part due to strength and excessive burden and spacing of the shot.

4.7. SOLID TEST BLOCK II

Information from the first test indicated that the strength of the material was too great for the explosives used creating only four fractures in two planes of orientation; the desired outcome required a large amount of fragmentation that could be sieved. This mix of material had to be improved to continue, thus the next series of specimens were varied by strength. The Glenium water displacer was not used for any of the remaining tests, to ensure the strength of the mix relied only on the mortar mix. Eliminating the Glenium also reduced the cost of each test specimen.

Three different mix configurations were used in the next test series: 100% mortar (no additives), 75/25 mortar to Missouri River sand mix, and a 50/50 mortar to Missouri River sand mix. The compressive strength of the mixes was altered by replacing a portion

of mortar mix with Missouri River sand, while keeping the same required amount of water as if they were completely mortar. This provided material that could be readily mixed and worked in the forms.

Eliminating the Glenium water displacer increased the cure time of the blocks to require a full 28-day cure. Following this cure time, the new blocks were tested using the procedure described in Section 5.3. Unlike the previous tests, the burden and spacing for this block series was changed to 7x7 in from the outside corner of the test specimen. The results showed that the fragmentation generated by the explosives increased with each decrease in strength. The fragmentation within the immediate vicinity the blast hole, using the 50/50 mix, was visually similar to that expected on a full-scale blast. This mix was selected as the mix design used as the basis for the remainder of testing. The strength data for the various mortar mixes, as well as the initial rock core values, can be found in Appendix A.

With the mix selected, the burden and spacing variable needed to be adjusted, since the 7x7 in pattern continued to create overly large fragments at the perimeter of the test specimen. The next test series advanced the burden and spacing towards the outside corner of the specimen, along a 45-degree line. The configuration used 5x5 in, which fragmented that section of the block more thoroughly than the 7x7 in configuration, but still had some excessively large blocks of material remaining in the muck pile. The final configuration tested was 4x4 in from the corner. This adequately fragmented the material surrounding the blast hole, with fracturing to the edges of the block. This burden and spacing parameter was used for the remaining tests in this project.

4.8. CAPROCK SIMULATION TESTING

After finalizing the mortar mix and burden and spacing parameters, the majority of the remaining tests were to ascertain the behavior of caprock relative to the blast hole configuration. The solid 50/50 mix blocks were tested at this configuration for future comparisons to the capped tests. The fragmentation on these tests was easily sieved and covered a broad spectrum of sizes. Following solid block testing, layered blocks were poured to simulate caprock laden rock benches.

To simulate the bedding plane that separates a caprock layer from the underlying rock, different configurations were considered to comprise a representative cap layer. In nature, rock joints are classified into three categories; closed, infilled, and open. Closed rock joints are tightly pressed together with no material in between. An infilled joint has material like mud, shale, or some other media filling the slightly separated rock layers. An open joint is mostly void with the rock structures touching in only a few places if any. Out of these, only closed, tightly-cemented joints were considered. The reason for selecting this joint condition is that, based on the information provided in the literature, this condition would have the least impedance to blast energies. If caprock problems are present at a tight bedding plane, then further infill material would only exacerbate the issue. The next variable to address was determining whether the material could be weakly bonded with a cold joint poured in the mortar, or whether a fill medium such as putty or paper was required to prevent the layers from completely bonding together. A concrete test cylinder was poured with a layer of mortar, left for a day to become firm, and finished with another layer of mortar. This process was completed during the pouring of the previous series of solid blocks to save time. The cold joint in the cylinder was

examined after removal from the cylinder and found to be tight, but weak enough that it broke free when struck with a small, light mallet. This formation was determined to be adequate for use in the layered test specimens and no infill material was used.

For the remainder of this thesis, the scaled model tests will have a specific nomenclature when labeling each series of tests. Up to this point, all of the testing was performed on solid test specimens. These are referred to as the solid series tests. For the caprock tests, they are counted starting with Caprock Series 1, sometimes referred to just as Series 1. There were three caprock series tests performed, and they are numbered consecutively.

4.8.1. First Series of Layered Specimens. The first series of layered blocks were poured with the cold joint at varying heights; three blocks were poured with a 3 in layer on the top, three with a 2.25 in layer, and three with a 1.5 in layer. The cap layers were dyed to aid in the identification of fragments after blasting. (The type and amount of dying agent used was changed throughout the remaining testing, as the first dyes used were mostly ineffective.) The layered specimens were then tested against three varying powder column depths, which were changed respective to the thickness of the caprock layer. In individual blocks, powder column depths were set even with the seam, half the distance into the caprock layer, and that same distance below the seam.

4.8.2. Second Series of Layered Specimens. Once the first series of layered tests was complete the next set of test specimens, Caprock Series 2, were poured. These specimens were to see the influence of caprock strength on the fragmentation. Often with sedimentary rocks, the upper layers are exposed to weathering which results in the removal of weak layers down to a more solid and strong layer. This can often result in a

remaining top layer that is harder than the rock below, sometimes up to twice as strong. It can be difficult to drill and even more difficult to blast. This series of tests examined the change in fragmentation by varying the compressive strength of the top layers.

The lower sections of these test specimens used the 50/50 mix as established earlier. The mix on the upper layers was adjusted with cap layers consisting of the 75/25 mortar to sand mix, and the 100% mortar mix. These layers were set at 2.25 in thickness, but the powder column was tested at differing heights as in the previous series.

4.8.3. Third Series of Layered Specimens. Caprock Series 2 and 3 specimens were constructed simultaneously. The third series specimens were formed to examine the effect of two layers of cap rock instead of a single massive layer. The lower portions of the specimens were poured using the 50/50 mortar to sand mix to a height of 9 in. The middle layer was poured using the 75/25 mortar to sand mix for a layer height of 1.5 in. The blocks were capped off by a top layer of 100% mortar mix, giving the top layer a height of 1.5 in as well as shown in Figure 4.4. These blocks were tested with powder column heights at 3 in, 2.25 in, and 1.5 in. Based on the ineffectiveness shown in the first series of artificial caprock tests, tests loaded below the lower cap layer were deemed unnecessary.

4.8.4. Multiple-Hole Tests. For the final series of tests, extra specimen blocks poured from previous series were blasted using two loaded holes instead of the single-hole setup previously used. This series was designed to determine if there were significant changes in fragmentation and breakage of caprock, from multiple blast holes, as opposed to single-hole scenarios. The tests were performed in the same manner as described in Section 4.3 with only two differences which are described as follows.

Figure 4.4. Two-Layer Cap Test Specimen

4.8.4.1. Drilling and loading multiple-hole blocks. The blocks were drilled at

the 4x4 in location as determined in Section 4.7, with the second hole located at 4x8 in,

or one more hole spacing. To properly blast two holes, they both needed to be adequately

timed to be representative of the sequential timing employed in mines and quarries. The

first hole, nearest the corner of the test specimen, could be initiated in the same manner as

in previous tests. However, the second hole needed special consideration to ensure that it

was initiated with an appropriate delay.

4.8.4.2. Timing additional scaled holes. The first element addressed in firing the

second hole was the amount of time required to initiate the second hole at the correct

time. The scale of the test specimen was such that 1'=16' on a full-sized bench. On a full-

scale limestone bench, the use of nonelectric detonators is one of the preferred initiation

methods for cost savings and ease of use. Commonly used delays for nonelectric

detonators are either 17ms or 25ms between hole initiations. At a 1/16th scale, this meant

that an approximately 1.06-1.56 ms delay is needed between two holes at this smaller scale. Once this required delay range was established, the difficulty arose of how to properly initiate this second hole with a miniscule amount of time elapsed from the initiation of the first hole.

There were no commercially available blasting caps with this delay built into them, so an external timing method was required. This left a couple options; the first option used a delay box for electric caps and fire zero delay blasting caps at 2 ms apart, or the second option, use additional detonating cord as a delay. The electric cap delay box method would have been adequate, but zero delay blasting caps did not have the required fidelity to initiate both caps in the proper order after they had been energized from the delay box. This lack of dependability left the detonating cord delay method as the most reliable method for blasting this test series.

A detonating cord delay is made by measuring a required additional amount of detonating cord and using it as a passfire between charges. Air blast was a concern at the test site, as the additional length of detonating cord was exposed during blasting. For this reason, the delay of 1.06ms was selected as the required delay. For this application, the manufacturer's data sheet for FireLine 8/40 was consulted for the detonating velocity the detonating cord. This speed, 22304 ft/s, was then multiplied by the required delay of 1.06ms to obtain the appropriate length of detonating cord required for the delay of 23ft 7 3/4in. This calculated delay length was added to the amount of detonating cord already required for blasting a single hole, for a total length of 26ft 7 3/4in. This total calculated length was the length required for both loading and timing the second hole.

The second hole was loaded first, as it was furthest to the back of the loading pocket underneath the test bench. It was loaded similar to the single hole setup, but instead of the center location used on the 3-foot sections of detonating cord, the fold in the detonating cord for the wire loop was marked 1.5 foot from the end of the long section. This section was guided through the loop and pulled to the appropriate powder column height, as described in Section 5.3. Once the appropriate height was achieved, a section of board was inserted into the loading pocket acting as a divider between the two blast holes, preventing the detonating cord from short circuiting and eliminating the required delay (by sympathetic detonation). The extra length of detonating cord was then partially looped around a section of rubber tractor tread to eliminate small loops, kinks, and cross-overs that could introduce a cutoff or improper timing. The end of this length was routed back to the loading pocket to be tied in with the first hole to be initiated. The first hole was loaded in the usual manner.

A bunch-block was used to connect the blasting cap to both sections of detonating cord leading to each separate hole. Bunch blocks are used to bind multiple strands of detonating cord or nonelectric shot line to a detonator. The ends of both lengths of detonating cord were seated in the bunch block within 6 in of their matched respective ends. This eliminated the need to measure a specific location on each end to match to the detonator, as the timing would stay consistent regardless of position near the end of the detonating cord. These blocks were covered and initiated using the single detonator in the same manner as described in Section 4.3.

4.8.4.3. Improved crib construction. The second element that required adjustment was the manner in which the crib was constructed. Immediately following the

firing of the first two-hole test, the crib was decimated from the additional force of the extra explosives, requiring a more robust solution. A new crib was fashioned out of 2x12 in boards with the same inner dimensions as the previous crib, but a much more resilient construction. Instead of a single layer of 2x12 in boards, three layers were used to construct each of the four sides. With the addition of each layer, a steel corner bracket was screwed to the boards, reinforcing the corners. The screws used to fasten the corner brackets to the boards were long enough to penetrate the board layer behind them as well, binding two layers together at a corner instead of a single layer and a bracket. Doing this for the three layers eliminated most of the flex that was present with the first crib design. Long screws were also used to fasten the boards to each other through their faces at each quarter of their length. This prevented the boards from sliding against each other and flexing independently, reducing the amount of force transferred to a single steel corner bracket that would be susceptible to bending. The finished construction was a more resilient crib shown in Figure 4.5.

This crib survived all of the subsequent two-hole tests with no visible damage to the crib. After test results were collected, the two-hole test was determined as the upper limit of what the test bench could accommodate. The additional detonating cord destroyed the plywood at the bottom of the bench significantly faster than the single hole tests and the plywood had to be replaced multiple times to obtain an intact corner for the test specimens to rest on.

Figure 4.5. Reinforced Crib Construction

4.9. DATA COLLECTION

Following blasting, specimens were measured and collected for sieve analysis. Care was taken when uncovering and collecting the specimens, limiting further agitation of the fragments to prevent unintended breakage of the larger fragments.

4.9.1. Sieving Broken Specimens. After completion of blasting for each series of tests and insitu photography, samples were transported off-site for measurement of fragmentation. The specimens were taken to the Civil Engineering Lab in Butler Carlton hall on the Missouri University of Science and Technology campus for sieving and weighing. Machines in this lab were large enough to accommodate most test specimens without the need to split the broken material and recombine results. Only the two-hole tests produced enough broken material to warrant a division of material. The division on

these tests was necessary to prevent a sieve from becoming full and blinding, which was not an issue for the single hole samples.

The samples were sieved using 12 different increments. The lower range consisted of the pan, #30, #16, #8, #4, ½ in, and 1 in sizes. These were to provide an exponential distribution of the material when analyzed. The upper size region was given more scrutiny because the behavior of oversize fragments was the subject of this thesis and each large fragment represented a larger percentage of the overall fragmentation than the mean size or fines region. These sizes consisted of 1 ¼ in, 1 ½ in, 2 in, 3 in, and 4 in sieves. Fragments in the upper size range were sorted by hand through larger screens because the larger fragments were more friable and susceptible to breakage from shaker agitation. The two smallest increments, the pan and #30 sieve, were collected separately but should be considered combined because the sand that constituted the 50/50 mortar to sand mixture could not pass the #30 sieve. The cement mixture, however, was able to fall through to the pan. Many of the caprock pieces were at the 4 in limit (representing 5ft 4in at a full scale), or could slip sideways to the 3in limit (representing 4ft at a full scale), but most remained near the top of these sieve sizes. The samples were weighted at each of these sieve sizes, the results recombined when split, and that data was entered into an Excel spreadsheet for analysis.

4.9.2. Picture Analysis. Photographs were taken during the field analysis portion of the experiment to assess the fracture patterns in the caprock layers and determine the mechanisms present during the blast causing specific patterns that were observed in the field.

Primary fractures were the first items identified in the photo. They extended in rays radiating away from the blast hole. In most of the tests, counterpart fractures extended in opposite directions from the hole. For the purpose of this project, these fractures were counted as individual fractures instead of pairing them together. The rational was that some fractures extended until they terminated into the faces of the block. These were often short fractures leading directly from the hole to the face. Opposite these were long fractures that extended out, sometimes terminating into the side of the block, but also ending within the material. These fractures lead in opposite directions, but were of differing lengths and the mechanics causing their creation was not necessarily the same. This is described in Section 6.2.1. While the short fractures were likely the result of compressive stresses, there is a possibility that a large portion of the rearward fractures developed due to the reflection of tensile stress waves from the faces.

Following the identification of the primary fractures, secondary features were identified, when present. Craters were measured for their depth, beginning at the surface of the specimens to the start of the intact blast hole collar. The craters were measured for their breadth from the center of the blast hole to the radial fracture. The craters were assumed to have a conical shape for estimation purposes. The calculated crater volume was compared to scaled depth of burial calculations to determine any correlation between the rise of the powder column height into the caprock layer and crater size. This information was used to compare any significant decrease in the volume of oversize caprock material relative to the extra use of explosives.

The results of the caprock testing are described in Section 5. This section describes the general behavior and characteristics of the small-scale caprock

fragmentation tests, primarily focused on the observations at the test site, with an emphasis on the types of occurring caprock fractures. Further analysis is discussed in Section 6.

5. RESULTS

Data collected from each small-scale test consisted of photographs and measurements taken at the blast site, and size data obtained from sieving the blasted fragments. As stated in the previous section, the results from each series of tests determined the criteria for the subsequent series. Tables containing test configurations and sieve data can be found in Appendix A. Photographs not shown in this section can be found in the Appendix B. In the photographs found in this section, and the following sections, the captioned test number refers to the test number listed in the first column of Table 1 in Appendix A. This thesis refers to the tests by the captioned number, and not the number written on the blocks.

5.1. SOLID BLOCK RESULTS

Solid block tests were used to determine the appropriate burden and spacing, as well as the appropriate mortar mixture for the small-scale caprock tests. A successful test setup produced results with a respective amount of fragmentation without excessive chunks or fines. Indicators for test adjustment were the amount of pulverized material around the blast hole and distribution of the breakage. A blast was expected to have more finely pulverized material adjacent to the blast, leading to larger fragments toward the perimeter of the blocks. In addition, the blast was expected to produce a clean, mostly straight face in the remaining section of the block.

The first test was conducted on a test block comprising of 100% mortar and Glenium mix with the blast hole centered in the block. This burden and spacing was

based on initial powder factor calculations and the assumption that the overall test bench

geometry would cause this block to fracture diagonally and throw fragments to the

overall corner of the bench. This was not the case, as this blast configuration caused the

test specimen to break into four equal quarters.

This orthogonal splitting indicated that the burden and spacing should be adjusted

for the blast to break towards the outside corner, as would occur during a standard bench

blast. Almost absolute minimal fragmentation was present in the test specimen, making

particle sizing easy to measure at four approximately 90lb fragments. Both orthogonal

fractures were clean breaks with no pulverized material surrounding the blast hole. Low

amounts of fragmentation would have been indicative of excessive burden and spacing,

but the complete lack of fragmentation indicated that the material strength of the test

specimen was too strong for this type of application.

The solid specimens that followed were poured with a mortar mix of 75%

mortar/25% sand and a 50%/50% mortar to sand mix. The specimens were blasted using

the same blast hole design, but with the burden and spacing reduced equally toward the

outside corner. The 50%/50% mortar mix was found to provide the best degree of

fragmentation, with the burden and spacing of 4 in from the outside faces of the block

providing the most breakage.

At the determined optimal mix and spacing, the test specimens displayed

fragmentation that could easily be analyzed, and breakage modes assessed. Figure 5.1

shows the extent of this breakage.

The blasts cleaved a mostly straight face with only the outside corner of material

fragmented. The material immediately surrounding the blast hole was reduced to the

smallest constituent particles, with fragments increasing in size with respect to horizontal distance from the blast hole. The majority of larger fragments were produced by diverging radial fractures originating from the blast hole. From the top of the powder column to the surface of the block, the breakage pattern became a cratering scenario. Some fractures radiating from the hole arced toward the top surface of the block, leaving a crater similar to those discussed in Livingston's work. Figure 5.2 shows the top of one of the 5"x5" burden solid block tests, post-blast, without any fragments removed. The approximate radius of the crater at the surface is outlined in black.

Figure 5.1. Solid Block Test Breakage at 4" x 4" Spacing, Test 5 8/17/16

Separation at the crater radius reveals cleavage of some larger fragments that were initially the result of the radial fracturing process. In Figure 5.2, the displayed crater

outline is limited to a half crater, facing the outside corner of the test bench. The half-crater result was present in most of the later tests where cratering occurred. Full-circle craters were only present with tests from later series where depths of burial were small.

Figure 5.2. Surface Radius of Crater in Solid Block, Test 1 6/7/16

The distribution of fragments at the surface can easily be counted. Approximately 15 distinct fragments that once comprised the surface of the block can be identified in Figure 5.2. Most of the fractures observed in this fashion were radial, originating at the blast hole and orienting toward a free face, with the exception of the long fracture seen

extending diagonally back from the blast hole. Coarser reduced fragmentation in upper portion of the block is to be expected due to the absence of explosives in the stemmed portion of the blast hole.

Material toward the top of the block was less fragmented and more organized than the material underneath. The presence of cratering in these solid blocks indicated a transitional region in massive formation blasting where explosive energy converts to a horizontal release to a vertical cone near the top surface. This presence corresponded with the theory that the upper portions of the blast should be considered separate from the lower portion of the blast, but not displaying a distinct delineation between the two regions. The main blast feature present was the surface crater that extended down to the top of the powder column. No other significant features were present in the solid block tests.

Thorough fragmentation of the block in front of the blast hole was present at every level. The remaining block that represented the in-situ, post-blast bench maintained a fairly uniform face once the fragments were removed. The profile of the face and spent blast hole is shown in Figure 5.3, with the breakage of the face at a 45-degree angle from the rest of the block. The newly formed face was broken cleanly, with visible damage to the bench limited to the large fracture extending toward the back of the block.

The remainder of the solid block tests produced similar results; the photographs of each test not presented in this section are shown in Appendix B. After completing visual observations, the fragments of each test were sieved to obtain the breakage profile of each test so they could be compared to their caprock counterparts.

Figure 5.3. Clean-blasted Block Face, Test 1 6/7/16

5.2. CAPROCK SERIES 1 RESULTS

The first series of caprock tests was the largest series in this project. This series was configured to test both the influence of the height of the caprock layer on cap breakage, as well as the influence of the powder column height on cap breakage. The construction of these caprock blocks is explained previously in Section 4. Three caprock heights and three powder configurations were tested respectively. The thicknesses of the caprock sections tested were 3 in, 2.25 in, and 1.5 in. The powder column heights tested were halfway into the caprock, at the caprock seam, and then 1.5 times the caprock thickness. In this series, both layers of the blocks used the same 50%/50% mortar mix design.

For most of this test series, the breakage at the surface of the blocks was significantly less than that of the solid block tests. Figure 5.4 shows the surface breakage of a caprock layer of similar material when explosives are loaded to the bedding plane, and the caprock layer stemmed. The amount of radial fracturing present in this

photograph is significantly less than that shown in Figure 5.1, or any of the other solid

block tests with approximately half of the same radial fractures present in the cap layer.

In Figure 5.4, four radial fractures can be counted, two perpendicular with the outside

faces, one angled 45 degrees to the free face, and the long fracture extending toward the

back of the block. In other tests of this series, there were typically two 45-degree

fractures extending radially from the hole. Two other features can be seen in this

photograph. An arcing, annular fracture can be seen in the square fragment of cap in the

lower left corner of the picture. This arc is broken at a distance from the blast hole

approximately the same as the caprock thickness. Another annular fracture lays

perpendicular to the blast hole at a distance of 5-6" back from the blast hole. This fracture

is present in a number of other tests as well, although the extent of this fracturing varied.

This mode of fracturing is discussed further in Section 6.

Figure 5.4. Surface Breakage of Caprock Layer, Test 7 8/18/16

The breakage of this cap varied greatly from the surface breakage of the solid block tests, but the material that comprised the substrate layer fragmented in the same fashion as its solid counterpart. Substrate breakage can be seen in Figure 5.5 as well as with the other tests in the appendices. The substrate layer broke consistently with each test, with crushing and fragmentation closest to the blast, and larger fragments toward the outer edge of the block. The lower portions fractured to a clean face similar to that seen with the solid block tests.

Figure 5.5. Breakage of Substrate, Test 7 8/18/16

Caprock layer fragments had a maximum thickness equal to the thickness of the original caprock, while the particles frequently broke away from the fragments of the lower layer at the artificial bedding plane. Breakage along this plane proved to be a distinct separation point that terminated the vertical breakage of both the cap and substrate layer. Three regions of breakage could be observed from these tests. The first region is the substrate layer that comprised the majority of the block and was in direct contact with the explosives. The second region of the blast was the blast crater, where cratering was present. The third region of breakage was the portion of the cap layer that was not part of the crater. There were additional fractures that extended into the block as seen in the solid block tests. The long fractures extended towards the back sides of the block in both the cap and lower layers. While these cracks followed a similar direction in both layers, they did not necessarily follow the same path.

Post-blast conditions of the caprock test blocks were similar to that of the solid block tests with a 45-degree clean-blasted free face. The only variances were areas where the fractures of the top layer and substrate diverged along the general 45-degree direction. In some instances, this left an overhang, and in others a section was removed from what would be a relatively smooth vertical face.

The first series of caprock tests showed the influence of cap thickness versus loading height in similar, cemented layers. Breakage was varied across the spread of tests, with general trends consisting of minimal caprock breakage for thicker layers and lower powder column heights, and thinner layered, high powder column test obtaining the most breakage, as listed in Table 6 in Appendix B. This information enabled the implementation of the Series 2 tests.

5.3. CAPROCK SERIES 2 RESULTS

The second series of small scale caprock tests assessed the influence of additional material strength on the same representative cap layer as in the previous tests. Series 2 caps were poured using two different mortar mixes. As with previous mixtures from the solid block tests, a 75% mortar/25% sand mix and a 100% mortar mix were used to comprise the artificial caprock layer. The purpose of this series was to demonstrate the results of blasting a weak substrate layer beneath a competent, or exceedingly strong cap. For the two-layer blocks in this series, the bedding plane remained at a depth of 2.25 in, which provided the most meaningful results in the previous series. Along with the single cap layer hardness tests, a second configuration was poured to simulate layers of increasing hardness. For this, the substrate layer was limited to 9 in height, with two additional cap layers poured at 1.5 in height each. The bottom layer remained the 50% mortar/50% sand mix, while the central layer was comprised of 75% mortar/25% sand mix, and the top with 100% mortar mix. The purpose for the top two layers occupying the top 3 in of the block, rather than the 2.25 inches used for the first part of this series, was due to the difficulty of working with the thin layers of mortar and maintaining the desired consistency and integrity of the test specimen. The middle layer was dyed in these multi-layer specimens to aid in the distinguishing and sorting of fragments. The configuration of the three-layer blocks can be seen in Figure 5.6.

The breakage of the harder, upper layers in both the single-layer cap and two-layer cap specimens in this series was blocky, with minimal or no cratering present. Individual caprock fragments and fractures were easily counted and characteristic features were readily identified. There were very few fine caprock fragments remaining

near the blast hole, and most caprock fragments were generated from radial fracturing. Some of the fractures that were present in the similar strength caprock tests were no longer present, or were less pronounced. The breakage of the softer, lower strata was characteristic with the remaining breakage from the previous series.

Figure 5.6. 3-Layer Test Block Post-Blast, Test 21 11/15/16

The principle aspects of this blasting method were tested by changing powder column height in varying strata thicknesses, hardness, and layer counts. This led to the final aspect that was tested; a sequential blast of a characteristic blast hole configuration within varying test blocks.

5.4. SCALED SEQUENTIAL HOLE RESULTS

The third series of small-scale caprock blasting tests determined the influence of two sequential blast holes on the breakage of artificial caprock. Until now, all of the testing had examined how the breakage of caprock performed with a single blast hole. From the results of previous series, the fracturing of material on top of the remaining bench extended beyond the point where a subsequent hole in the blast would have been located. Caprock Series 3 tests employed a second blast hole shot in sequence with the first to ascertain if the pre-conditioning of the remainder of the bench was a product of the test design, or remained present with additional blasting. Two holes were drilled in each test block at the 4"x4" spacing, then timed and loaded with detonating cord.

The blasting results from this series revealed more of the same characteristics that were present for the outer hole in the previous series. However, the addition of the second hole altered some of the remaining features that were present as a result of the first hole. The larger fragments that appeared at the edges of the block in the soft substrate layer were broken more than in the single blasthole tests. Also, the material that would have comprised one side of the 45-degree face was fractured and the face extending between the two holes was more parallel with the original face of the block. The long fractures in the cap that extended back into the block from the first blast hole were more open and exacerbated as shown in Figure 5.7. The corresponding substrate photo is shown in Figure 5.8 as well. In addition, comparing the two photographs shows that the annular fracture can be considered as an exclusive feature of the cap layer.

This series completed the collection of data from the field. The results of Series 3 were sieved in a similar fashion to the previous series. The results of all collected sieve

data are discussed in the next section along with an analysis of the characteristics that

appear in the cap breakage throughout the caprock tests.

Figure 5.7. Caprock Breakage 2-Hole, Test 30 11/22/16

Figure 5.8. Substrate Block Fractures 2-Hole, Test 30 11/22/16

6. ANALYSIS

There are many different inferences that can be deduced regarding the data collected for the scale model tests. The purpose of these was to determine if the mechanics produced adverse breakage that could not necessarily be observed in the field due to soil, mud, water, or some other environmental aspect that would obscure these features. Direct comparisons to the behavior of an in-situ rock mass are difficult due to lack of control over the same aspects within a full-scale rock bench, which makes physical model testing very useful. The analysis conducted on the test blocks, and the observed behavior trends are used to infer aspects of the behavior of a full-scale bench. This analysis is primarily divided into two parts; the first part covers the fragmentation of the test specimens as measured by sieve analysis, and the second part focuses on the photographic analysis of the blocks.

6.1. FRAGMENATION OF TEST BLOCKS

The first test aspect examined the fragmentation of the substrate layers of the caprock tests. All of the substrate layer fragments, as well as the solid block fragments, were classified using a set of rotary sieves. The larger fragments, above 1 in, had cracks and fractures permeating throughout. This fracturing caused the fragments to be friable with additional breakage probable as described in Section 2.6.3. Due to the fragile nature of the larger fragments, fragments above 1" were sorted separately by hand using a stationary set of sieves. The substrate layer was classified separately from the cap

material and examined per individual factors to approximate the effects of the varying

cap and loading configurations on the fragmentation of the lower bench.

The cap material was sorted in the same manner as the larger fragments of

substrate. As shown in the previous section, the fragmentation of the cap layers was

coarse compared with the underlying material, often breaking into only a few fragments.

The larger cap fragments often had distinct shapes, as radial fracturing was the primary

mode of breakage.

6.1.1. Plotting Test Fragmentation. For this thesis, the sieve data obtained from

the test specimens was plotted on a series of line graphs. The y axis of these line graphs

shows the cumulative percentage of the test specimens retained per sieve size, beginning

with the smallest sieve.

The percentages for the pan material were excluded from the plots as they should

be considered together with the #30 sieve. The pan weights and percentages are listed in

the tables in Appendix A. The individual grains of sand in the mortar mix were retained

on the #30 sieve, so as one of the smallest possible elements of the mortar, this was

determined as the lowest size considered for this study. The sand did cause the blocks to

break along grain boundaries, but it did effectively reduce the block strength uniformly.

The plotted fragmentation ranged across the entire combined size range, including

both the smaller, machine sieved particles, and the larger hand-screened fragments. Due

to the large discrepancy in scale between the largest and the smallest screen sizes, the x-

axis of the fragmentation plots is logarithmic. This allows the plot to represent each

screen interval accurately, without requiring an overly large plot area. Each series

represented in the plots is depicted by a separate color. Where two different aspects of the

same series are represented, such as in Figure 6.3 and 6.4 in Section 6.1.2, the series are still divided by color, and then subdivided by line type.

In addition to displaying cumulative percentages, these plots are also able to show how the rapidly the large counts of the larger fragments affect the graphs. Regions of the graph where the plotted series remain relatively flat represent screen sizes that retained small amounts of the test specimen. Conversely, graph regions that have sharply rising plots represent a large portion of the test specimen retained on the respective screen. The following subsections describe the behavior of the plotted fragmentation from the graphed data and how it compares to common fragmentation prediction models.

6.1.2. Fragmentation Profiles of the Caprock Model Lower Layers. The fragmentation profiles of the lower layers of the scaled-model tests were all relatively consistent in fragmentation regardless of configuration. A majority of the fragmentation profiles trended in an almost straight-line progression across the examined sieve sizes, with slight variations. This subsection examines the fragmentation of the substrate layers of the small-scale caprock test blocks, the overall fragmentation of the small-scale caprock test blocks, and the comparison between the two. In addition, the results from the sequential-hole tests are discussed.

General results showed a slightly coarser breakage through the mid-sized fragments on the solid blocks than the substrate of the capped blocks, as shown in Figure 6.1. This coarse shift in fragmentation can be attributed to the inclusion of large fragments from the stemmed region of the blast. Figure 6.1 shows that the breakage profiles of material in the lower layers of the capped specimens have consistent trends and typically produced smaller mean fragment sizes than that of their solid counterparts.

In the larger size region of the graph, each series takes a large jump in cumulative percentage around the 1.25-1.5in. range. For the displayed caprock series, the slopes of these series increase moderately in this range. However, the solid series has the shallowest rise across the lower and middle size ranges, and then produces the steepest ascension in the 1-2in. range. This difference in breakage shows that instead of a steady rise in breakage, the middle range of sizes is almost absent. Blast energies in the solid blocks were dispersed, providing a more thorough breakage of the upper block instead. In addition, Figure 6.1 displays that the substrate fragmentation profiles of each average series do not significantly change depending on the cap scenario. In the majority of these scenarios, the capped blocks were loaded so that all, or nearly all, of the substrate blasthole lengths were in contact with the explosives.
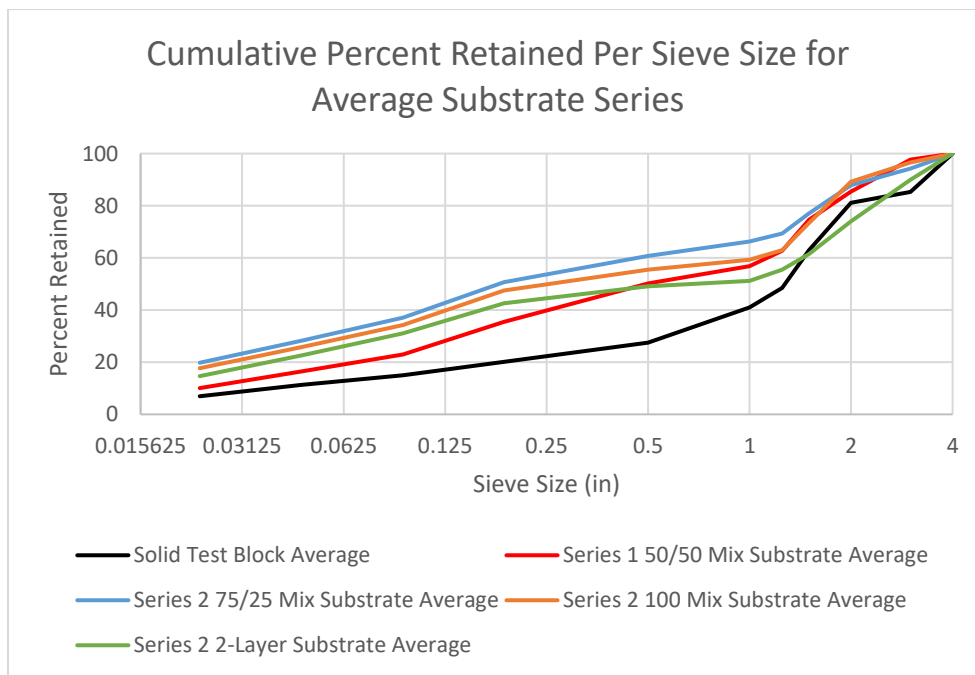
Figure 6.1. Average Substrate Fragmentation Cumulative Percent Retained

In the above figure, the average trends of substrate fragmentation for each significant set of tests are compared. They are divided by cap layer mix to show the influence of the cap layer on the breakage of the substrate. With the exception of the 2-layer cap tests, the substrate broke consistently, and were indistinguishable in fragmentation at sieve sizes above 1.5in.

While the lower layers of the caprock test blocks generated fragments finer than those from the solid blocks, the combined fragmentation profiles of the capped test blocks indicated a much different result. With the broken cap data added to the substrate data, the complete fragmentation profiles for each test block are shown in Figure 6.2. With the fragmentation of the whole test specimen compared to the solid block breakage, it is difficult to distinguish any significant difference in the coarseness of breakage. Contrary to anticipated results, the data shown in Figure 6.2 illustrates that while there were cap fragments caught on the 4in. screens, the profiles do not indicate a large deviation in fragmentation from that of the solid block tests. The intermingling of the different plotted curves between the 1-2in. screen sizes of both the solid and capped block series make breakage in the large size region of the graph indistinguishable from one to the next. A potential cause of this is the lack of lamination of the lower layers of the test specimens that would be present in limestone formations such as the Bethany Falls or Winterset. This caused the large vertical fragments at the extents of the 45-degree fractures to remain intact. If a lack of laminations is the explanation for the large vertical fragments at the extents, it follows that even though the explosive column detonates from end to end, the forces imparted to the rock are primarily exerted radially from the column with little to no noticeable vertical component. Another potential reason for these large

vertical fragments is the nature of the single-hole test design. The large vertical fragments could be eliminated either by dividing the substrate into more layers, or using additional blastholes to increase the amount of breakage.
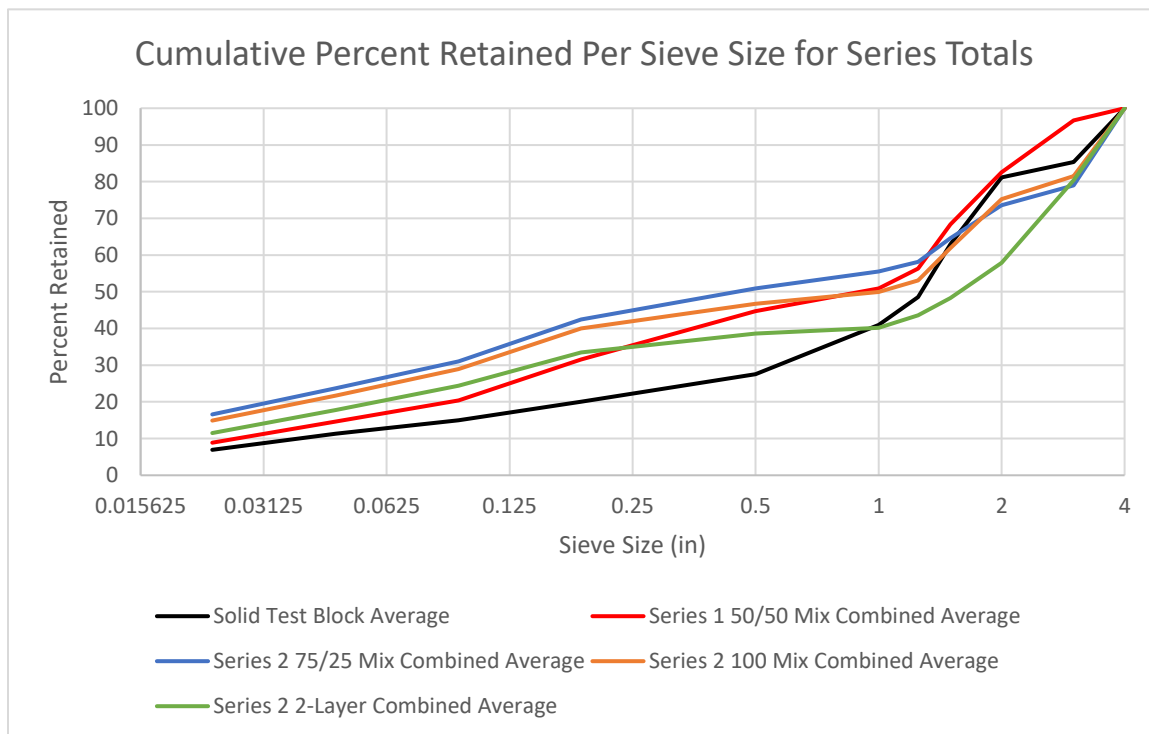
Figure 6.2. Complete Sample Fragmentation Per Series

A primary observation about the total fragmentation profiles is that there is a distinct change in the breakage profile of the test specimens when the material above the powder column is excluded from material sizing. This is most easily shown in Figure 6.3. Figure 6.3 shows the difference between the complete sample averages, and their respective lower layer averages. Due to the greater influence of individual fractures on

the reduction of large particle sizes, the broken cap material shifts the fragmentation curve to the coarse side, and makes the curves less uniform. The most notable change in fragmentation in Figure 6.3 can be seen at the 1in. screen size. At this size, each cap series has a discrepancy in cumulative fragmentation ranging from approximately 7-15 percent reduction in breakage. This coarse breakage is made up in the 2-4in. size range, indicating that the mid-range fragments (0.25-1in.) are not as influential as their larger counterparts.
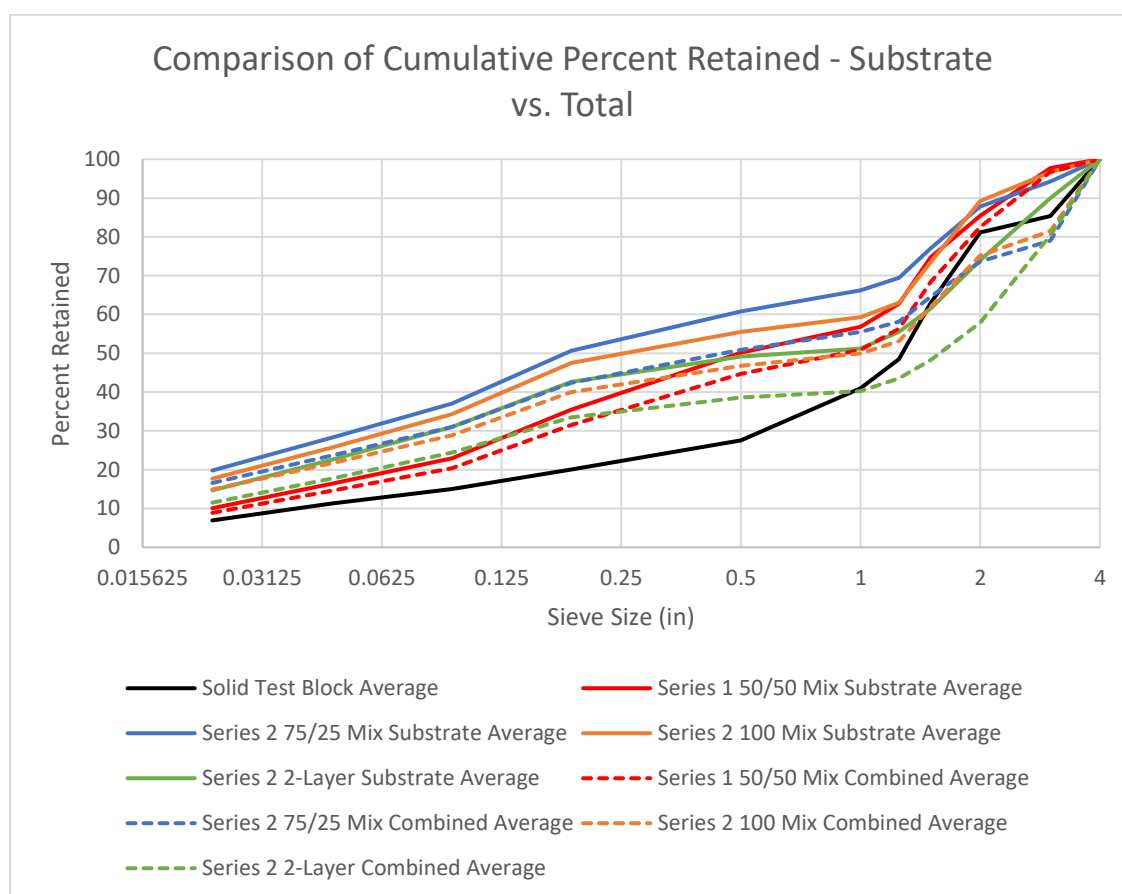
Figure 6.3. Comparison of Single Hole Cap Fragmentation Profiles with Substrate Profiles (Solid Lines) and Combined Cap and Substrate Profiles (Dashed Lines)

The solid colored lines in Figure 6.3 represent the substrate fragmentation of the respective test series similar to the previous charts. The dashed lines represent the combined fragmentation profile of both the substrate and cap for their respective series. The gap between the solid and dashed lines of the same color represents the change in fragmentation that the caprock breakage produced. In each case, the fragmentation of the fines to mid-range fragments, in both the substrate and overall, were more prevalent than in the solid block tests. However, from about the 1/2in. to 1in. range, the caprock test curves flatten out. The lack of slope in this region indicates that there were little to no additional fragments in this size range. Following this section, the curves steepen and arc until they reach the 100% mark. The curves in this upper section all tend to coalesce, as is the nature of this type of analysis. The distinguishing feature of the upper portion of the plotted fragmentation, above 1.5in, is that the substrates trended to have smaller breakage than the solid block series, but the majority of combined series had coarser breakage above this size range. The practical explanation for this is that the caprock tests had more fines and larger oversize fragments compared to the solid tests, but in the mid-range of approximately 1/4in. to 1in. was nearly absent. This indicates that the caprock layer has a significant influence on not only the overall breakage profile, but the breakage of the substrate as well.

The results of the two-hole sequential tests show similar results in Figure 6.4, with the lower substrate having a finer fragmentation profile compared to the total counterparts. This confirms the hypothesis that the upper part of the blast should be considered separately from the lower portion. It should be noted that the breakage of the lower layers in the two-hole tests was not as course as the single hole counterparts. This

can be attributed to a lack of large corner fragments that were seen along the 45-degree

break in lower layers of the single hole tests. Similar to the results in Figure 6.3, the

overall breakage profiles of the sequential hole blasts still shift to the coarse side

confirming, that the cap material does influence the overall fragmentation profile.
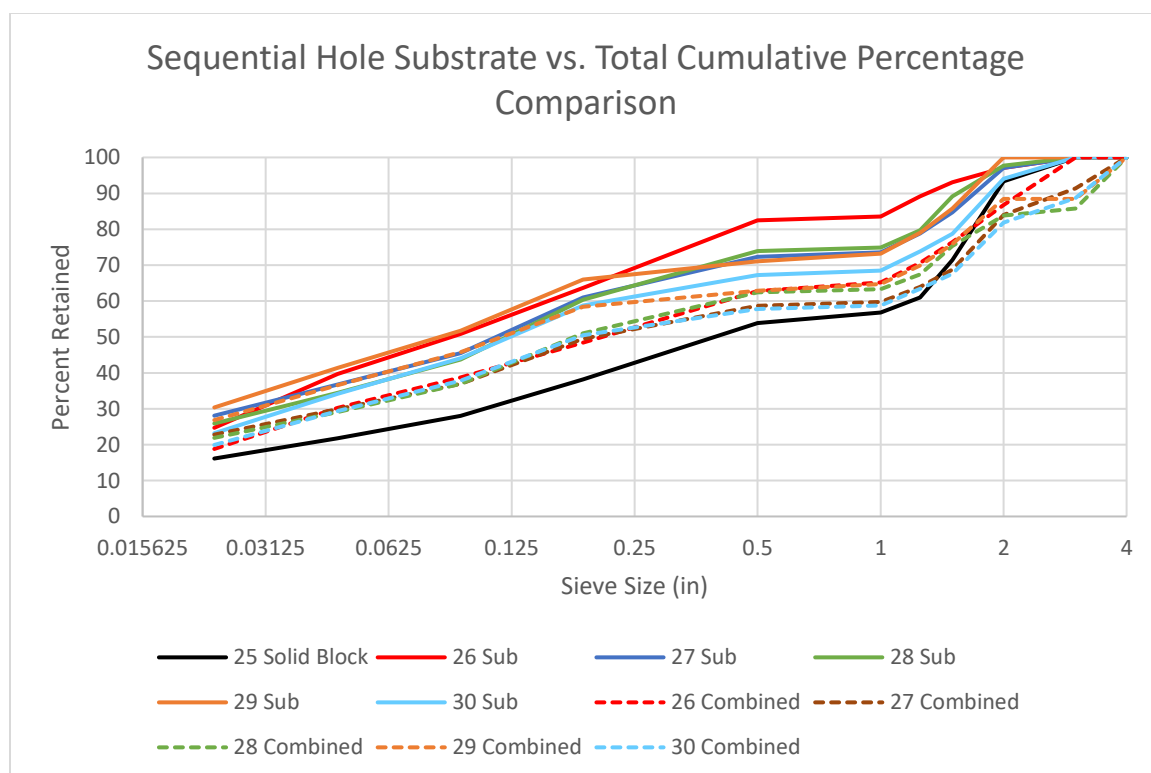
Figure 6.4. 2-Hole Fragmentation Total vs. Substrate with Test Substrate Profiles (Solid)
and Combined Cap and Substrate Profiles (Dashed)

Figure 6.4 is in similar form to the substrate and combined comparison performed

in Figure 6.3. Figure 6.4 compares the substrate and combined fragmentation of the 2-

hole tests, and displays similar results. Like in Figure 6.3, there is a larger number of

fines generated in the 2-hole caprock tests compared to the 2-hole solid test, with an inflection around the 1.5in. size, where there is a larger presence of oversize compared to the solid test. This validates the results of the single hole tests, because similar behavior was displayed in both cases.

The last general fragmentation comparison needed is the comparison of the single-hole series fragmentation with the sequential-hole series fragmentation to see how the addition of the second hole affected the breakage of the test blocks. Figure 6.5 is in similar form to Figure 6.4 in that it shows the breakage profiles of the sequential-hole tests relative to their single-hole series counterparts.
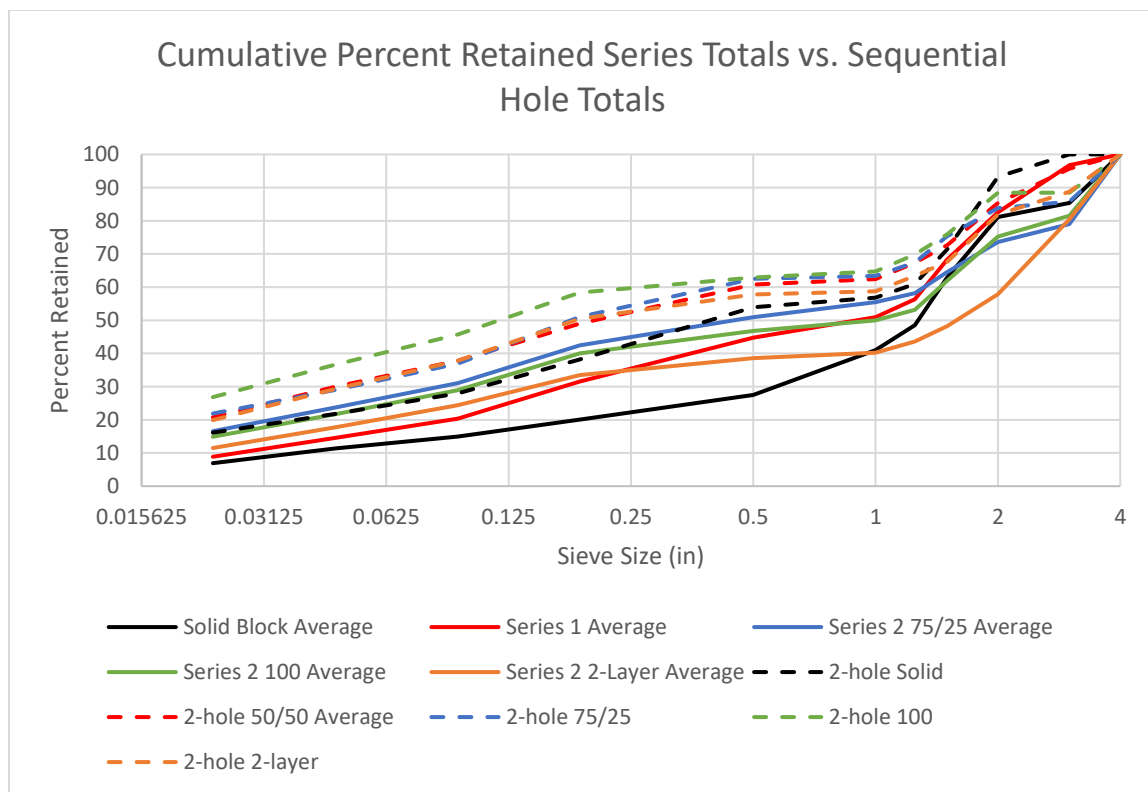
Figure 6.5. Single-hole Vs. Sequential-hole Fragmentation Illustrating Finer Fragmentation of 2-hole Tests Compared to Single-hole Tests

Figure 6.5 compares the solid block test average, as well as the single-hole averages, and the sequential hole tests plotted side by side. The single-hole tests are denoted by the solid colored lines. The sequential hole tests are represented by the dashed lines, and are colored respective of their single-hole counterparts. The general trend of the sequential-hole test breakage profiles is similar in shape to the single-hole tests. However, the sequential hole tests indicate that the additional hole produces a significantly smaller breakage profile compared to the single-hole tests, as indicated by the larger percentage of fines and mid-range fragments. This is most likely a result of the explosives in the second blasthole acting upon a normal amount of rock, nearly equal to the burden and spacing, as opposed to the initial hole which is removing rock at twice its designed volume.

With the general breakage of the small-scale caprock tests described, the results need to be compared to existing models to verify the results of the models. The following subsection examines the behaviors of three fragmentation prediction models and compares them to the results found in this subsection.

6.1.3. Comparison of Single Blasthole Substrate to Fragmentation Models.

The data collected from the single hole, scaled-model tests was compared to the estimations generated from the Kuz-Ram and Swebrec fragmentation models. Factors within these models used to describe rock mass and explosives application were set as close as possible to the criteria used to describe the test blocks in Table 1 in Appendix A. This exercise was to see if the models can be adapted to fit some of the data obtained from the scale-model tests, as that application is a significant departure from the intended use of the prediction models.

The first part of this subsection examines how the models behave when configured using the final design values for the solid 50/50 mix scaled test blocks. Two versions of the Kuz-Ram as well as the Swebrec model were entered into a spreadsheet for ease of operation. Initial input values for these models were taken directly from the solid block test configurations. Explosive inputs were set at a 4in burden and spacing, and a 9in powder column height. Properties of the detonating cord were entered as well. The concrete properties of 600psi compressive strength, 160lbs/cu. ft. density, massive formation designation, and no jointing were entered as well. These conditions represented the solid block scale model tests.

Figure 6.6 shows the models were evaluated at the same sieve apertures as used in the scaled model tests. The models assessed the topsize, and smaller fines regions close to the obtained sieve values. However, the slope of the curve at the 50% mark is far steeper than that seen in the laboratory tests, and the 50% failing value is much lower than the scaled model tests. This indicates a couple of things about the model. The fragmentation of the solid test blocks had a larger 50% failing sieve size than the models predicted, around 1.25in instead of 0.5in. In addition, the slope of the prediction curves at the 50% mark is much steeper than the slope that that of the scale-model tests.

Examining the formulas for each of the models, these discrepancies can be closely described as a difference in the value of the mean (50%) fragment size as well as the exponent used with the Rosin-Rammler curve. The mean size is a function of the effective powder factor, the amount of explosives per volume of rock. The exponent is calculated using criteria from Lilly's method of rock mass assessment, as well as blast geometry.
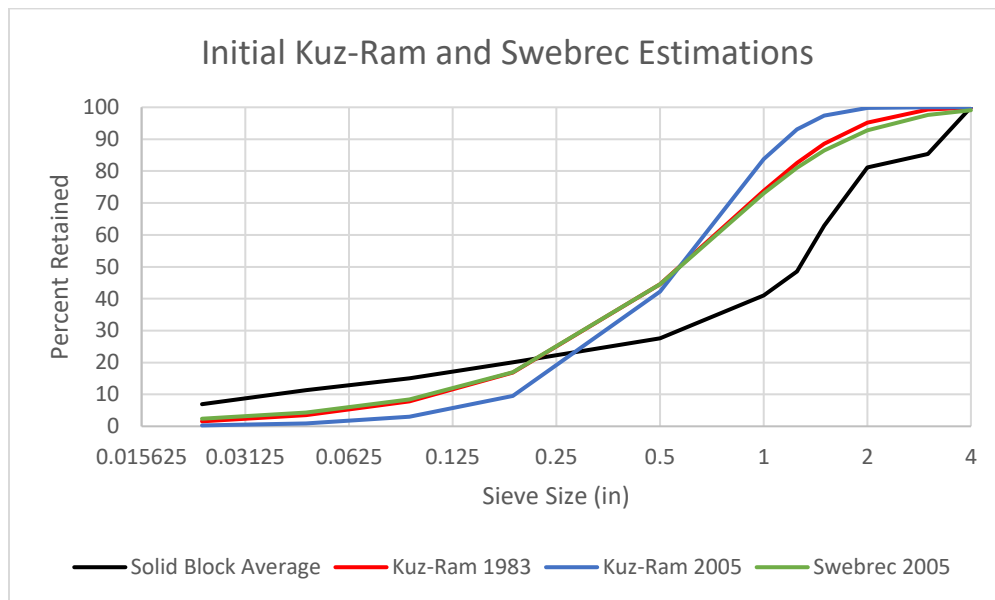
Figure 6.6. Kuz-Ram and Swebrec Estimation of Test Blocks

After close examination, the models could be adjusted to better accommodate this inappropriate application. Both the mean size and exponent of uniformity, shown in Equations 1 and 2 in Section 2.3, are dependent on the burden and spacing of the blast to calculate useful values. To adapt the estimation calculated in the semi-empirical models, the 4x4 in burden and spacing of the blasthole was adjusted to reflect the actual geometry of blasted material. The corners of the test blocks fractured to an approximate 45-degree angle, which exceeded the extents of the 4x4 in burden and spacing of the original blasthole. The 16 square inches of surface area used to calculate the effective volume of rock was doubled to 32 square inches because of the actual 45-degree breakage angle. This is due to the fact that these single-hole blasts were made on the corner of the test blocks. To adjust the models for this additional material volume, the root of 32 square inches, approximately 5 5/8 in, was used as the value for the burden and spacing for these

models. The result in doing so is much different as shown in Figure 6.7. The curves

shown in Figure 6.7 are more representative of the general breakage profiles of the

scaled-model tests and is only valid for this specific geometric configuration. Subsequent

blastholes provide a different blast geometry than the first hole in these tests. This is

because the rock mass has different boundaries than those encountered by the first hole.

The first blasthole in these tests broke to two orthogonal faces because the block starts

out square. The second hole broke to two oblique faces as a result of the angled face left

from the first hole. Because the geometries for the first and second blastholes are

different, each scenario needs to be assessed separately and then combined afterwards

instead of evaluated in a single estimation.
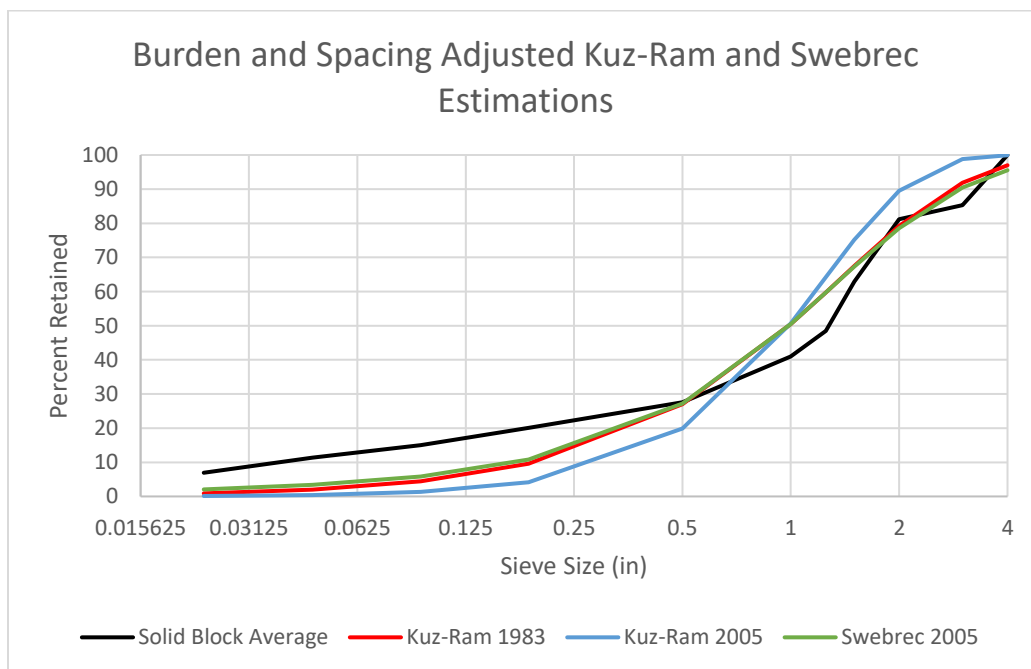
Figure 6.7. Burden and Spacing Adjusted Kuz-Ram and Swebrec Estimations

Figure 6.7 shows the adjusted Kuz-Ram and Swebrec models converge better in the upper size region, but the estimated mean size (50% retained) is smaller and the fines are underestimated. These estimations can be made closer to the solid block test average by substituting the calculated mean size in the models with the observed mean size of the tests, as shown in Figure 6.8. To do this, the A factor was then adjusted until the 50% passing values were nearest each other. This still left some regions of discrepancy between the estimation curves, but the mean size, and extents are close to what the test data displays.
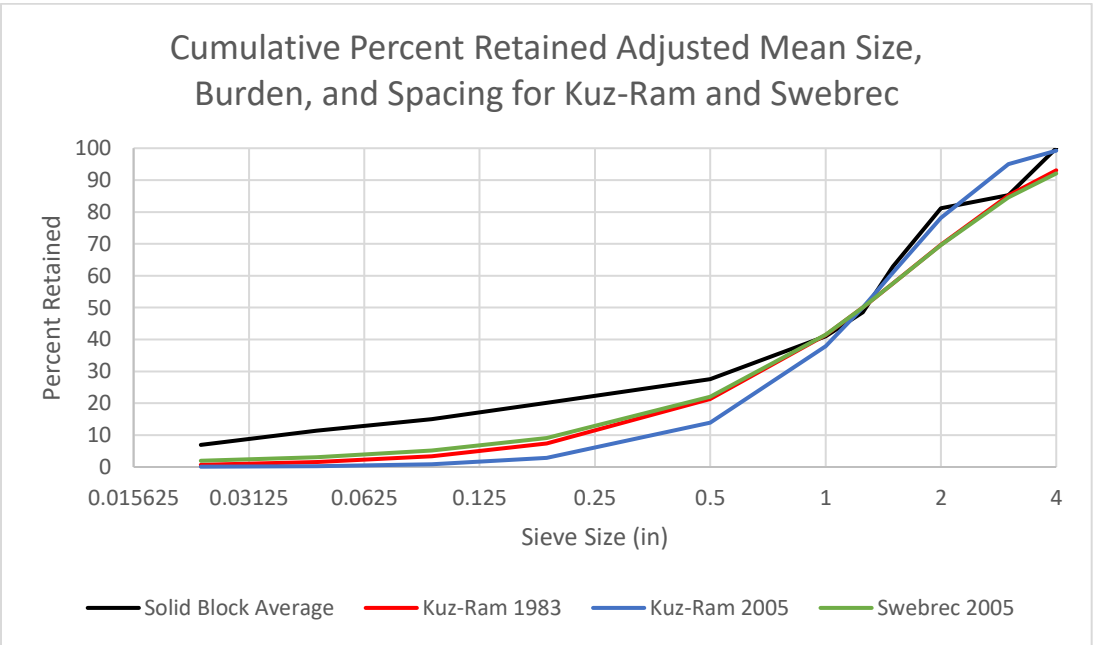
Figure 6.8. Plots of the Kuz-Ram and Swebrec Models, with Mean Size, Burden, and Spacing Adjusted to Fit

These estimations were close enough to validate the results of the models and confirm that they can predict breakage for small scale blasting as well. However, the

models required major adjustment to fit the solid block tests. These models are also effected by the change in explosives from TNT (Kuz-Ram 1983), ANFO (Kuz-Ram 2005 and Swebrec 2005) to detonating cord, although to a small degree. The calculations performed in these models are based on the relative weight strength (RWS) of the explosives used in relation to a reference value. Velocity of detonation is not considered in these equations, so high brisance, lower gas volume explosives like detonating cord are treated similar to TNT or blasting agents. There is no distinguishing between their differences in explosive properties but simply a difference in strengths.

However, the largest influence is still the difference in the amount of rock blasted instead of the burden and spacing of the blast hole. This is a geometrically dependent portion of the model. It was intended to provide average values from a full-scale, multiple blasthole shot. By restricting it to a single hole that has a much different volume output of fragments, the biggest concern is making sure the model is calculating the appropriate amount of blasted material. This modification to these models may be applicable for other geometric configurations. They were originally intended as an approximation for a complete bench blast.

6.2. OBSERVED CAPROCK FRACTURE PATTERNS

Along with the plotted fragmentation data, the photographic data provided a large amount of information into the origin of large fragment production. Many observations can be made from this information regarding the conditions that cause the unique breakage patterns of the cap layers. These observations include the radial breakage patterns of the tests which are directly related to the explosive column, the transient

fracturing occurrences, and the overall surface breakage estimation and comparison of the scaled depth of burial for individual tests. Lastly, this section will discuss issues with the collection of cap data.

6.2.1. Radial Fracture Patterns. Specific fracture patterns occurred in the cap layer, surrounding the blastholes in the scaled-model tests. These fracture patterns had distinct characteristics similar to those found by Livingston and others. The primary fractures initially extended radially from the blasthole until other blast conditions, such as approaching a free face could affect their directions. Radial fractures were counted as originating at the blasthole and extending outward. The radial fractures extending towards a free face often had a counterpart that extended from the blasthole in the opposite direction. These fractures, although counted separately, were treated as a pair with their partner fracture opposite the blasthole. On average, six major radial fractures were a common occurrence in the simulated cap rock. Two of these fractures developed orthogonal to the faces, maintaining a 90-degree angle of breakage from the blasthole. These radial fractures were often accompanied by fractures that extended backwards past the blasthole. These partner fractures became thinner as they progressed towards the back faces of the test block, terminating at, or most of the distance to the face. They are similar to fractures that appeared in scale model testing performed by Tariq (Tariq S. , 1995). The remaining two of the 6 fractures extended from the blasthole and oriented 45 degrees from either of the original block faces defining the extent of fragmentation. Depending on the situation, these fractures either fractured in a straight line or feathered out to the face. Figure 6.9 is a good example of the two short fractures that extended from the blasthole to the two original block faces and the 45-degree fractures that formed the newly blasted

face. Also shown in this picture is one of the partner fractures that extended towards the back of the block. This thin fracture is considered the partner to the orthogonal fracture that developed opposite the blasthole. On this test, only one of these fractures presented itself in the cap strata. In the substrate material, there were 2 of these fractures that extended to the back of the block, indicating that the mechanisms of breakage between the substrate and caprock are different. One of the lower fractures formed trending a similar direction with the thin fracture above, but broke independent from the caprock strata as shown in Figure 6.10. Although the breakage shown in Figure 6.9 is an excellent example of some of the individual types of fractures encountered in the cap strata, it was also one of the poorest cap breakages with only three fragments produced.

The last two typical fractures in the cap opposed each other and formed the 45-degree breakage angle. In certain instances, an additional two radial fractures developed perpendicular to the 45-degree break, extending diagonally to the front corner of the specimen and extending back toward the center of the block at the same angle. The inconsistent appearance of this diagonal break contributed little to the overall fragmentation, only splitting the square corner fragment a few times.

Of these described radial fractures within the cap, five are considered as contributing to the fragmentation of the blast. These fractures are classified as such due to their relatively straight paths from the blasthole, and the fact that they develop toward the open faces of the block. The two short orthogonal fractures, the two 45-degree fractures that form the new face, and the inconsistent 45-degree fracture that forms from the blasthole to the outside corner of the block fall within the bounds of the fragmented section of the test specimen. The additional fractures that extend towards the back sides

of the block, or through the middle, are considered to be a result of the face-bound

fractures reaching the face and expanding. The expanding outer fractures provide the

leverage needed to force the extension of fractures to the back of the block.
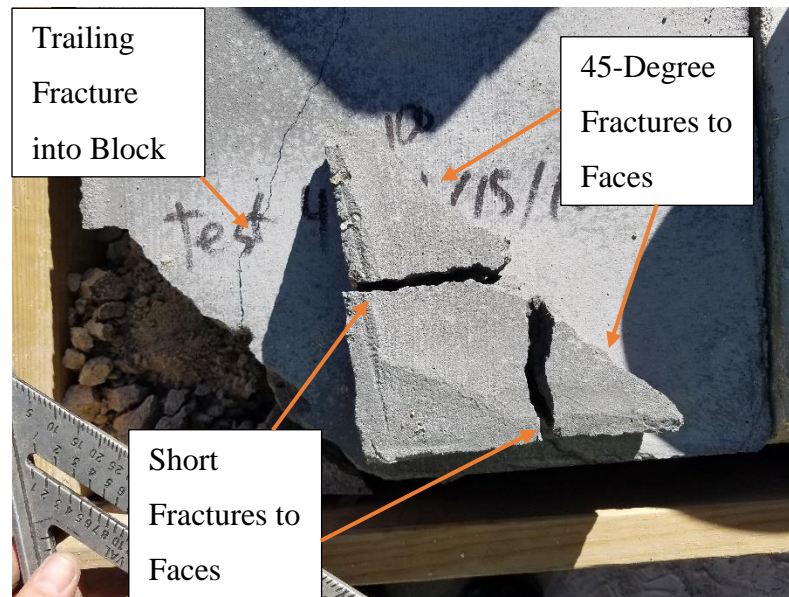
Figure 6.9. Test 18 Basic Cap Fractures, with Cap Material Repositioned (Center) for
Comparison to the Breakage of Substrate (Bottom Left)

The long, backwards fractures are similar to those discovered by Tariq and

Worsey (S. M. Tariq). They found that long backward-extending fractures like these are a

result of the momentum of expanding material furthering crack elongation. From a

single-hole perspective, like the majority of tests in this work, it is difficult to predict the

effects these fractures would have on fragmentation. If there was enough time delay

between holes in a sequentially timed blast for these fractures to develop within a rock

bench, they would likely behave as a predominant vertical joint set for the subsequent rows of the blast.
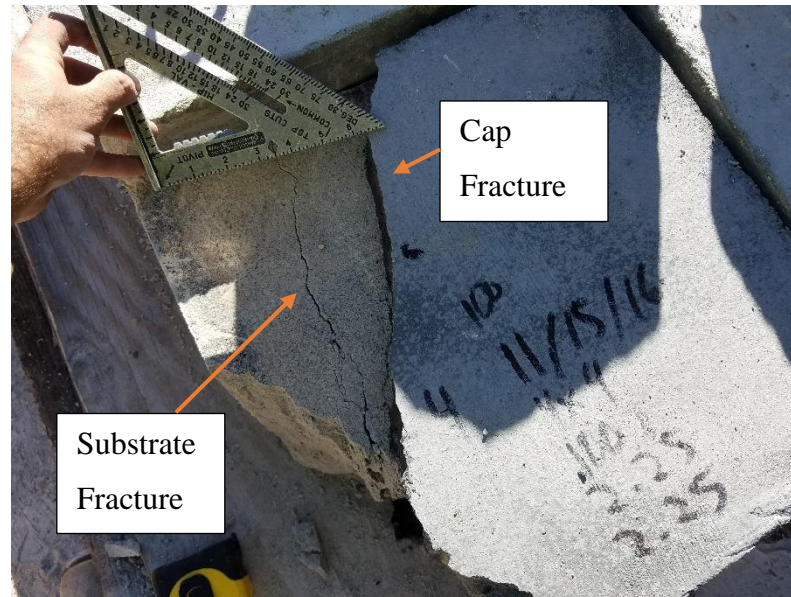
Figure 6.10. Test 18 Diverging Cap and Substrate Fractures

The presence of a vertical joint set like this would likely restrict blast energies from subsequent holes to within the fracture boundaries. The other possibility is that these cracks do not develop within a rock bench at all. This could be a possibility due to fast enough blast timing, or the confinement of a continuous rock bench restricting expansion of blasted rock. This speculation is from an overall blast standpoint. From a caprock perspective, if these fractures became prevalent, they would likely worsen caprock problems. This is due to the fractures dividing the caprock into large chunks that

are not likely to fragment. If we were able to orient these fractures so that they intersect the adjacent blastholes, it would increase the uniformity on the breakage of the cap.

This describes the primary occurrences of radial fractures that developed in the cap layers of the block. The amount, length, and direction of fractures varied as conditions changed throughout the cap. In some instances, fractures combined or coalesced instead of maintaining their own path. However, these radial fractures all originated from the blasthole and were present in some form throughout the entirety of the tests. These commonplace fractures were sometimes accompanied by inconsistent, transient fracturing.

6.2.2. Transient Fracture Patterns and Characteristics. In addition to the regularly occurring fractures in the cap, as discussed in the previous section, there were two types of transient fractures that appeared, but were either formed as an indirect result of the blast, or not regularly occurring. These patterns of breakage are described as transient because their presence was inconsistent and not tied to a specific test series. One of these features, the annular fracture, appeared behind the blasthole, just past the point of an additional burden and is shown in Figure 6.11. This fracture was a result of flexure of plates formed within the caprock. Flexure of the cap layer was indicated by the separation of the large plates from the substrate that formed backwards from the blasthole. The remainder of the cap layers were still adhered to the intact substrate and had to be loosened with a rubber mallet to inspect the remaining substrate for tensile fractures. These flexural plates tended to form in pie slice shapes centered on the blasthole, and as previously stated, the length of these plates exceeded the burden or spacing of the blasthole.
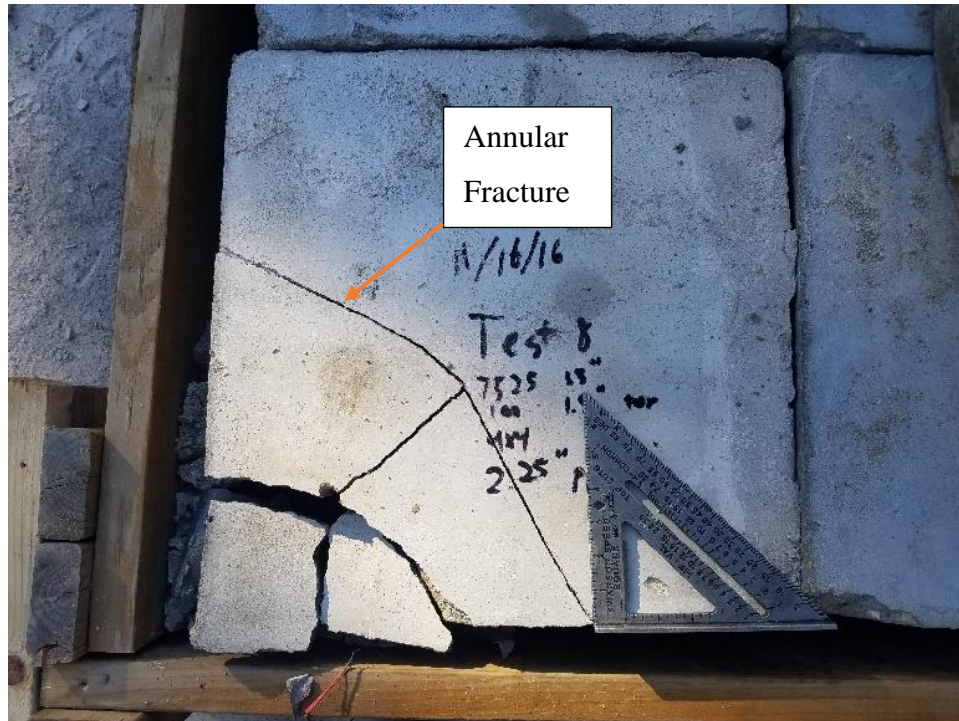
Figure 6.11. Annular Fracture and Large Plates

This is a possible source of uncharacteristic oversize as a result of caprock. These slabs are not considered as part of the fragmentation generated from the blasthole because they fall within the burden and spacing relegated to subsequent holes. In the sequential hole tests these fractures were present, although slightly different in shape. In these tests however, the fracture extended from the block edge, ran parallel with the row of the two holes, and hooked around to the adjacent edge past the second hole. It is not clear whether the annular cap fracture from the first hole interfered with the cap breakage above the second blasthole. An examination of the residence time needed for the annular fracture to fully form between holes needs to be performed. Aside from that, the distance of the annular fracture toward the back of the block from the first blasthole extended across for the second blasthole as well. Even though it is difficult to determine the

formation of the annular breakage between holes, the presence of the annular fracture behind both sequential holes indicates that trying to eliminate this oversize by changing blast timing would likely not show a significant increase in cap breakage. This is due to the long delay time between rows of a full-scale blast.

The annular fracture scenario alludes to the possibility that overly large boulders, on top of a conventional bench blast, can be created as a result of preconditioning of the rock strata by previous holes in the blast. In the field, large caprock fragments can be found with blasthole collars still present, and not fractured from its respective blasthole. This preconditioning could potentially cause the large oversize by opening up the aperture of the bedding plane, preventing sufficient blast energies from subsequent blastholes from penetrating the strata. Following this premise, any infilling, or foreign material in the bedding plain, such as a clay or wet shale seam, could potentially prevent direct fracturing of the cap layer as well. In testing, these large fragments were the only source of overly large breakage, and likely a result of a heaving mechanism.

The scaled-model tests showed that a degree fracturing was always present in the cap layer surrounding the blasthole collar, regardless of setup. The degree of cap fracturing for the first hole in the multiple-hole tests was similar to the fracturing of the single-hole tests. There was less cap fracturing surrounding the second blasthole in the multiple-hole tests than the first blasthole. This is a similar result to Livingston's work, shown in Figure 2.8 in Section 2.6.3. When this logic is applied to full-scale caprock blasting, large slabs with intact blasthole collars remaining can be considered a result of the preconditioning of the caprock from a previous blasthole.

Cratering was the second transient fracture pattern present in the caprock test specimens. Cratering occurred in the caprock layer in some of the tests. These craters formed an approximate 45-degree angle with the top of the block, with cratering extending upward from the approximate location of the top of the powder column, or the artificial bedding plane, whichever was higher. The fragmented material contained within the crater is of no concern to this study because the fragments within the craters were small enough that they became difficult to separate from the substrate breakage and were not relevant to the examination of oversize for this project. The importance of cratering within the cap layer is more related to the volume of the crater relative to the volume of the cap layer for a uniform single blasthole test. When cratering is present in caprock, a small portion of the volume is removed from the cap. Instead of that rock being used to create large surface fragments, it is broken to a finer fragmentation in keeping with the substrate material. Cratering was only observed for the single-hole caprock tests. The breakage generated during the multiple-hole tests made it difficult to observe in-situ post-blast conditions.

Calculating the volume and mean size of the crater for a full-scale blast can be performed for breakage or flyrock estimation purposes as described by Roth and performed in the author's master's thesis (Coy, 2014). The breakage of the crater is dependent on the scaled depth of burial as discussed in detail in Section 2.6.2.1. Since the caprock tests were covered, the crater fragments were either easy to identify, or were pulverized to a point where they were indistinguishable from the substrate material. This cratered material provides no risk of oversize.

6.2.3. Caprock Test Surface Breakage and Scaled Depth of Burial. The breakage of fragments on the surface was too coarse to obtain a usable fragmentation profile. The only meaningful display of this data is in the cumulative fragmentation profiles in Figures 6.2, 6.3, and 6.4. For the analysis of the cap layer itself, a count of the fragments was conducted to associate the amount of breakage with the blasting scenario. Figures 6.12 and 6.13 depict the difference in surface breakage between a solid block test and an equivalent caprock test.

The individual fragments on the surface were totaled as could be distinguished from the surface. Only fragments that were distinguishable from the substrate material were included in the count. This was the intended purpose for the dye the cap layers. This method did not account for fragments that were small enough to become lost in the substrate material. Those small fragments presented no risk of oversize and were still included in the overall fragmentation profiles, as shown in Section 6.1.

Figure 6.12. Test 5 Solid Block Surface Breakage

Figure 6.13. Test 13 3" 50%/50% Mix Cap Surface Breakage

The cap fragment counts were compared for differing cap configurations and scaled depths of burial. Scaled depth of burial calculations were performed using the U.S. unit scaled depth of burial equation found in the ISEE Blasters' Handbook and shown in Section 2.6.2.1. The assumption made for these calculations was that the length contributing factor for the SDOB equation was limited to a value of 8 as recommended in the Blasters' Handbook (ISEE, 2011). The explanation for this assumption was that due to the distinct difference in breakage caused by the artificial bedding plane, the effective length of the explosive charge was relatively short. Calculated SDOBs ranged from 0.69-1.83 ft/(lb^3), which placed all blast configurations within the range where a complete crater should form on each blast, and when unrestricted, eject most or all of the cratered material (ISEE, 2011). As shown in the photographs, and represented by the data, cratering did not necessarily occur in each scenario. However, the amount of explosives

changed only slightly. All of the tests measured within the SDOB range should have provided a complete crater, and should have broken the upper strata. Despite this, cratering was not a consistent phenomenon across the test spectrum.

In general, the count of cap fragments decreased as both the seam thickness and scaled depth of burial increased. Most of the test results showed that lower SDOB values produced higher cap fragment totals. This was the usual result for all tests except the 1.5 in cap thickness tests, where the cap fragment count decreased as SDOB decreased. Differing results at the 1.5in cap thickness could be attributed to failing stemming material, or the lack of overlying burden confining the blast. Even through fragment count decreased as SDOB decreased in the 1.5in cap tests, this thin cap layer had the highest amount of breakage of any cap configuration, comparable with the surface breakage of the solid block tests, as shown in Figures 6.14, 6.15, and 6.16. If cap breakage was problematic, thin caprock layers would not be the primary cause. Aside from the 1.5 in cap layers, the remaining cap tests broke into low, single digit fragment counts.

Figure 6.14. Test 9 1.5 in Cap 50%/50% Mix Surface Breakage

Figure 6.15. Test 10 1.5 in 50%/50% Mix Cap Surface Breakage

Figure 6.16. Test 11 1.5 in 50%/50% Mix Cap Surface Breakage

Test specimens constructed with the same seam thickness and using scaled depth of burial were compared to determine if the different mortar mixes comprising the various cap layers had an effect on the cap breakage. The fragment count results were nearly identical for each state, or differed only by one or two fragments. Even though the difference in strength between the cap layers mixes in these tests was approximately double, or even 4 times that of the weak 50% mortar/ 50% sand cap mix, it did not have as much effect on the tests as the thickness of the cap layer did. The lack of fracturing and transience of cratering made a comparison of surface fragment count unusable for assessment. The count of surface fractures and fragments can be found in Table 6 in Appendix A.

As shown in both Figure 6.17 and 6.18, only four primary fractures could be counted, generating two free cap fragments, while in Figure 6.8, five primary fractures can be seen. Each of these three tests generated a square fragment with orthogonal sides equal to the burden and spacing of the shot. In addition, they each generated at least one angled fragment, with Test 18 having two angled fragments. All three show a single fracture extending towards the back. In Figure 6.17, two transient fractures appeared in the form of hoop fractures, indicating flexure of the cap layer at their locations. With the difference in breakage from the blasthole limited to a single fracture, there is no definitive evidence that the strength of the cap material had a substantial difference on the breakage of the cap layer for these tests.

The two-layer tests fractured poorly as well. While the substrate fragmentation was comparable with the rest of the tests, the middle cap and top layers broke poorly. In the two-layer tests, the middle layers typically generated more fragments than the upper

layers. This is effectually similar to the single layer results, where there are one or two

fractures different so that analyzing by fragment count is unproductive.

Figures 6.19 through 6.21 are taken from Test 21. Figure 6.19 displays the surface

layer, where there was a 45-degree break straight across with an additional orthogonal

fracture. In Figure 6.20, the middle layer breakage is shown with the two orthogonal

fractures, a 45-degree fracture for the new face, and an additional diagonal fracture that

split the 4x4 in square. There were additional tailing fractures that extended towards the

back of the block in the middle layer as well. Figure 6.21 shows the final profile of the

block after blasting.
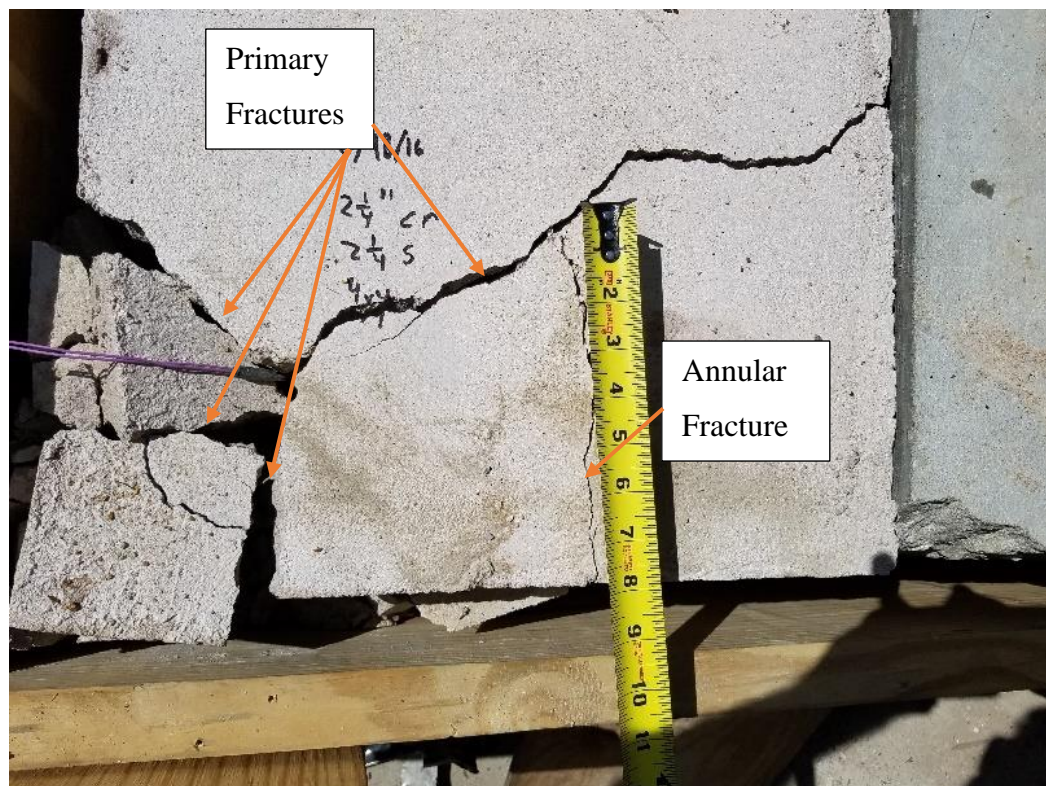
Figure 6.17. Test 7 2.25 in 50%/50% Mix Cap Surface Breakage
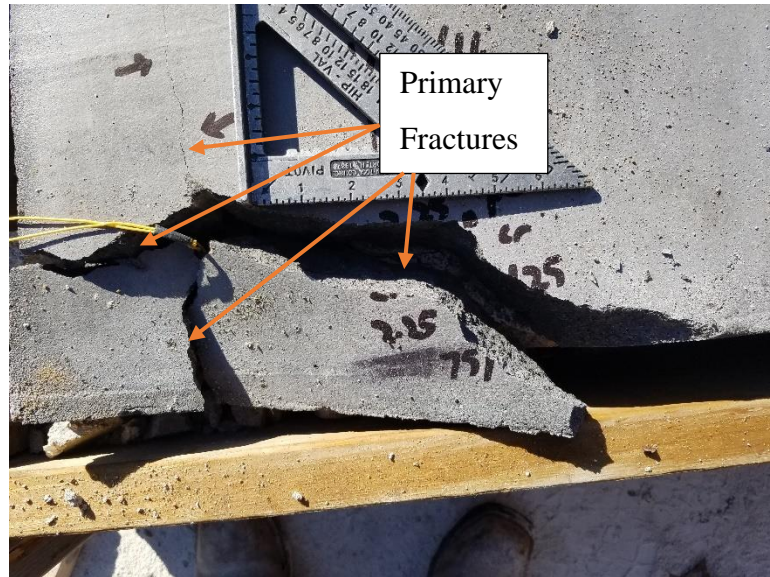
Figure 6.18. Test 15 2.25 in 100% Mix Cap Surface Breakage
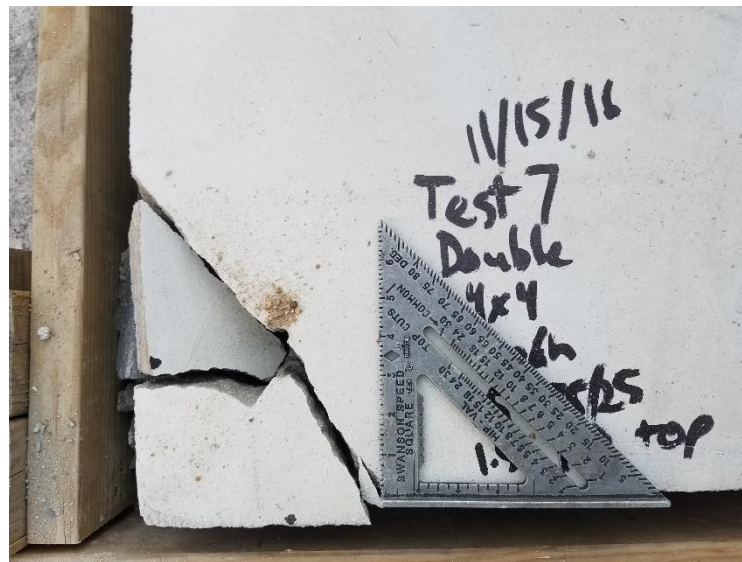
Figure 6.19. Test 21 2-Layer Cap Test Top Layer

Figure 6.20. Test 21 2-Layer Cap Test Middle Layer

Figure 6.21. Test 21 2-Layer Cap Side Profile

This test, when compared to the solid block and 3in loaded single layer tests

(shown in Figures 6.12 and 6.13), demonstrates that the additional bedding plane between

the two cap layers further reduced the surface fracturing when loaded even with the lower bedding plane. The cap fragments were limited vertically by their adjacent bedding planes. The fragments broke to these adjacent bedding planes, giving the fragments a thinner vertical dimension than that of the single-layer cap tests. However, the overall breakage of these thin cap layers remained poor and plate-like because radial fracturing played a role similar to the single-layer cap tests. The middle cap layer (dyed black in Figure 6.21) had fracture patterns similar to the single layer cap tests, while fracturing in the top cap layer (top, white layer in Figure 6.21) was minimal. At lower loading heights, the fracturing of the middle cap layer became poorer and broke similar to the top cap layer.

Neither the surface nor middle caprock layer in this test received the degree of fragmentation experienced by the 1.5 in single cap layer, even though both of the thinner seams were 1.5 in thickness, and the top layer was loaded the same as in Test 9. Their breakage was more consistent with the coarse breakage of the thicker layered tests. This would indicate that in some circumstances, the upper layers of a bench, while fracturing independently, may have an overall combined behavior similar to that of thicker cap strata.

One additional point to make on the surface breakage of these tests is that the detonating cord that was used has a very high velocity of detonation, and produces a shattering effect on brittle materials. This shattering effect creates the fractures in the cap. A different explosive would likely have a lower velocity of detonation. If a blasting agent were used in this configuration, the degree of fracturing in the cap could be even less.

This concludes the analysis of the photographic data. Many observations were made regarding the nature of the fracturing process in the test blocks, some more useful than others. It is clear that the means of photographic data collection and analysis used in this study is not yet a straightforward process. The known issues with data collection are discussed in the following subsection.

6.3. ISSUES WITH CAP DATA COLLECTION AND ANALYSIS

Many observations and calculations of the data produced by the scaled-model tests provided insight into the blast phenomena present when blasting with caprock. However, there were issues that arose when collecting and processing the data. These issues should be remedied for future work. The following subsections discuss the lack of population when measuring test data, classification of caprock fractures, and crater assessment.

6.3.1. Lack of Population in Data. A single break can make a large percentage difference in data collection and analysis. The breakage count of the tested cap fragments was, in some cases, as low as two fragments. This made graphical representations of the data unusable, because changes in the low fragment count caused large percentage differences for each respective series of inquiry. The lack of resolution for these tests obscures any sort of reasonable comparison using typical fragmentation or statistical analysis methods due to extremely low population.

6.3.2. Classification of Caprock Fractures. In addition to problems with resolution, there were also issues regarding the classification of fractures and free fragments. Utilizing a simple fracture or fragment count can give a general idea of the

level of breakage of a cap strata, if the degree and orientation of fractures match those present in the comparative test. However, a test with a number of prominent radial fractures might not have the same fracture pattern as another test with the same number of prominent fractures. This method does not take into account the length and orientation of fractures. From a quantitative standpoint, this method needs more development before more observational data and conclusions can be garnered from it.

6.3.3. Crater Assessment. The third issue with cap data collection was the accurate measuring of crater volume and crater fragmentation. In the author's master's thesis, crater volumes and mean fragmentation were predicted and measured. The tests were designed for trenching purposes, and in those tests, the scaled depth of burial was set to produce the strongest intensity flyrock conditions for the blasthole and explosives used. There were no free faces other than the surface of the ground. With those conditions, craters were round and had a distinguishable depth, making identification, and estimation a relatively straightforward process. In comparison, the testing method in this thesis was designed to represent excavation in quarries which uses an entirely different geometry.

These scaled model tests in comparison had two free faces, thin upper cap layers, and SDOBs smaller than those utilized in the cratering studies, making the craters appear irregular and misshapen. Craters that formed at higher SDOBs were often a semicircular crater profile projecting out to the blasted corner. While the craters tended to extend to the open corner, there was little breakage directed toward the back of the block. This occasionally produced an eccentric profile for the craters.

With the thinner cap layers, such as the 1.5" series, the formed craters were wide and shallow, with an irregular bottom, making measurement and estimation of their contribution to the overall fragmentation more difficult. A gross approximation was the best measurement that could be performed in this circumstance, and even then, the approximation would not provide useable information for Roth's estimation method (Roth). Estimating fragment size is based on an accurate estimation of the volume of rock blasted, as previously discussed. Approximation of the mean fragment size for the crater would be inaccurate in this case because of the irregularity in the size and shapes of the craters produced in the cap. Estimations aside, actual data for fragmentation within the crater could not be obtained as the majority of particles were small enough to be mixed with the breakage of the substrate, and were not significant to the study of oversize.

6.4. RECLASSIFICATION OF OVERSIZE

In quarry operations, rock that cannot pass through the crusher is considered oversize. This material is removed from the primary crusher feed material and stockpiled for secondary breakage, most commonly at the face. The breakage of the cap in the scaled-model tests would represent massive slabs in a quarry setting. Few, if any quarries would have a crusher that could be fed such slabs. In most of these tests, the entire cap breakage could be considered oversize. Even in the two-layer cap tests, where the vertical dimension of fragments is limited, still produced slabs that would be unacceptable as crusher feed in a full-scale setting. Though the results of breakage in the cap layers varied by a handful of fragments, they still all produced breakage that would necessitate secondary breakage.

While the information provided from this study was mostly qualitative in nature, it allowed for some reasonable conclusions and numerous opportunities to further this research. This analysis provides information for better understanding of caprock breakage under certain situations, and displays many aspects that would have gone unnoticed or ignored in a production setting. The sections that follow provide the conclusions obtained from this analysis, as well as possible future undertakings to further this work.

6.5. SMALL SCALE MODELING ISSUES AND CLARIFICATIONS

The small-scale modeling used in this dissertation is not a direct representation of a full-scale bench blast. It was intended as a means to examine and identify possible sources of oversize as a result of caprock blasting. The tests performed in this dissertation were intended to bring to light the existence of massive caprock breakage phenomena without interference from additional geologic features. There are additional configurations that need to be examined.

There are configurations of single-hole tests that still need to be examined. These configurations include blasting from a straight face, from an included corner, and from an angled face that would represent the end of a previous blast. Each of these conditions should be examined to see if there are any changes from the outside corner configuration. The outside corner blast design used in this dissertation allowed for tests to be performed in succession with relative ease. However, it is just one possible configuration. An outside corner is usually used for the first hole in a blast, and a square corner such as this is usually not the case for subsequent bench blasts. Along with the change in

configuration, the use of any modeling techniques, such as those in Section 6.1.3, will require major adjustment to fit the situation as well.

These configurations still only represent a single point region of a blast. Once the cap blasting effects of the different configurations have been identified, the scale model testing will have run its course. The two-hole tests in this dissertation were almost too much for the test bench. Once the requisite single hole configurations have been tested, full-scale field testing will become a more viable option. Scaled-models are used to identify regions or phenomena that require further scrutiny in a controlled situation. However, the next step in testing is to examine a bench blast. The prediction models discussed in this work were made for a full-scale bench blast. Also, the additional holes at full scale would likely smooth out some of the inconsistencies in the fragmentation data. With more of the blasted material generated in the center of a blast pattern, odd fragmentation near the edges of the blast becomes less relevant.

7. CONCLUSIONS

The examination of caprock requires much consideration for rock extraction by blasting in quarries. Aspects of caprock phenomena were examined using model blasting and the following conclusions are made.

7.1. ESTABLISHMENT OF A SCALE-MODEL FOR CAPROCK

Though only a few scenarios were tested, the scaled-model caprock tests were productive, and provided new information and opened numerous possibilities for future testing. Once the targets were poured to the desired configuration, performing the actual test was a straightforward, iterative process. This test can be modified to fit many scenarios and potentially uncover more blast phenomena not readily observed by other means. The first characteristic was the discrepancy between the cap and the substrate rock.

7.2. CAPROCK HAS A SEPARATE FRAGMENTATION FROM SUBSTRATE

Breakage of the caprock must be assessed separately from the substrate. Data obtained from the scale-model test clearly indicated that there was a difference in breakage between a uniform rock bench and one with a thick upper layer of caprock. The data supports the proposition that a single bedding plane near the top of a powder column not only produces coarser breakage than that of a solid block, but also produces a distinct difference in breakage between the cap layer and the underlying strata. While the primary fractures can form in similar directions in both strata, they do so independently, even with

a relatively strong and cemented joint comprising the artificial bedding plane. The primary factors found to influence caprock breakage are the thickness of the cap layer, location of the bedding plane, and depth to the top of the powder column. The strength of the cap material did not produce large changes in cap fragmentation in this study. In addition to these factors, there is also the influence of inconsistent phenomena such as cratering and annular fracturing on the caprock breakage.

7.2.1. Influence of Cratering on Caprock Breakage. The presence of cratering has a small effect on caprock breakage. When cratering was present, the degree of loading into the cap layer determined the volume of the crater and the fragmentation of the crushed material. When cratering was not present, the cap layer fractured in a coarse manner, with a minimal amount of radial fractures present at the collar. While a cratering scenario does slightly improve the fragmentation of the cap layer, it is not necessarily the desired scenario for actual quarry blasting. Slabs that would be present without cratering are still present, but with a corner section removed. Using small enough scaled depths of burial to make full craters would result in large amounts of flyrock and not reduce the effective size of slabs or boulders. From a blast energy perspective, cratering represents explosive energy that is not being spread throughout the cap layer, but focused on a small volume of the cap layer.

7.2.2. Preconditioned Bench as a Potential Source for Uncharacteristic Oversize. Caprock slabs larger than the burden and spacing of the blast pattern are a result of cap preconditioning from previous blastholes. While the breakage immediately surrounding the collar of the blasthole can be easily controlled by adjusting the burden and spacing, the presence of some prominent, inconsistent fracturing formed during

blasting with caprock can cause problems. In some tests, a large annular fracture formed

beyond where the next row and column of blastholes would be located in the blast

pattern. This circular fracture created large, chevron shaped slabs when combined with

radial fractures extending from the blasthole. These are similar in shape to fragments that

appeared during the author's master's research and seen after bench blasting at a full

scale. These plates are likely the largest oversize generated during caprock operations.

This is due to their dimensions extending beyond the burden and spacing of the adjacent

holes, and is a possible explanation why caprock slabs, observed in quarries, can still

retain the collars of blastholes instead of breaking properly.

7.3. CAPROCK MITIGATION

As stated in the previous section, preconditioning of the cap layer by annular

fracturing can produce uncharacteristically large oversize, beyond that of the typical blast

pattern. If these fractures can be prevented, the worst of the oversize will be mitigated.

The cap layer would need to be preconditioned in such a way to preclude the formation of

annular fractures to accomplish this. A blasting configuration that fractures the cap

without heaving must be shot before the main blast, so that the cap only fractures

radially. When the cap layer heaves as a result from the main blast, the cap fragments will

separate at the established fractures, rather than allow the annular fracture to form. This

will prevent the occurrence of uncharacteristic oversize from annular fracturing before it

can occur.

Based on the data of this study, the recommendation of author is to load powder

high enough in to the caprock to crack it but not necessarily high enough to produce

flyrock problems. For the purpose of reducing the oversize, without causing additional flyrock, the burden and spacing of the explosives near the cap must thereby be reduced accordingly. This can be practically accomplished by drilling and loading shallow satellite holes between the normal production holes and shooting them prior to the rest of the blast before annular fractures can develop, preventing their formation. By increasing the amount of explosives in the cap layer, breakage of the cap layer should increase as well.

Drilling the satellite holes in the cap layer should be performed with careful consideration. No additional breakage is needed in the lower layers, so blast energies need to be confined to the cap as much as possible. For this reason, satellite hole depths should be limited to the cap layer without penetrating into the substrate. Doing so should also reduce or prevent the heaving mechanism that causes the annular fracture. This would likely limit cap fragment size to within the burden and spacing of the satellite hole pattern. Breakage in the caprock layers of the small-scale tests was minimal, even around the blasthole collar. The fragments within the burden and spacing of the small-scale caprock tests often had a large dimension equal to the burden and spacing. To reduce or eliminate the need for this material to be re-handled and broken again before the crusher, burden and spacing of the satellite holes should be limited to the size of material desired for crusher feed.

7.4. BLAST INITIATION WHEN CAPROCK IS PRESENT

Fully activated sequential timing is required when caprock is present to eliminate the risk of disconnects and cutoffs during blasting. When a blast is connected to a firing

system, there exist connections that extend from the main firing line down into the blastholes to the detonator. Slack in these connections is often removed so that excess connecting materials on the surface do not whip and interfere with the shot timing. This eliminates loops and accidental crossovers in the blasting lines. If a slab of rock heaves before the respective blastholes are energized, blasting lines could be stretched taught and possibly snapped or severed, leading to a cutoff situation. Cutoffs in blasting are a hazard as they must to be reconnected and initiated or removed from the muckpile and disposed of to reduce danger to operators. They also result in reduced breakage of the substrate layers of the rock bench.

7.5. BUDGETING FOR OVERSIZE

Almost the entire caprock layer must be considered separately when trying to budget for oversize material. As previously stated, the breakage of the caprock must be considered as a separate element from that of the substrate. When attempting to optimize the revenue at a particular quarry, the operator would use an optimization program similar to that proposed by Calnan, but with two separate iterations. The substrate layers would go through a normal iteration of his model, while the caprock layers would go through a separate iteration. The caprock iteration would have an additional cost factor to represent the additional breakage required for the material to go back into the processing stream. By evaluating these two sections of the bench separately, the operator can determine if the cap material is a profitable, salable product. For budgetary purposes, both optimizations can be combined to yield the best overall cost minimization for the quarry.

7.6. USING SEMI-EMPIRICAL MODELS TO ESTIMATE FRAGMENTATION WITH CAPROCK

Semi-empirical models such as Kuz-Ram and Swebrec can be used to estimate the fragmentation of quarry blasts to a high degree of success. They could be made to estimate the breakage of the substrate layers in the small-scale tests. However, when caprock conditions were introduced, the mathematical models severely underestimated the mean size, and volume of fines generated. They were adjusted to match the actual data, but after all the work to adjust them, the solution was too contrived to be feasible for implementation in a caprock-heavy blasting operation. The models cannot be considered predictive when they would require constant adjustment to fit blasting in-situ caprock formations.

In addition, the general use of these estimation techniques is overshadowed by the fact that a large portion of the caprock layer will need to be set aside for secondary breakage before being taken to the crusher. As discussed in Section 2.3.1.3, the Rosin-Rammler curve is used to describe an aggregate of material that has undergone the same breakage process. The conclusion in Section 7.2 states that the breakage mechanism for the cap layers is different from the substrate layer. In addition, boulders produced by caprock are classified as oversize. Oversize is typically broken by a hydraulic impactor, which is an entirely different mechanism of breakage. The combination of these different mechanisms makes using a single descriptive curve inappropriate for caprock scenarios.

7.7. FINAL CONCLUSION

Along with these conclusions there is the potential for the further development and expansion of the scaled-model caprock tests. The work performed for this

dissertation produced many observations and conclusions that would not have been easily

observed in the field. The future of this potential work is described in the following

section.

8. FUTURE WORK

The testing described in this dissertation established a solid base for examining the breakage of caprock-laden benches. The data provided gave some insight into the conditions that cause poor cap breakage. However, there is room for improvement, not only with the testing methods, but also with the collection and processing of information. This proposed future work is beyond the scope of this thesis.

8.1. IMPROVEMENTS TO TEST BENCH

While the test setup used in this dissertation was fairly straightforward, it was not without flaws. The bench was near its durability limit with the single-hole blast, requiring the crib to be repaired multiple times. Blasting for the sequential hole tests required an entire redesign of the crib, but still damaged the bench significantly. Reinforcement to the test bench would improve durability and reduce the amount of maintenance needed to operate the tests. An improvement in durability would allow more sequential holes to be tested, allowing for multiple sequential holes, perhaps even multiple rows, and varying initiation patterns to be tested.

The first improvement to test bench durability would be to place ½" steel plate underneath the plywood that the test block and bumper blocks rest on. This would reduce the amount of wood that is removed from consecutive blasts, conserving resources and minimizing the downtime needed to change it out. The other piece of bench equipment that could use reinforcement is the crib used to contain the horizontal throw of fragments.

Steel banding could be used to reinforce the wood crib and keep the corners from pulling apart.

8.2. ADDITIONAL TEST SCENARIOS

A limited variety of caprock scenarios were tested in this dissertation. The success of this testing has opened p many potential avenues to investigate further. There are a myriad of geologic scenarios involving caprock that can be encountered, and to better understand the behavior of the caprock, additional testing will need to be conducted with respect to additional bedding and jointing. The substrate, for instance, could be thinly layered to mimic a thinly bedded limestone with a large cap. This would limit the maximum vertical dimension of fragments from the substrate, making the blast fragmentation results much finer. The current drawback to constructing these specimens is the one day wait between pours. It could potentially require up to a month of pouring mortar daily to construct a target, then another month to test the finished product. The method of constructing targets requires further investigation.

Another possible scenario includes vertical joint sets at various spacings and angles relative to the blasthole. This could show how the amount of damage to in-situ blocks is further limited by blast geometry and vertical geology. In addition, the conditions of the bedding planes could be examined. Clay-infilled bedding planes could be simulated to represent the mud and clay seams below the cap in formations like the Winterset limestone to test the supposition that these features increase the dominance of caprock.

Changes in blast geometry are needed for future testing. The scaled-model tests need to be altered so that an oblique diagonal, repeatable face is produced as would be seen in quarry blasting. This would ensure the shape of the face post blast is the same shape as the starting face. The square shape of the blocks made the tests easily poured and repeated, but the natural tendency of benches to have an angled face after blasting must be better represented.

8.3. MODELING IMPROVEMENTS

Lastly, a regression model to analyze additional data more accurately could be constructed. All of the data, once placed in numerical form must be analyzed for interrelated properties and influences. In the case of the testing performed for this dissertation, this means a multivariable, non-linear regression model. The basic concept would take sieve data, and other size data from a spreadsheet or database, and construct the constraints based on the statistics mentioned previously to approximate the behavior of the variables. Once this regression method is constructed, this scaled model testing will be better enabled to bridge the gap between field blasting and simulation of caprock.

APPENDIX A.

SCALED MODEL TEST DATA

Table 1 Scaled Model Test Configurations

Test Number	Date	Series #	Series	Mix	Burden (in)	Spacing (in)	Seam height (in)	Stemming (in)	SDOB (U.S.)
1	6/7/2016	Solid	Solid	50/50	5	5	0	3	1.37708996
2	6/7/2016	Solid	Solid	50/50	5	5	0	3	1.37708996
3	6/8/2016	Solid	Solid	50/50	5	5	0	3	1.37708996
4	6/8/2016	Solid	Solid	50/50	5	5	0	3	1.37708996
5	8/17/2016	Solid	Solid	50/50	4	4	0	3	1.37708996
6	8/17/2016	Solid	Solid	50/50	4	4	0	3	1.37708996
7	8/18/2016	1	Layers	50/50	4	4	2.25	2.25	1.14818538
8	8/18/2016	1	Layers	50/50	4	4	2.25	1.125	0.80482851
9	8/18/2016	1	Layers	50/50	4	4	1.5	2.25	1.14818538
10	8/18/2016	1	Layers	50/50	4	4	1.5	1.5	0.9192808
11	8/19/2016	1	Layers	50/50	4	4	1.5	0.75	0.69037622
12	8/19/2016	1	Layers	50/50	4	4	3	4.5	1.83489913
13	8/19/2016	1	Layers	50/50	4	4	3	3	1.37708996
14	8/19/2016	1	Layers	50/50	4	4	3	1.5	0.9192808
15	11/15/2016	2	Layers	75/25	4	4	2.25	2.25	1.14818538
16	11/15/2016	2	Layers	75/25	4	4	2.25	1.125	0.80482851
17	11/15/2016	2	Layers	75/25	4	4	2.25	1.6875	0.97650694
18	11/15/2016	2	Layers	100	4	4	2.25	2.25	1.14818538
19	11/15/2016	2	Layers	100	4	4	2.25	1.125	0.80482851
20	11/15/2016	2	Layers	100	4	4	2.25	1.6875	0.97650694
21	11/15/2016	2	2 layer	100-75/25	4	4	3	3	1.37708996
22	11/15/2016	2	2 layer	100-75/25	4	4	3	2.25	1.14818538
23	11/15/2016	2	2 layer	100-75/25	4	4	3	1.5	0.9192808
24	11/21/2016	3	2-hole	100+Glenium	4	4	0	2.25	1.14818538
25	11/21/2016	3	2-hole	50/50 all	4	4	0	2.25	1.14818538
26	11/22/2016	3	2-hole	50/50 all	4	4	3	2.25	1.14818538
27	11/22/2016	3	2-hole	50/50 all	4	4	1.5	2.25	1.14818538
28	11/22/2016	3	2-hole	75/25 top	4	4	2.25	2.25	1.14818538
29	11/22/2016	3	2-hole	100 top	4	4	2.25	2.25	1.14818538
30	11/22/2016	3	2-hole	100 top 72/25 r	4	4	3	2.25	1.14818538

Table 2 Scaled Model Test Substrate Sieve Data (lbs)

Test Num	4"	3"	2"	1.5"	1.25"	1"	0.5"	#4	#8	#16	#30	Pan
1	0	0	26.7	3.4012	1.0934	0.3036	1.573	0.9988	1.2452	0.7546	0.7436	0.8448
2	0	0	31.3	0.6864	0.2992	0.2794	1.0186	0.9306	1.5532	0.9636	1.089	1.2936
3	0	0	30.4	1.386	1.3288	0.9262	2.1934	1.265	1.3992	0.7194	0.6182	1.056
4	0	0	27	2.123	1.21	1.1506	2.3232	1.023	1.0274	0.572	0.55	0.8492
5	3.565	0	3.688	5.12	1.707	5.276	1.404	0.992	1.013	1.478	1.373	1.02
6	4.661	2.433	6.586	2.805	2.512	2.08	2.81	1.882	1.024	0.952	0.786	0.64
7	0	8.58	4.814	2.498	1.49	0.827	2.26	2.02	1.192	0.708	0.677	0.868
8	2.084	1.589	3.199	3.034	1.468	1.666	2.323	2.469	1.57	0.995	1.099	0.803
9	2.101	3.74	2.014	3.535	0.713	2.043	3.56	2.459	1.217	1.255	1.136	0.379
10	0	4.728	3.499	2.665	2.312	2.691	5.646	4.248	2.288	2.81	2.068	0.561
11	0	4.581	4.278	3.733	1.582	2.63	4.618	4.034	2.109	1.965	2.349	1.125
12	0	1.814	1.917	2.76	1.862	1.935	4.806	3.911	1.638	1.173	2.077	1.427
13	0	0	3.018	4.803	1.906	0.951	3.962	3.502	1.975	1.731	1.656	1.96
14	0	2.746	0.659	3.098	2.003	2.282	6.647	5.928	2.868	4.507	3.232	1.523
15	0	3.55	4.641	3.498	1.441	2.434	2.621	4.209	2.482	2.275	2.448	2.903
16	6.5	0	3.748	1.925	0	2.113	4.056	5.333	3.181	3.002	3.345	4.26
17	0	2.435	2.387	2.077	1.491	0.98	3.401	4.039	2.993	3.095	3.344	3.351
18	0	0	4.725	2.979	1.359	1.076	2.702	4.579	2.754	2.593	2.888	3.565
19	3.248	4.04	2.759	4.181	1.14	1.298	1.768	3.946	2.483	2.297	2.367	2.366
20	0	2.624	6.259	2.228	0.814	1.018	2.54	3.223	2.337	2.25	2.264	2.228
21	2.474	1.781	3.301	2.271	1.377	0.76	1.315	2.674	2.059	1.974	1.177	1.771
22	5.162	5.271	1.389	0.122	0.832	0.107	2.027	2.976	2.332	2.306	2.131	2.032
23	0	5.771	5.011	2.195	1.05	0.713	1.717	3.376	2.144	1.863	2.104	2.282
24	21.91	13.453	9.161	4.78	1.118	0.734	3.467	1.745	0.516	0.318	0.257	0.538
25	0	3.618	11.844	5.632	2.274	1.561	8.473	5.506	3.371	3.055	3.282	5.438
26	0	1.307	1.834	1.768	2.572	0.499	8.521	5.824	5.058	6.822	5.38	5.837
27	0	1.207	5.157	2.446	2.171	0.507	4.7	6.441	3.623	3.612	4.542	7.114
28	0	0.881	3.286	3.625	1.853	0.404	5.197	6.406	3.592	3.273	3.922	6.041
29	0	0	6.594	3.141	2.691	0.977	2.364	6.64	4.771	5.124	5.813	8.266
30	0	2.227	5.785	1.838	2.036	0.453	3.21	5.53	3.723	4.148	4.252	4.49

Table 3 Scaled Model Tests Cap Sieve Data (lbs)

Test Num	4"	3"	2"	1.5"	1.25"	1"	0.5"	#4	#8	#16	#30	Pan
1	0	0	0	0	0	0	0	0	0	0	0	0
2	0	0	0	0	0	0	0	0	0	0	0	0
3	0	0	0	0	0	0	0	0	0	0	0	0
4	0	0	0	0	0	0	0	0	0	0	0	0
5	0	0	0	0	0	0	0	0	0	0	0	0
6	0	0	0	0	0	0	0	0	0	0	0	0
7	0	1.34	0.83	0.163	0	0	0	0	0	0	0	0
8	0	2.202	0.501	0.341	0	0	0.269	0	0	0	0	0
9	0	0	0.299	2.051	0	0.222	0	0	0	0	0	0
10	0	0	1.273	0.608	0.447	0.494	0	0	0	0	0	0
11	0	1.032	3.265	0.501	0	0.05	0	0.107	0	0	0	0
12	3.231	2.496	0	0	0	0	0	0	0	0	0	0
13	0	0	6.357	0	0	0	0	0	0	0	0	0
14	0	0	0	0	0	0	0	0	0	0	0	0
15	6.089	0	0	0	0	0	0	0	0	0	0	0
16	7.52	0	0	0	0	0	0	0	0	0	0	0
17	5.689	0	0	0	0	0	0	0	0	0	0	0
18	5.806	0	0	0	0	0	0	0	0	0	0	0
19	6.024	0	0	0	0	0	0	0	0	0	0	0
20	4.725	0	0	0	0	0	0	0	0	0	0	0
21	3.297	2.59	0	0	0	0	0	0	0	0	0	0
22	3.299	2.686	0	0	0	0	0	0	0	0	0	0
23	4.876	4.876	0	0	0	0	0	0	0	0	0	0
24	0	0	0	0	0	0	0	0	0	0	0	0
25	0	0	0	0	0	0	0	0	0	0	0	0
26	0	6.598	4.319	1.707	0.696	0.93	0	0	0	0	0	0
27	4.409	2.586	2.635	0	0	0	0	0	0	0	0	0
28	6.48	0	0.56	0	0	0	0	0	0	0	0	0
29	6.064	0	0	0	0	0	0	0	0	0	0	0
30	4.941	0.782	0.487	0	0	0	0	0	0	0	0	0

Table 4 Scaled Model Test Total Sieve Data (lbs)

Test Num	4"	3"	2"	1.5"	1.25"	1"	0.5"	#4	#8	#16	#30	Pan
1	0	0	26.7	3.4012	1.0934	0.3036	1.573	0.9988	1.2452	0.7546	0.7436	0.8448
2	0	0	31.3	0.6864	0.2992	0.2794	1.0186	0.9306	1.5532	0.9636	1.089	1.2936
3	0	0	30.4	1.386	1.3288	0.9262	2.1934	1.265	1.3992	0.7194	0.6182	1.056
4	0	0	27	2.123	1.21	1.1506	2.3232	1.023	1.0274	0.572	0.55	0.8492
5	3.565	0	3.688	5.12	1.707	5.276	1.404	0.992	1.013	1.478	1.373	1.02
6	4.661	2.433	6.586	2.805	2.512	2.08	2.81	1.882	1.024	0.952	0.786	0.64
7	0	9.92	5.644	2.661	1.49	0.827	2.26	2.02	1.192	0.708	0.677	0.868
8	2.084	3.791	3.7	3.375	1.468	1.666	2.592	2.469	1.57	0.995	1.099	0.803
9	2.101	3.74	2.313	5.586	0.713	2.265	3.56	2.459	1.217	1.255	1.136	0.379
10	0	4.728	4.772	3.273	2.759	3.185	5.646	4.248	2.288	2.81	2.068	0.561
11	0	5.613	7.543	4.234	1.582	2.68	4.618	4.141	2.109	1.965	2.349	1.125
12	3.231	4.31	1.917	2.76	1.862	1.935	4.806	3.911	1.638	1.173	2.077	1.427
13	0	0	9.375	4.803	1.906	0.951	3.962	3.502	1.975	1.731	1.656	1.96
14	0	2.746	0.659	3.098	2.003	2.282	6.647	5.928	2.868	4.507	3.232	1.523
15	6.089	3.55	4.641	3.498	1.441	2.434	2.621	4.209	2.482	2.275	2.448	2.903
16	14.02	0	3.748	1.925	0	2.113	4.056	5.333	3.181	3.002	3.345	4.26
17	5.689	2.435	2.387	2.077	1.491	0.98	3.401	4.039	2.993	3.095	3.344	3.351
18	5.806	0	4.725	2.979	1.359	1.076	2.702	4.579	2.754	2.593	2.888	3.565
19	9.272	4.04	2.759	4.181	1.14	1.298	1.768	3.946	2.483	2.297	2.367	2.366
20	4.725	2.624	6.259	2.228	0.814	1.018	2.54	3.223	2.337	2.25	2.264	2.228
21	5.771	4.371	3.301	2.271	1.377	0.76	1.315	2.674	2.059	1.974	1.177	1.771
22	8.461	7.957	1.389	0.122	0.832	0.107	2.027	2.976	2.332	2.306	2.131	2.032
23	4.876	10.647	5.011	2.195	1.05	0.713	1.717	3.376	2.144	1.863	2.104	2.282
24	21.91	13.453	9.161	4.78	1.118	0.734	3.467	1.745	0.516	0.318	0.257	0.538
25	0	3.618	11.844	5.632	2.274	1.561	8.473	5.506	3.371	3.055	3.282	5.438
26	0	7.905	6.153	3.475	3.268	1.429	8.521	5.824	5.058	6.822	5.38	5.837
27	4.409	3.793	7.792	2.446	2.171	0.507	4.7	6.441	3.623	3.612	4.542	7.114
28	6.48	0.881	3.846	3.625	1.853	0.404	5.197	6.406	3.592	3.273	3.922	6.041
29	6.064	0	6.594	3.141	2.691	0.977	2.364	6.64	4.771	5.124	5.813	8.266
30	4.941	3.009	6.272	1.838	2.036	0.453	3.21	5.53	3.723	4.148	4.252	4.49

Table 5 Compressive Strength Data for Rock Cores and Mortar Mixes

Compressive Strength					
Date	Sample	Size	Shape	Compressive Strength (psi)	Average Values (psi)
1/27/2016	Jeff. City White	2"x4"	Cylinder	13395	13590
1/27/2016	Jeff. City White	2"x4"	Cylinder	13549	
1/27/2016	Jeff. City White	2"x4"	Cylinder	13826	
1/27/2016	Jeff. City Gray	2"x4"	Cylinder	7039	6694
1/27/2016	Jeff. City Gray	2"x4"	Cylinder	5655	
1/27/2016	Jeff. City Gray	2"x4"	Cylinder	7388	
2/25/2016	100% Mortar + Glenium	2"x2"	Cube	3370	3723
2/25/2016	100% Mortar + Glenium	2"x2"	Cube	3882	
2/25/2016	100% Mortar + Glenium	2"x2"	Cube	3917	
3/14/2016	100% Mortar	2"x2"	Cube	2436	2447.333333
3/14/2016	100% Mortar	2"x2"	Cube	2471	
3/14/2016	100% Mortar	2"x2"	Cube	2435	
11/16/2016	100% Mortar	2"x2"	Cube	2323	2381.333333
11/16/2016	100% Mortar	2"x2"	Cube	2438	
11/16/2016	100% Mortar	2"x2"	Cube	2383	
11/16/2016	75% Mortar 25% Sand	2"x2"	Cube	1471	1500
11/16/2016	75% Mortar 25% Sand	2"x2"	Cube	1584	
11/16/2016	75% Mortar 25% Sand	2"x2"	Cube	1445	
11/16/2016	50% Mortar 50% Sand	2"x2"	Cube	583	600.3333333
11/16/2016	50% Mortar 50% Sand	2"x2"	Cube	649	
11/16/2016	50% Mortar 50% Sand	2"x2"	Cube	569	

Table 6 Caprock Breakage Fracture and Fragment Count

Test	Seam Thickness	SDOB	Main Radial Fractures	Number of Surface Fragments	Mix	Seam Thickness/SDOB
7	2.25	1.148185	4	3	50/50	1.959613872
8	2.25	0.804829	8	5	50/50	2.795626617
9	1.5	1.148185	Uncountable	15	50/50	1.30640924s
10	1.5	0.919281	10	10	50/50	1.631710356
11	1.5	0.690376	10	7	50/50	2.172728378
12	3	1.834899	4	2	50/50	1.634967263
13	3	1.37709	8	5	50/50	2.178506911
14	3	0.919281	Uncountable	Uncountable	50/50	3.263420712
15	2.25	1.148185	4	2	75/25	1.959613872
16	2.25	0.804829	7	5	75/25	2.795626617
17	2.25	0.976507	5	4	75/25	2.304131079
18	2.25	1.148185	5	3	100	1.959613872
19	2.25	0.804829	5	5	100	2.795626617
20	2.25	0.976507	8	6	100	2.304131079
21 Top	3	1.37709	3	2	100	2.178506911
Bottom	3		5	3	75/25	
22 Top	3	1.148185	4	2	100	2.612818497
Bottom	3		6	4	75/25	
23 Top	3	0.919281	6	6	100	3.263420712
Bottom	3		7	5	75/25	
26	3	1.148185	Uncountable	Uncountable	50/50 all	2.612818497
27	1.5	1.148185	Uncountable	Uncountable	50/50 all	1.306409248
28	2.25	1.148185	4	4	75/25 top	1.959613872
29	2.25	1.148185	3	2	100 top	1.959613872
30 Top	3	1.148185	4	6	100	2.612818497
Bottom			Uncountable	Uncountable	75/25	

APPENDIX B.

SCALED MODEL TEST PHOTOGRAPHS

This appendix contains additional photographs, covering each of the tests. These photographs are not used in the main text. Caprock tests, as well as relevant solid block tests are shown in order, listed by the test number used in Table 1 in Appendix A. Pictures shown include surface breakage for each test. Substrate breakage is shown for the first few tests to demonstrate breakage below the cap, then the remaining photos are of surface breakage.

Test 1

Figure 1 Surface Breakage Test 1

Figure 2 Side Breakage Test 1

Test 2

Figure 3 Surface Breakage Test 2

Figure 4 Side Breakage Test 2

Test 3

Figure 5 Surface Breakage Test 3

Figure 6 Side Breakage Test 3

Test 4

Figure 7 Surface Breakage Test 4

Figure 8 Broken Face Profile Test 4

Test 5

Figure 9 Surface Breakage Test 5

Figure 10 Side Breakage Test 5

Test 6

Figure 11 Surface Breakage Test 6

Figure 12 Side Breakage Test 6

Test 7

Figure 13 Surface Breakage Test 7

Figure 14 Substrate Breakage Test 7

Figure 15 Broken Face Test 7

Test 8

Figure 16 Surface Breakage Test 8

Test 9

Figure 17 Surface Breakage Test 9

Test 10

Figure 18 Surface Breakage Test 10

Test 11

Figure 19 Surface Breakage Test 11

Test 12

Figure 20 Surface Breakage Test 12

Test 13

Figure 21 Surface Breakage Test 13

Test 14

Figure 22 Cap Fragments and Blasted Face Test 14

Test 15

Figure 23 Surface Breakage Test 15

Test 16

Figure 24 Surface Breakage Test 16

Test 17

Figure 25 Surface Breakage Test 17

Test 18

Figure 26 Surface Breakage Test 18

Test 19

Figure 27 Surface Breakage Test 19

Test 20

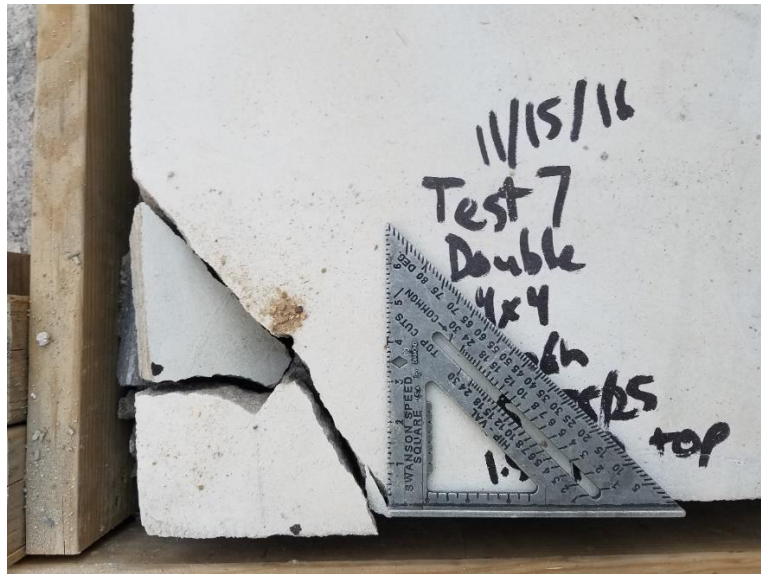Figure 28 Surface Breakage Test 20

Test 21

Figure 29 Top Layer Breakage Test 21

Figure 30 Middle Layer Breakage Test 21

Test 22

Figure 31 Top Layer Breakage Test 22

Figure 32 Middle Layer Breakage Test 22

Test 23

Figure 33 Top Layer Breakage Test 23

Figure 34 Middle Layer Breakage Test 23

Test 24

Figure 35 Block Breakage Test 24

Test 25

Figure 36 Block Breakage Test 25

Test 26

Figure 37 Block Breakage Test 26

Test 27

Figure 38 Block Breakage Test 27

Test 28

Figure 39 Surface Breakage and Annular Fracture Test 28

Figure 40 Block Damage Test 28

Test 29

Figure 41 Surface breakage Test 29

Test 30

Figure 42 Top Layer Breakage Test 30

Figure 43 Middle Layer and Block Breakage Test 30

BIBLIOGRAPHY

Ash, R.L. *Influence of Geological Discontinuities on Rock Blasting*. University of Minnesota, 1973.

Aswegen H.V, Cunningham C.V.B. "The estimation of fragmentation in blast muckpiles by means of standard photographs." *Journal of the South African Institute of Mining and Metallurgy* (1986): 469-474.

Atlas Powder Company. *Explosives and Rock Blasting*. Dallas, TX, 1987.

Bauer, A. "Application of the Livingston Theory." *Quarterly of the Colorado School of Mines* 56 (1961): 171-182.

Blair, D. P., & Minchinton, A. "Near-field blast vibration models." *Proceedings of the 8th International Symposium of Rock Fragmentation by Blasting*. Chile, 2006. 152-159.

Blair, D.P. "Statistical models for ground vibration and airblast." *Fragblast 3*. 1999. 335-364.

Blair, Dane and Minchinton, Alan. "On the damage zone surrounding a single blasthole." *Fragblast 1*. 1997. 59-72.

Brent, G. F., Rothery, M. D., Dare-Bryan, P. C., Hawke, S. J., Gomez, R., & Humeres, I. "Ultra-high intensity blasting for improved ore comminution." Sinha, Singh &. *Rock Fragmentation by Blasting*. London: Taylor & Francis Group, 2013. 163.

Calnan, Joshua. *Determination of Explosive Energy Partition Values in Rock Blasting Through Small-Scale Testing*. Theses and Dissertations-- Mining Engineering. 24., 2015. <http://uknowledge.uky.edu/mng_etds/24>.

Cattermole, J. M., & Hansen, W. R. "Geologic effects of the high-explosive tests in the USGS Tunnel area, Nevada Test Site." 1962.

Chiappetta, R.F. "History and Expansion of the Panama Canal." *Proceedings of the twenty-fourth annual Conference on Explosives and Blasting Technique*. New Orleans, LA, 1998. 867.

Cho, S.H., & Kaneko, K. "Rock Fragmentation Control in Blasting." *Materials Transactions* 45.5 (2004): 1722-1730.

Chung, S. H., & Mustoe, G. G. "Effects of particle shape and size distribution on stemming performance in blasting." *Discrete Element Methods: Numerical Modeling of Discontinua*. 2002. 288-293.

Cook, Melvin A. *The Science of Industrial Explosives*. Salt Lake City, UT: Ireco Chemicals, 1974.

Cooper, Paul W. *Explosives Engineering*. New York: Wiley-VCH, 1996.

Coy, Matthew. *Test Development to Determine the Feasibility of Rubber Tractor Treads for Use as Blasting Mats*. Rolla, MO: MST, 2014.

Cramer, J.R. *Contouring and Analysis of Rock Hardness and Point Load Strength Index Values for the Bethany Falls, Winterset, and Argentine Limestones in the Greater Kansas City Area*. Rolla, MO: University of Missouri at Rolla, 1983.

Crichton, G.A. *Crack Interaction in Hydraulic Fracturing of Cement Blocks*. Massachusetts Institute of Technology, 1980.

Cumerlato, C. L., Stachura, V. J., & Tweeton, D. R. "Application of refraction tomography to map the extent of blast-induced fracturing." *Symposium on the Application of Geophysics to Engineering and Environmental Problems*. Society of Exploration Geophysicists, 1989. 456-466.

Cunningham, C.V.B. "Fragmentation estimations and the Kuz-Ram model - Four Years On." *2nd International Symposium on Rock Fragmentation by Blasting*. Keystone, CO, 1987. 475-487.

—. "Methods of Evaluating and Predicting Fragmentation." *Blasting Technology, Instrumentation and Explosives Applications*. Boston, MA, 1995. 317-333.

—. "The Kuz-Ram fragmentation model - 20 years on." *Brighton Conference Proceedings*. European Federation of Explosives Engineers, 2005. 201-210.

—. "The Kuz-Ram Model for Prediction of Fragmentation from Blasting." *1st International Symposium on Rock Fragmentation by Blasting*. Lulea, Sweden, 1983. 439-453.

Dare-Bryan, P. C., Mansfield, S., & Schoeman, J. "Blast optimisation through computer modelling of fragmentation, heave and damage." *Proc 10th Int Symp Rock Fragm Blasting*. New Delhi, India, 2012. 95-104.

Derlich, S. "Underground nuclear explosion effects in granite rock fracturing." *Proc. Engineering with Nuclear Explosives*. American Nuclear Society, 1970. 505-518.

Donze F.V., Bouchez J., Magnier S.A. "Modeling Fractures in Rock Blasting." *International Journal of Rock Mechanics* (1997): 1153-1163.

Dyno Nobel. "FireLine 8/40 HMX LS Technical Information." Salt Lake City: Dyno Nobel, n.d.

Engin, I.C. "A practical method of bench blasting design for desired fragmentation based on digital image processing technique and Kuz-Ram model." *Fragblast 9*. 2010. 257-263.

Englman, R., Jaeger, Z., & Levi, A. "Percolation theoretical treatment of two-dimensional fragmentation in solids." *Philosophical Magazine B* 50.2 (1984): 307-315.

Esen, S., La Rosa, D., Dance, A., Valery, W., & Jankovic, A. "Integration and Optimisation of Blasting and Comminution Processes ." *EXPLO Conference*. Wollongong, NSW: The Australasian Institute of Mining and Metallurgy, 2007. 1-10.

Field J.E., Ladegaard-Pedersen A. "THE IMPORTANCE OF THE REFLECTED STRESS WAVE IN ROCK BLASTING." *International Journal of Rock Mechanics and Mining Sciences & Geomechanics Abstracts* 8.3 (1971).

Gheibie, S., Aghababaei, H., Hoseinie, S. H., & Pourrahimian, Y. "Modified Kuz—Ram fragmentation model and its use at the Sungun Copper Mine." *International Journal of Rock Mechanics and Mining Sciences* 46.6 (2009): 967-973.

Ghosh, A., Daemen, J. J. K., & Van Zyl, D. "Fractal-based approach to determine the effect of discontinuities on blast fragmentation." *The 31th US Symposium on Rock Mechanics (USRMS)* (1990).

Gil, Henryk. *The Theory of Strata Mechanics*. Amsterdam: Elsevier, 1991.

Gur, Y., Jaeger, Z., & Englman, R. "Fragmentation of rock by geometrical simulation of crack motion—I: Independent planar cracks." *Engineering fracture mechanics* 20.5 (1984): 783-800.

Hagan T.N., Just G.D. "Rock Breakage by Explosives, Theory, Practice and Optimization." *Proceedings of the Int. Soc. ofRock Mechanics, Denver*. Denver, 1974. 1349-1357.

Henrych, J., & Major, R. *The dynamics of explosion and its use*. Amsterdam: Elsevier, 1979.

Hino, K. "Fragmentation of Rock Through Blasting and Shock Wave Theory of Blasting." *The 1st US Symposium on Rock Mechanics (USRMS)*. American Rock Mechanics Association., 1956.

Hjelmberg, H. "Some ideas on how to improve calculations of the fragment size distribution in bench blasting." *1st International Symposium on Rock Fragmentation by Blasting*. Lulea, Sweden, 1983. 469-494.

Indian Institute of Technology - Roorkee. *Reflection, Transmission, and Standing Waves*. n.d. <WWW.IITR.AC.IN>.

ISEE. *ISEE Blaster's Handbook 18th Ed.* Cleveland, Ohio: International Society of Explosives Engineers, 2011.

Jaeger, Z., Englman, R., Gur, Y., & Sprecher, A. "Internal damage in fragments." *Journal of materials science letters* 5.5 (1986): 577-579.

Jhanwar, J. C., Cakraborty, A. K., Anireddy, H. N., & Jethwa, J. L. "Application of air decks in production blasting to improve fragmentation and economics of an open pit mine." *Geotechnical & Geological Engineering* 17.1 (1999): 37-57.

Jhanwar, J. C., Jethwa, J. L., & Reddy, A. H. "Influence of air-deck blasting on fragmentation in jointed rocks in an open-pit manganese mine." *Engineering Geology* 57.1 (2000): 13-29.

Johansson, C. H. and Persson, P.A. *Detonics of High Explosives*. London: Academic Press, 1970.

Johansson, D., & Ouchterlony, F. "Shock wave interactions in rock blasting: the use of short delays to improve fragmentation in model-scale." *Rock mechanics and rock engineering* 46.1 (2013): 1-18.

Johnson, C.E. *Fragmentation Analysis in the Dynamic Stress Wave Collision Regions in Bench Blasting*. Lexington, Kentucky, 2014.

Johnson, J. B., & Fischer, R. L. "Effects of mechanical properties of material on cratering: a laboratory study." 1963.

Katsabanis, L., & Liu, L. "Delay requirements for fragmentation optimization." *Measurement of Blast Fragmentation* (1996): 241-246.

Katsabanis, P.D., et al. "A review of timing requirements for Optimization of Fragmentation." *Proceedings of the 40th Conference on Explosives and Blasting Technique*. Denver, CO: ISEE, 2014.

Katsabanis, P.D., et al. "Timing effects on the fragmentation of small scale blocks of granodiorite." *Fragblast: International Journal for Blasting and Fragmentation* 10.1-2 (2006): 83-93.

Kolle, J. J., & Fort, J. A. "Application of dynamic rock fracture mechanics to non-explosive excavation." *The 29th US Symposium on Rock Mechanics (USRMS).* American Rock Mechanics Association, 1988.

Kopp, J.W. *Stemming ejection and burden movements from small borehole blasts.* Bureau of Mines. Twin Cities, MN: U.S. Deptartment of the Interior, 1987.

Kosheleve, E. A. "Development of a camouflet cavity as a result of an explosion in soft ground." *Journal of applied mechanics and technical physics* 16.2 (1975): 223-228.

Kutter H.K., Fairhurst C. "On the fracture process in blasting." *International Journal of Rock Mechanics and Mining Sciences & Geomechanics Abstracts* 8.3 (1971).

Kuznetsov, V.M. "The Mean Diameter of the Fragments Formed by Blasting Rock." *Journal of Mining Science* (1973): 144/148.

Langefors U., and Kihlstrom B. *Rock Blasting.* New York: John Wiley & Sons, 1978.

Larson, W.C. *Effects of Jointing and Bedding Separation on Limestone Breakage at a Reduced Scale.* Twin Cities, MN: Bureau of Mines, 1974.

Latham, J. P., Van Meulen, J., & Dupray, S. "Prediction of fragmentation and yield curves with reference to armourstone production." *Engineering geology* 87.1 (2006): 60-74.

Lilly, P.A. "An Empirical Method of Assessing Rock Mass Blastability." *The AUSIMM/IE Aust Newman Combined Group, Large Open Pit Mining Conference.* University of Queensland, 1986. 89-92.

Livingston, Clifton W. "Fundamentals of rock failure." *The 1st US Symposium on Rock Mechanics (USRMS).* American Rock Mechanics Association, 1956.

Lownds, C. M. "Prediction of fragmentation based on distribution of explosives energy." *Proceedings of the 11th Annual Symposium on Explosives and Blasting Research.* 1995. 286-297.

Lownds, C.M. "Computer modelling of fragmentation from an array of shotholes." *Proceedings of the 1st International Symposium on Rock Fragmentation by Blasting.* 1983. 455-468.

Lu, P., & Latham, J. P. "A model for the transition of block sizes during fragmentation blasting of rock masses." *Fragblast* 2.3 (1998): 341-368.

Ma, G. W., Hao, H., & Zhou, Y. X. "Modeling of wave propagation induced by underground explosion." *Computers and Geotechnics* 22.3 (1998): 283-303.

Margolin L.G., Adams T.F. "Numerical simulation of fracture." *The 23rd US Symposium on Rock Mechanics (USRMS)*. American Rock Mechanics Association, 1982.

McHugh, S. "Computational simulations of dynamically induced fracture and fragmentation." *First International Symposium on Rock Fragmentation by Blasting*. Lulea, Sweden, 1983. 407-418.

McKenzie, C. K. "Flyrock range and fragment size prediction." *Proceedings of the 35th Annual Conference on Explosives and Blasting Technique*. International Society of Explosives Engineers, 2009.

Morin M.A., Ficarazzo F. "Monte Carlo simulation as a tool to predict blasting fragmentation based on the Kuz-Ram model." *Computers and Geosciences* (2006): 352-359.

Nicholls, H. R., & Duvall, W. I. "Effect of charge diameter on explosive performance." U.S. Department of the Interior, 1966.

Onederra, I., Thurley, M. J., & Catalan, A. "Measuring blast fragmentation at esperanza mine using high-resolution 3d laser scanning." *Mining Technology* 124.1 (2015): 34-36.

Otterness, R. E., Stagg, M. S., Rholl, S. A., & Smith, N. S. "Correlation of shot design parameters to fragmentation." *Proceedings of the 7th annual symposium on explosives and blasting research*. Las Vegas, NV, 1991. 179-191.

Ouchterlony, F. "Fracture mechanics applied to rock blasting." *Congress of the International Society for Rock Mechanics: 01/09/1974-07/09/1974*. National Academy of Sciences, 1974. 1377-1383.

Ouchterlony, F., & Moser, P. "Likenesses and differences in the fragmentation of full-scale and model-scale blasts." *International Symposium on Rock Fragmentation by Blasting: 07/05/2006-11/05/2006*. Editec, 2006. 207-220.

Ouchterlony, F., Olsson, M., Nyberg, U., Andersson, P., & Gustavsson, L. "Constructing the fragment size distribution of a bench blasting round, using the new Swebrec function ." *International Symposium on Rock Fragmentation by Blasting*. Editec, 2006. 332-344.

Ouchterlony, Finn and Peter Moser. "Likenesses and differences in the fragmentation of full-scale and model-scale blasts." *International Symposium on Rock Fragmentation by Blasting*. Santiago, Chile: Editec, 2006. 207-220.

Ouchterlony, Finn. "Fragmentation monitoring of production blasts at MRICA." *International Symposium on Rock Fragmentation by Blasting*. The Australian Institute of Mining and Metallurgy, 1990. 283-289.

—. "The Swebrec© function: linking fragmentation by blasting and crushing." *Mining Technology* 2005: 29-44.

—. "What does the fragment size distribution of blasted rock look like?" *EFEE World Conference on Explosives and Blasting*. European Federation of Explosives Engineers, 2005. 189-199.

Persson, P. A. "The relationship between strain energy, rock damage, fragmentation, and throw in rock blasting." *Proceedings of the Fifth International Symposium on Rock Fragmenation by Blasting*. Montreal, Quebec, 1997. 113-120.

Persson, P.A., R. Holmberg and J. and Lee. *Rock Blasting and Explosives Engineering*. Boca Raton: CRC, 1994.

Porter D.D., Fairhurst C. "A study of crack propagation produced by the sustained borehole pressure in blasting." *The 12th US Symposium on Rock Mechanics (USRMS)*. American Rock Mechanics Association, 1970.

Preece, D. "3D computer simulation of bench blasting with precise delay timing." *PROCEEDINGS OF THE ANNUAL CONFERENCE ON EXPLOSIVES AND BLASTING TECHNIQUE*. ISEE, 2008. 191-200.

Rinehart, J. S., & Pearson, J. "Fracturing under impulsive loading." *The Third American Symposium on Mining Research*. 1952. 46-84.

Rollins, R. R. "Prediction of fragmentation by blasting." *The 30th US Symposium on Rock Mechanics (USRMS)*. American Rock Mechanics Association, 1989.

Rosin R, Rammler. "Laws governing the fineness of powdered coal." *Journal of the Institute of Fuel* (1933): 29-36.

Rossmanith, H.P. "The use of Lagrange diagrams in precise initiation blasting. Part I: Two interacting blastholes." *Fragblast* 6.1 (2002): 104-136.

Roth, Julius. "A model for the determination of flyrock range as a function of shot conditions." U.S. Department of the Interior, 1979.

Seaman L., Curran D. R., & Shockey, D. A. "Computational models for ductile and brittle fracture." *Journal of Applied Physics* 47.11 (1976): 4814-4826.

Siddiqui F.I., Ali Shah S.M., Behan M.Y. "Measurement of Size Distribution of Blasted Rock Using Digital Image Processing." *Journal of King Abdulaziz University* (2009): 81-93.

Singh, B., Roy, P. P., & Singh, R. B. *Blasting in Ground Excavations and Mines*. AA Balkema, 1993.

Siskind, D.E., R.C. Steckley and J.J. and Olson. *Fracturing in the Zone Around a Blasthole, White Pine, Mich.* Twin Cities, MN: Bureau of Mines, 1973.

Snelling, W.O. *The Effect of Stemming on the Efficiency of Explosives*. Bureau of Mines, 1928.

Sobin, O. A., & Smolyanitskii, A. A. "Calculations concerning concentrated single charges for ejection blasting in soils." *Soviet Mining,* 10.3 (1974): 296-299.

Stagg, M. S., & Rholl, S. A. "Effects of accurate delays on fragmentation for single-row blasting in a 6.7 m (22 ft) bench." *Proceedings of the 2nd International Symposium on Rock Fragmentation by Blasting*. Bethel CT, 1987. 210-230.

Stagg, Mark S. "Influence of blast delay time on rock fragmentation: one-tenth scale tests." *International Journal of Surface Mining, Reclamation and Environment* 1.4 (1987): 215-222.

Starfield, A.M. "Strain Wave Energy in Rock Blasting." *Proceedings of the 8th Symposium on Rock Mechanics*. American Rock Mechanics Association, 1966. 538-548.

Steiner, H.J. "The Significance of the Rittinger Equation in Present Day Comminution Technology." *Proceedings XVII International Minerals Processing Congress*. Dresden, 1991. 177-188.

Stimpson, B., & Yablonski, J. J. "Improving powder factor and cap-rock fragmentation in limestone quarrying." *CIM bulletin* 93.1041 (2000): 138-144.

Tariq, S. M., & Worsey, P. N. "An investigation into the effect of joint frequency and spatial positioning on pre-splitting." *Proceedings of the 11th Annual Conference on Explosives and Blasting Technique*. Cleveland, OH: International Society of Explosives Engineers, 1995. 287-296.

Tariq, S. M., & Worsey, P. N. "An investigation into the effect of varying joint aperture and nature of surface on pre-splitting." *Proceedings of the 12th Annual Symposium on Explosives and Blasting Research*. Orlando, FL, 1996. 186-195.

Tariq, S. M., Worsey, P. N., & Wilson, J. W. "Single decoupled blasthole tests and the significance of the results to presplitting and boulder busting." *Proceedings of the Twelfth Annual Symposium on Explosives and Blasting Research*. Orlando, FL: International Society of Explosives Engineers, 1996. 176-185.

Tariq, S., & Worsey, P. N. "An investigation into the effects of some aspects of jointing and single decoupled blast holes on pre-splitting and boulder blasting." *Rock Fragmentation by Blasting* (1996): 438.

Tariq, S.M. *Effects of Spatial Positioning and Surface Characteristics of Simulated Rock Joints on Presplit Blasting*. Rolla, MO: University of Missouri at Rolla, 1995.

Tawadrous, A.S. "Prediction of Fines Generated Around a Blasthole Using a State-of-the-Art Constitutive Model." *Blasting and Fragmentation* (2012).

Tulsa Geological Society. *Limestones of the Mid-Continent*. Tulsa, OK: Tulsa Geological Society, 1984.

W.R., Cattermole J.M. and Hansen. "Geologic Effects of the High-Explosive Tests in the USGS Tunnel Area Nevada Test Site." Professional Paper. 1962.

Wang, H., Latham, J. P., & Poole, A. B. "Producing armourstone within aggregate quarries." Magoon, O. T., & Baird, W. F. *Durability of Stone for Rubble Mound Breakwaters*. ASCE, 1992. 200-210.

Wang, H., Latham, J. P., & Poole, A. "Blast design for armour stone production. Part 1." *Quarry Management* (1991): 17-21.

—. "Blast design for armour stone production. Part 2." *Quarry Management* 18.8 (1991): 19-22.

Wang, Ping and L. Roy Xu. "Dynamic interfacial debonding initiation induced by an incident crack." *International Journal of Solids and Structures* 43 (2006): 6535-6550. <http://www.sciencedirect.com/science/article/pii/S0020768306000060>.

Wills, B.A. *Mineral Processing Technology*. Cornwall: Butterworth Heinemann, 1997.

Xu, K., & Lu, Y. "Numerical simulation study of spallation in reinforced concrete plates subjected to blast loading." *Computers & Structures* 84.5 (2006): 431-438.

Yang, R. and Kay, D.B. "Multiple Seed Wave (MSW) Vibration Modelling for Tunnel Blasting in Urban Environments." *Blasting and Fragmentation* (2011): 109-122.

Yang, R. L., & Scovira, D. S. "A model to predict the peak particle velocity for near field blast vibration-based on dominant charge, waveform broadening, delay time modeling, and non-linear charge weight superposition." *Blast Fragmentation* 2 (2008): 91-116.

VITA

Matthew Kurtis Coy was born in 1987. He grew up in rural Northeast Missouri and spent a lot of his time outdoors. During his school years, he participated in academic and athletic extracurricular activities. He was also an active member of the local 4-H youth organization, participating in shooting sports and many other activities. Matthew graduated from Highland High School in May 2006. From there he went on to the University of Missouri, Rolla (now Missouri S&T) to pursue an education in explosives. While at college, Matthew became involved in many organizations, primarily UMR and later S&T's Mucking and Pyrotechnics programs. Both of these programs involved lots of hard work and dedication but have provided him with many opportunities to travel and see places many people do not have the opportunity to see.

Matthew graduated from Missouri S&T with a Bachelor of Science in Mining Engineering in December 2010, and his Master of Science in Explosives Engineering in 2014. He graduated with his Ph.D. in Explosives Engineering in December 2017. At the time of finishing this dissertation, he was an instructor for the Proximate Pyrotechnics class, professional pyrotechnician, and blaster.